UNIVERSITEIT VAN PRETORIA
UNIVERSITY OF PRETORIA
YUNIBESITHI YA PRETORIA

In vitro P-glycoprotein activity of alkaloid-enriched fractions from *Solanum aculeastrum* and its synergistic potential with doxorubicin

by

Trevor Michael Burger

A dissertation submitted in fulfillment of the requirements for the degree

Magister Scientiae

in

Pharmacology

in the

Faculty of Health Sciences

at the

University of Pretoria

Supervisor
Mr Werner Cordier

Co-supervisor
Prof Vanessa Steenkamp

2016

Acknowledgements

I dedicate the work done in this study to my grandfather, Gerrit George de Koning, who battled prostate and colon cancer for many years.

To my supervisors:

Prof. Vanessa Steenkamp and Werner Cordier: Thank you for the knowledge and teachings you have passed down to me. Your help has been immense and I cannot express how grateful I am. You have pushed me throughout the project and taught me life lessons that will stay with me forever.

To my colleagues and staff of the department:

Alet van Tonder, Dr Gerda Fouché, Dr Gisela Joone, Prof. Duncan Cromarty, Prof. P Steenkamp and Tracey Hurrell: Thank you for all your advice concerning methodology and other aspects of my project. The help and suggestions have made the project a successful one.

To my close friends and fellow masters students:

Akanyang Rapholo, Hafiza Parkar, Keagile Lepule, Roxette Anderson, Tlabo Leboho, Tsholofelo Mokoka: Your help in the laboratory and emotional support throughout my project has been invaluable. I look forward to many more collaborations in the future.

To God and my family:

God: Thanks for giving me strength and providing guidance throughout the project and time at the University of Pretoria. I will always praise and give thanks to you.

Bryan Burger, Cedric Michael, Kim Michael and Melissa Ramos: Thank you for all the support and motivation throughout my project and my time at the University of Pretoria. My university career would not have been possible without your funding and amazing impact in my life.

To the National Research Foundation and Dr C Edgell:

NRF: Thank you for the financial support which made the project possible.

Dr C Edgell: Thank you for supplying the EA.hy296 endothelial hybrid cell line.

"*Science knows no country, because knowledge belongs to humanity, and is the torch which illuminates the world. Science is the highest personification of the nation because that nation will remain the first which carries the furthest works of thought and intelligence*" - **Louis Pasteur**

Table of Contents

Plagiarism declaration

University of Pretoria

Faculty of Health Sciences

Department of Pharmacology

I, Trevor Michael Burger,

Student number: u04429583

Subject of the work: *In vitro* P-glycoprotein activity of alkaloid-enriched fractions from *Solanum aculeastrum* and its synergistic potential with doxorubicin

Declaration

1. I understand what plagiarism entails and am aware of the University's policy in this regard.

2. I declare that this project (e.g. essay, report, project, assignment, dissertation, thesis etc) is my own, original work. Where someone else's work was used (whether from a printed source, the internet or any other source) due acknowledgement was given and reference was made according to departmental requirements.

3. I did not make use of another student's previous work and submitted it as my own.

4. I did not allow and will not allow anyone to copy my work with the intention of presenting it as his or her own work.

Signature TMBurger

Abstract

Cancer is one of the most life-threatening groups of diseases that affect humanity. Current treatment options include surgery, radiation treatment as well as chemotherapeutic agents such as alkylating agents, antimetabolites and antimitotic antibiotics. Resistance is often experienced due to overexpression of P-glycoprotein (P-gp) which leads to treatment failure. Due to prevalence of resistance and lack of effective combination treatment, novel treatment modalities are sought. *Solanum aculeastrum* Dunal, also known as the goat apple, is used to treat cancer, in the Eastern Cape. Literature is scarce concerning its anticancer activity, but steroidal alkaloids, such as solasodine and solamargine, are the proposed bioactive components. The aim of this project was therefore to assess the anticancer and P-glycoprotein inhibitory potential of alkaloid-enriched fractions from *S. aculeastrum* fruits as well as its synergistic potential with doxorubicin *in vitro*.

A crude extract was prepared by exhaustive ultrasonic maceration of *S. aculeastrum* fruits. Sequential liquid-liquid extraction was done to prepare one aqueous and two organic fractions from an acidified aliquot of the crude extract. Phytochemical screening for steroidal alkaloid employed thin layer chromatography (TLC), with ultra violet (UV) and spraying with Dragendorff's reagent. The extract and fractions were assessed for cytotoxicity in cancerous (A2780, Caco-2, DU145, HepG2, MCF-7, MDA-MB-231, SH-SY5Y, SK-Br3) and non-cancerous (3T3-L1, C2C12, EA.hy926, SC-1) cell lines using the sulphorhodamine B (SRB) assay, whereas P-glycoprotein inhibitory activity was determined utilising the rhodamine-123 assay. The aqueous fraction was further fractionated using High Performance Liquid Chromatography, followed by bioactivity screening (cytotoxicity and P-gp activity) of sub-fractions. Isolation of active components was by means of column chromatography, solid phase extraction and preparative TLC. Identities of isolated compounds were confirmed using Nuclear Magnetic Resonance (NMR) and Ultra-Performance Liquid Chromatography Tandem-Mass Spectrometry (UPLC-MS). The isolated compounds were also subjected to cytotoxicity and P-gp activity determination. Synergism was evaluated by combining doxorubicin with either the active isolated compound or the aqueous fraction using the checkerboard assay.

Phytochemical screening indicated the presence of steroidal alkaloids. The crude extract and aqueous fraction were the most cytotoxic in all cell lines, whereas the ether and chloroform fractions showed no cytotoxicity. The crude extract and aqueous fraction were most cytotoxic towards the SH-SY5Y neuroblastoma cell line, with half-maximal inhibitory concentrations (IC_{50}) of 10.72 µg/ml (crude) and 17.21 µg/ml (aqueous) respectively. Dose-dependent P-gp inhibition was observed for the crude extract (5.9 to 18.9-fold at 100 µg/ml) and the aqueous fraction (2.9 to 21.2 at 100 µg/ml). Sub-fractions 10 and 11 were the most active (cell density reduction: 91.06 and 91.72%, P-gp inhibition: 7.13 and 12.69-fold). Isolation and structural elucidation yielded the steroidal alkaloid solamargine as the bioactive component with an IC_{50} of 15.62 µg/ml and 9.1-fold P-gp inhibitory activity at 100 µg/ml against the SH-SY5Y cell line. The crude extract, aqueous fraction and solamargine also showed dose-dependent cytotoxicity and P-gp inhibition against primary cell lines. The steroidal alkaloid solasonine was also isolated but was found to be inactive. No synergistic combinations with doxorubicin were found in any of the cell lines tested. Additive effects were noted for combinations of doxorubicin with the aqueous fraction as well as solamargine against the SH-SY5Y cell line with FIX values of 0.71 and 0.51 respectively. In the C2C12 cell line, antagonistic interactions were noted with FIX values > 2.

The crude extract and aqueous fraction displayed potent non-selective cytotoxicity, and noteworthy P-gp inhibition against various cancer types, which was attributed to the steroidal alkaloid solamargine. Solamargine and the aqueous fraction were also shown to enhance doxorubicin through additive effects in select cell lines as well as indifferent and antagonistic responses in others. Although P-gp inhibition was present concurrently with cytotoxicity, it is not the proposed mechanism of the enhanced effect. Other processes need to be investigated.

Keywords: cytotoxicity, fractionation, P-glycoprotein, *Solanum aculeastrum*, solamargine, solasonine, steroidal alkaloids, structural elucidation

Abbreviations

ATCC	American Type Culture Collection
ATP	Adenosine triphosphate
B	Blank
^{o}C	Degrees centigrade
CAM	Complementary and alternative medicine
CI	Combination index
COSY	Correlation spectroscopy
CSIR	Council of Scientific and Industrial Research
δ_c	Chemical shift
dH_2O	Distilled water
DMEM	Dulbecco's Modified Eagle's Medium
DMSO	Dimethyl sulphoxide
EMEM	Eagles Minimum Essential Medium
F-10	Sub-fraction 10
F-11	Sub-fraction 11
F-Aq	Aqueous fraction
FaDD	Fas-associated death domain
Fas	Fas receptors
FCS	Foetal calf serum
g	Gram
g	Relative centrifugal force
Hams-F12	Ham's-F12 nutrient medium
HPLC	High performance liquid chromatography
HMBC	Heteronuclear Multiple Bond Correlation
HMRS	High Resolution Mass Spectrometry

HSQC	Heteronuclear Single Quantum Coherence
IC_{50}	Concentration which inhibits 50 percent cell growth
IGF-1	Insulin-like growth factor 1
J	Coupling constant
L	Liter
LLE	Liquid to liquid extraction
µg	Microgram
µl	Microliter
µm	Micrometer
µM	Micromolar
m/z	Mass to charge ratio
MDR	Multi-drug resistant
mg	Milligram
ml	Milliliter
min	Minute
M	Molarity
NC	Negative control
nM	Nanomolar
nm	Nanometer
NMR	Nuclear magnetic resonance
PBS	Phosphate buffered saline
PC	Positive control
pH	Hydronium ion concentration
Rf	Retention factor
RPMI	Roswell Park Memorial Institute-1640
SPE	Solid phase extraction
SRB	Sulphorhodamine B

TLC	Thin-layer chromatography
TNFR I	Tumour necrosis factor receptor I
TRADD	TNFR-I-associated death domain
UV	Ultraviolet
UPLC-TOF-MS	Ultra-Performance Liquid Chromatography
VC	Vehicle control
v/v	volume to volume
w/v	weight to volume

List of Figures

List of Tables

Chapter 1: Literature review

1.1 Cancer

Cancer is one of the most life-threatening groups of diseases that afflicts humanity.[1] According to the World Health Organisation (WHO), there were 14.1 million new cases of cancer in 2012 and 8.2 million cancer-related deaths noted between 2008 and 2012.[2] In 2012, lung cancer appeared with the highest incidence globally, whereas Kaposi sarcoma was the least diagnosed type of cancer (Table 1).[3] In terms of breast carcinoma, 6.3 million new cases were recorded in a five year period (2008-2012) with an incidence increase of 20% and mortality increase of 14%.[4] In South Africa, more than 100 000 people are diagnosed with cancer per annum, with prostate and breast cancer being the leading diagnosed cancers in men and women, respectively.[5]

Cancer involves unregulated cellular division and proliferation which may lead to the formation of tumours. Cancerous cells have classical hallmarks (Figure 1) which differentiates it from normal cells. The most prominent hallmark includes a limitless replicative potential due to disruption of growth regulating factors (e.g. retinoblastoma protein or p53 tumour suppressor gene).[6] Furthermore, cancer cells evade programmed cell death or apoptosis by invoking survival factors such as insulin-like growth factor 1 (IGF-1) or by mutations in the p53 gene.[6] Other hallmarks include tissue invasion and metastasis, insensitivity to antigrowth signals, sustained angiogenesis and a self-sufficient supply of growth signals.[7]

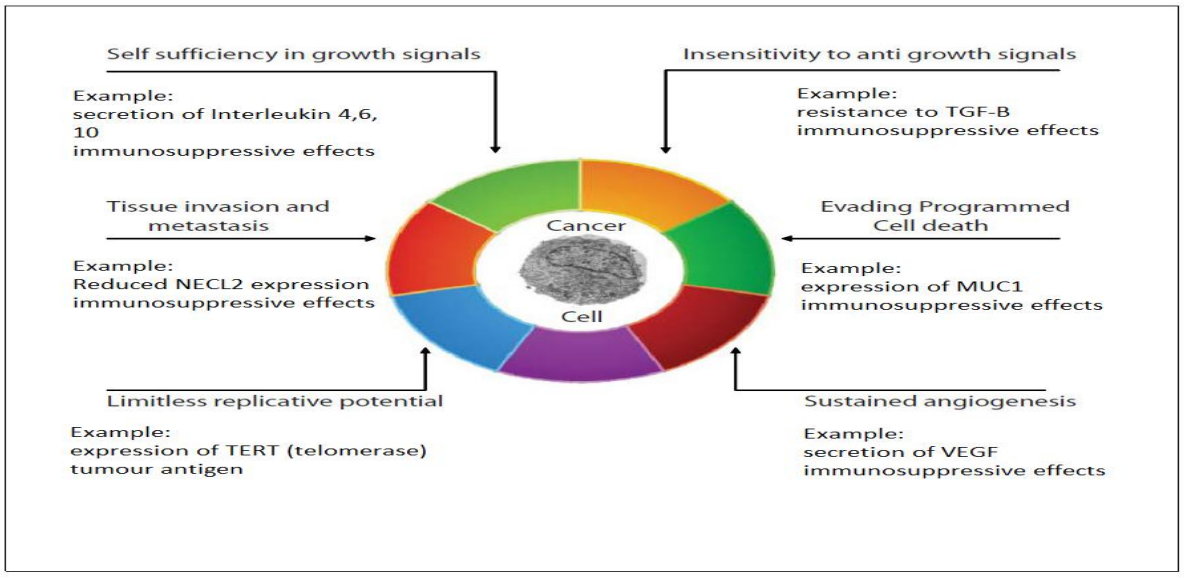

Figure 1: Classical hallmarks of cancer.[8]

Table 1: Global frequency and amount of new diagnosed cases of 20 cancer types in 2012.[3]

Rank	Cancer	New cases diagnosed in 2012 (1,000s)	Percent of all cancers (excl. non-melanoma skin cancer)
1	Lung	1,825	13.0
2	Breast	1,677	11.9
3	Colorectum	1,361	9.7
4	Prostate	1,112	7.9
5	Stomach	952	6.8
6	Liver	782	5.6
7	Cervix uteri	528	3.7
8	Oesophagus	456	3.2
9	Bladder	430	3.1
10	Non-Hodgkin lymphoma	386	2.7
11	Leukaemia	352	2.5
12	Pancreas	338	2.4
13	Kidney	338	2.4
14	Corpus uteri (endometrium)	320	2.3
15	Lip, oral cavity	300	2.1
16	Thyroid	298	2.1
17	Brain, nervous system	256	1.8
18	Ovary	239	1.7
19	Melanoma of skin	232	1.6
20	Gallbladder	178	1.3
21	Larynx	157	1.1
22	Other pharynx	142	1.0
23	Multiple myeloma	114	0.8
24	Nasopharynx	87	0.6
25	Hodgkin lymphoma	66	0.5
26	Testis	55	0.4
27	Kaposi sarcoma	44	0.3

1.2 Cancer treatment

Current anticancer therapy ranges from surgical intervention (excision of cancerous growth) to chemotherapy (treatment by cytotoxic and other drugs) or radiation treatment (treatment using X-rays or similar forms of radiation).[1] However, many drawbacks of current treatment exist, such as the expensive cost and wide panel of adverse effects.[9,10] A variety of anticancer agents are used, and these are divided into different classes based on chemical structure and mechanism of action (Table 2).[11] Examples include alkylating agents such as cyclophosphamide (which damage cancer cell DNA), antimetabolites which includes methotrexate (act as false DNA and RNA building blocks) and anti-tumour antibiotics like actinomycin-D (which disrupts cell-cycle enzymes). The increasing incidence of cancer in the absence of effective anticancer drugs has led to the search for novel compounds.[12]

Compounds that target mediators of the cell cycle have been a focus of many cancer based studies.[13] The effects of compounds generally result in cell cycle arrest which allows anti-proliferation (e.g. p53) mediators to repair damaged DNA or activate apoptotic signalling.[14]

Table 2: Different types of anticancer agents used in anticancer therapy.[11]

Anticancer agent type	**Examples**	**Mechanism of action**
Alkylating	Cyclophosphamide, lomustine, busulfan	Damage cancer cell DNA directly, influencing cell-cycle
Anti-metabolites	Methotrexate, gemcitabine	Act as false building blocks in DNA and RNA synthesis
Anti-tumour antibiotics	Actinomycin-D, mitomycin-C	Interfere with enzymes in DNA replication
Topoisomerase inhibitors	Etoposide, topotecan, mitoxantrone	Interfere with topoisomerase in DNA replication
Mitotic inhibitors	Paclitaxel, vinblastine, estramustine	Stops mitosis of cancer cells

Cellular death can either follow an apoptotic or necrotic pathway. Apoptosis (or programmed cell death, Figure 2) is characterized by nuclear condensation, fragmentation and packaging of the non-viable cells into apoptotic bodies and is a strictly-controlled process.[14] Necrosis (Figure 2) is the result of adenosine triphosphate (ATP) depletion and is characterized by breakdown of the plasma membrane, inflammation and changes in nuclear morphology, being an uncontrolled process.[14] In the necrotic process after cellular damage has occurred, the cell's organelles swell and there is a leaking of cellular contents on the surrounding tissues which leads to inflammation. Cancer therapy opts for apoptotic death to avoid inflammation of neighbouring cells and promote ordered cellular death.[15]

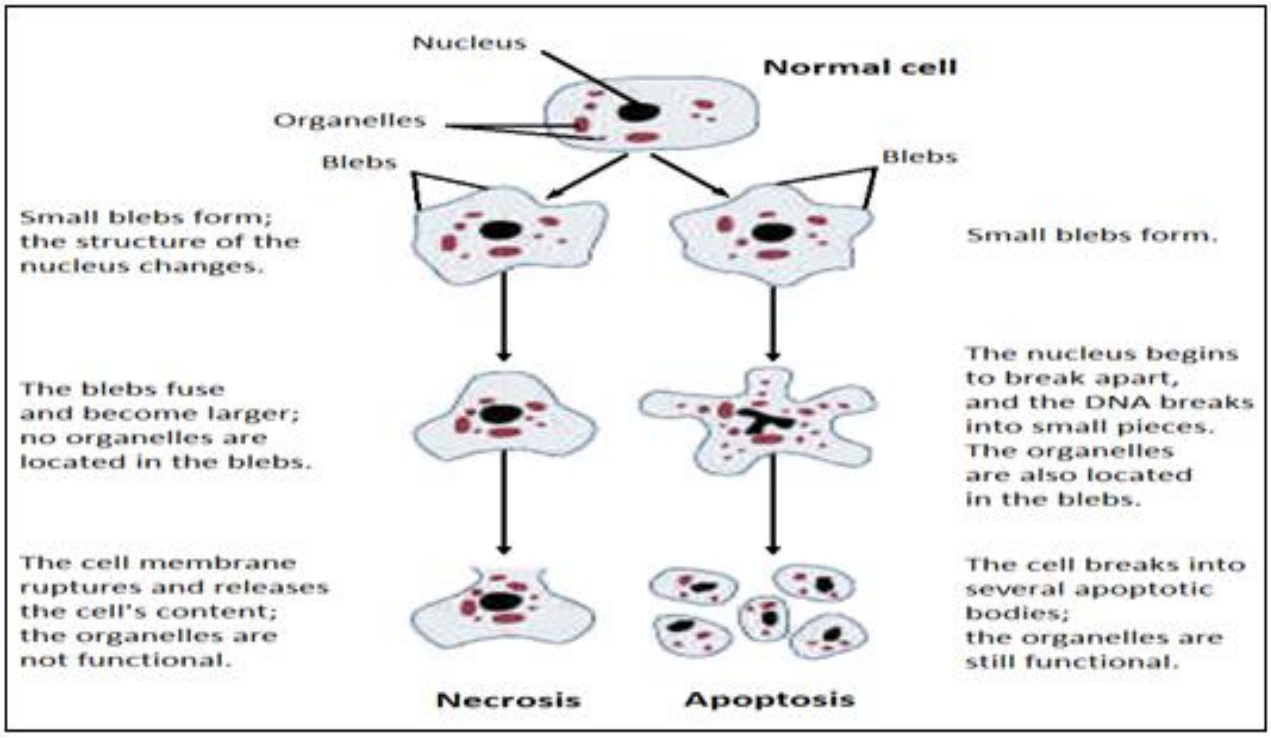

Figure 2: Overview of necrotic and apoptotic processes.[16]

Many of the anticancer agents mentioned in Table 2 have been shown to be effective in various cancer types, however, resistance is often observed which leads to treatment failure. Resistance elicited by cancers can either be to a single agent (mono drug resistance) or to multiple drugs (multidrug resistance).[17]

1.3 Multi-drug resistant cancer and P-glycoprotein

Multi-drug resistant (MDR) cancer refers to the ability of cancer cells to survive even in the presence of cytotoxic anti-tumour agents.[18] Resistance elicited by cancers pose a severe threat to successful treatment, where up to 90% treatment failure has been noted in cancer patients due to resistance.[19] The latter is often achieved by over-expression of particular proteins in cancer cells which help lower the intracellular concentration of many cytotoxic drugs. Other mechanisms of resistance include detoxifying enzymes (which disables the anticancer agent) and defective apoptotic pathways (which allows continuous growth of cancer cells in the presence of cell damage).[20] Proteins that decrease intracellular concentration include cell-membrane transporters which result in a reduced uptake and increased efflux of drugs in cancerous cells.[21]

P-glycoprotein (P-gp) is a 170 kDa ATP-binding cassette membrane transporter (Figure 3) which is expressed in various tissues throughout the body (e.g. small intestine and blood-brain barrier).[22] This protein affects the distribution (e.g. viral protease inhibitors), clearance (e.g. paclitaxel) and absorption (e.g. digoxin) of different molecules in the cell.[23] P-gp up-regulation is associated with the majority of drug-resistant cancers and acts as an efflux pump for many anticancer agents (e.g. doxorubicin, paclitaxel and vincristine).[24]

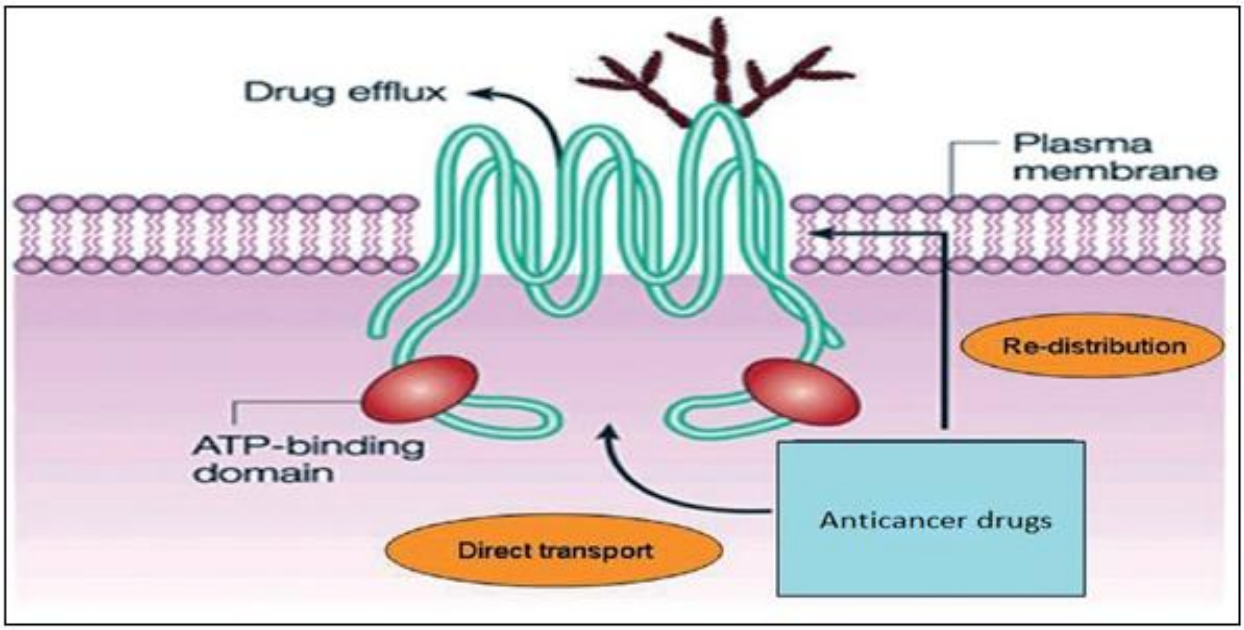

Figure 3: The structure and efficacy of P-glycoprotein.[25]

In MDR cancers expressing high levels of P-gp, anticancer drugs will be extruded from the intracellular space, and thus cannot elicit their mechanism of action. This leads to treatment failure and the prolongation of cancer. When anticancer agents are issued with a P-gp inhibitor, drug accumulation will occur, and thus high concentrations can be obtained with greater cytotoxic effect (Figure 4). This may lead to treatment success and destruction of the cancer cells. Elucidating the various substrates of P-gp may help in the selection of specific drugs which will be effective against cancer (even in the presence of P-gp) and help develop better treatment regimens.[23]

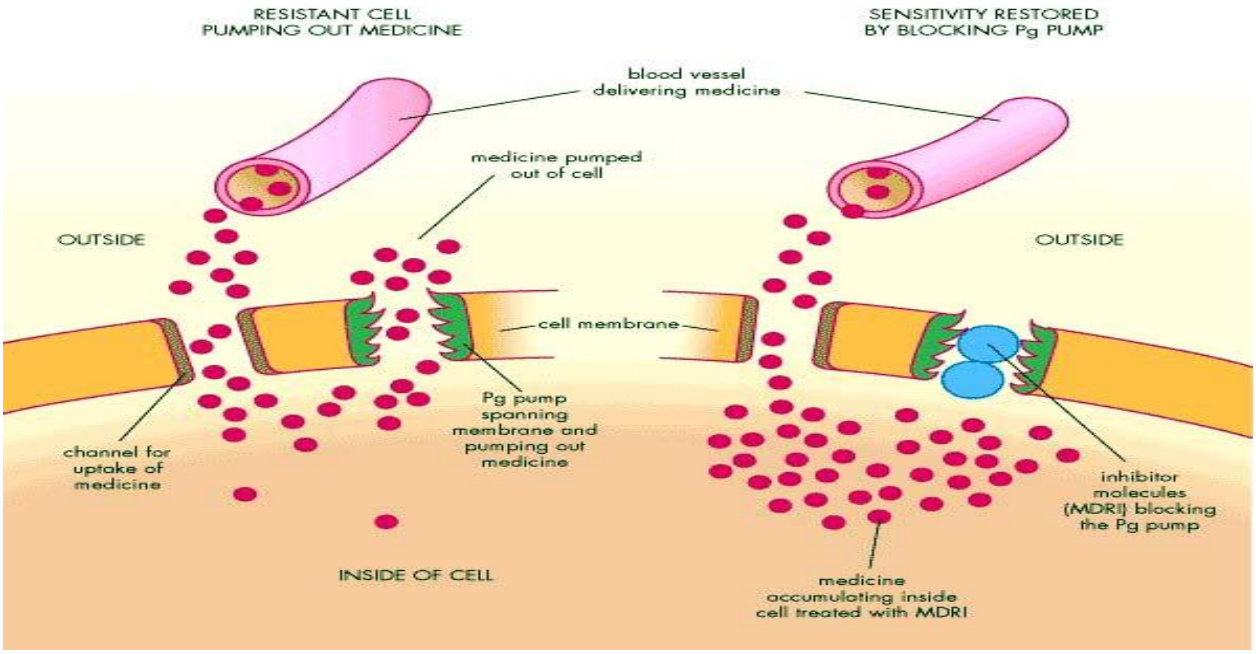

Figure 4: Illustration of how P-gp inhibitors would increase intracellular drug concentrations.[26]

Examples of inhibitory molecules include verapamil and cyclosporin A, which are first generation P-gp inhibitory drugs and bind non-specifically to the transporter.[27] Verapamil (antihypertensive/anticonvulsant) in particular is a phenylalkylamine, which blocks L-type calcium channels and has been used clinically for many years due to its rapid pharmacodynamics.[28,29] The inhibitor is also known to decrease the transport of P-gp substrates in a dose-dependent manner.[30]

1.4 Combination therapy and doxorubicin

Cancer is very often genetically diverse from one cell to the next. Due to this there is a high risk of a small number of cells being resistant to a given treatment which leads to treatment failure. Thus the probability of a single anticancer agent eliciting a significant effect on a single cancer pathway is very low. Multiple drugs in combination targeting many cancer hallmarks will have a greater chance of a possible cure.[31] Combination therapy where drugs are combined at a lower concentration leads to a reduced number of side effects. [32]

An example of a current combination therapy includes capecitabine (5-fluorouracil which is a pyrimidine analogue acting as a false building block) and docetaxel (interferes with microtubule dynamics) which is used for the treatment of anthracycline-pretreated patients with metastatic breast cancer. Clinical data showed that the combination resulted in a significantly higher efficacy, patient survival rate and reduced tumour progression than either drug alone.[33]

Doxorubicin is a front line chemotherapeutic agent used alone and in combination to treat a variety of blood cancers, solid tumours and soft tissue sarcomas.[34] There are two proposed mechanisms of action for doxorubicin. Firstly, through DNA intercalation and interference of topoisomerase-II effectuated DNA repair (inhibits cancer cell replication) which leads to apoptosis through cell cycle arrest, as well as the generation of free radicals which causes cellular damage. Although doxorubicin has potent anticancer activity, cardiotoxicity is a major side effect thus its use alone is problematic.[35]

Combination therapy involving doxorubicin (at low doses) acting synergistically with other compounds may be an effective way of decreasing cardiomyopathy while retaining efficacy.[36] Many studies have shown that herbal therapy and natural compounds enhance the effect of known anticancer agents.[37]

1.5 Herbal remedies

Worldwide, complementary and alternative medicines (CAM) are used for alleviation of various diseases, including cancer.[38] People in rural and disease-stricken areas use CAM out of desperation, general belief that it is safe, lack of medical facilities or the fact that CAM are more cost-effect.[38] As CAM definitions differ from country to country, accurate estimation of use worldwide is challenging.[39] Many CAM's, such as herbal remedies, are commonly used in the treatment of cancer. A multinational survey reported that 35.9% of cancer patients had or were presently using CAM.[40] Herbal therapies have been reported to be used by 5.3% of patients prior to cancer diagnosis and 13.9% after diagnosis.[41]

Many current anticancer agents are phytochemicals or derivatives thereof. Examples of such phytochemicals include vinblastine and vincristine (isolated from *Catharanthus roseus)*, which have been shown to elicit anticancer activity towards leukemias, lymphomas and other types of cancer.[41,42,43] Taxanes (isolated from *Taxus canadensis*) such as paclitaxel are used clinically in the treatment of breast, lung and ovarian cancer. Other examples include betulinic acid, etoposide, silvestrol, combretastatin which have a wide variety of anticancer properties and affinities (Table 3).[41,42,43]

Table 3: Phytochemicals used in cancer treatment.[42]

Phytochemical/s	**Plant of origin**	**Use in cancer treatment**
Betulinic acid	*Zizphus sp.*	Melanoma cell lines
Combretastatin	*Combretum caffrum*	Colon, lung and leukemia cancers
Etoposide and teniposide (semi-synthetic derivatives of epipodophyllotoxin)	*Podophyllum peltatum*	Lymphomas, bronchial and testicular cancers
Paclitaxel	*Taxus brevifolia*	Ovarian cancer, advanced breast cancer, small and non-small cell lung cancer
Silvestrol	*Aglailia sylvestre*	Lung and breast cancer cell lines
Vincristine and vinblastine	*Catharanthus roseus*	Leukemias, lymphomas, testicular, breast and lung cancers

1.6 Solanum genus

Solanaceae or the nightshades are a family of flowering plants which can range from crops and shrubs to highly toxic plants.[44] The family consists of 94 genera which consists of 2 000 species.[47] This family contains toxic alkaloids, which include solanine, atropine, nicotine, scopolamine and hyoscyamine.[46]

The *Solanum* genus has been reported to possess anticancer[47], antihepatoxic[48], anti-inflammatory[49] and hypotensive properties.[50] Many medicinal molecules have been isolated from the *Solanum* genus and some include alkaloids, saponins and flavonoids.[51,52,53] The existence of high levels of alkaloids may explain the toxicity (neurological and gastrointestinal effects) associated with the genus and may contribute to the bioactivity (which includes anticancer activity, P-gp inhibition and pro-apoptotic nature).[54,55] Studies done by Koduru *et al.* (2006, 2007) showed that steroidal alkaloids (tomatadine and solasodine) from *S. aculeastrum* had potent anticancer and antioxidant activity.[51,56]

The fruits of *S. aculeastrum* Dunal. (Figure 5), also known as the goat apple, is used in the treatment of cancer, especially breast carcinoma in the Eastern Cape.[58] Other uses include treatment of human and livestock diseases as well as jigger wounds and gonorrhoea.[57,58] Traditional treatment includes cooking the fruits of *S. aculeastrum* in water until they rupture. The mixture is then filtered and administered orally daily to alleviate symptoms, as well as decrease disease progression.[56] Literature is scarce concerning the anticancer activity of the fruits, but it is proposed that steroidal alkaloids (such as solamargine and solasonine) are responsible for its bioactivity.[59,60]

The steroidal alkaloids are known to induce apoptosis and incur anticancer activity in cancer cell lines by interfering in the mitotic process.[61] Steroidal alkaloids from the Solanaceae family have also been shown to elicit P-gp inhibitory activity and decreasing resistance by sensitising cancer cells to known anticancer agents.[62] In a previous study, solamargine was shown to enhance the cytotoxicity and efficacy of known anticancer agent cisplatin against ZR-75-1 and SK-BR-3 breast carcinoma cell lines by potentiating the apoptotic effect.[63] Solamargine has also been shown to down regulate P-glycoprotein in a multi-drug resistant leukemia cell line.[64,65] These findings illustrate the classes potential to overcome chemoresistance. The bioactivity elicited by steroidal alkaloids warrants further investigation in combination with other chemotherapeutic agents in the hope of overcoming multi-drug resistance and increasing treatment success against an array of cancers.

Figure 5: *Solanum aculeastrum* fruits. [66]

1.7 Aim and objectives

The aim of the study was to determine the cytotoxic and P-gp inhibitory activity of a crude extract and steroidal alkaloid-enriched fractions from *S. aculeastrum*. Furthermore the aim was to determine whether the fractions acted synergistically with doxorubicin to increase cytotoxic effects against cancerous cell lines.

The objectives of the study were to:

- Prepare a crude extract and alkaloidal enriched-fractions from *S. aculeastrum* fruits using standard ultrasonic maceration and liquid-liquid extraction techniques, respectively
- Determine the cytotoxic effects of the extract and alkaloid-enriched fractions in a panel of cell lines using the sulphorhodamine B staining assay:

  Cancerous (A2780 ovarian carcinoma, Caco-2 colon adenocarcinoma, DU145 prostate carcinoma, HepG2 hepatocarcinoma, MCF-7 breast ductal carcinoma, MDA-MB-231 breast carcinoma, SH-SY5Y neuroblastoma and SK-Br3 epithelial breast carcinoma)

  Non-cancerous (3T3-L1 pre-adipocyte, C2C12 myoblast, EA.hy926 endothelial hybrid and SC-1 fibroblast)
- Evaluate the P-glycoprotein inhibitory activity of the crude extract and alkaloid-enriched fractions in susceptible cell lines using the rhodamine-123 accumulation assay
- Isolate the bioactive phytochemicals from the alkaloid-enriched fraction displaying the greatest P-glycoprotein inhibitory activity.
- Evaluate the active phytochemical(s) for bioactivity through the following:
  - Cytotoxicity towards non-cancerous and cancerous cell lines
  - P-glycoprotein inhibitory activity
  - Synergistic potential with doxorubicin

Chapter 2: Materials and methods

Ethics approval (167/2015) to carry out the study was obtained from the Ethics Committee at the University of Pretoria (Appendix I). A list of reagents is provided in Appendix II.

2.1 Preparation of crude extract and alkaloid-enriched fractions

2.1.1 Collection of plant material

Ripened fruits of *S. aculeastrum* were received as a gift from the Makana Botanical Gardens, Grahamstown, Eastern Cape (South Africa) and the identity confirmed by the in-house botanist, Karin Cockburn. Fruits were sliced open, air-dried at room temperature and stored in amber bottles. Plant material was ground to a fine powder using a mill (Yellowline A10, Merck (Pty) Ltd) and stored in an air-tight, amber container.

2.1.2 Preparation of crude extract

One hundred and fifty grams of plant material was soaked in 1.5 L of absolute methanol, sonicated for 30 min and shaken for 2 h. Extracts were incubated at 4°C for 16 h and the procedure repeated five more times (10% and 5% w/v for the first two and last three extractions, respectively). Supernatants were pooled, centrifuged at 500 *g* for 1 min, filtered using a vacuum-filtration system (0.2 µm filters, Waters Corporation) and concentrated through *in vacuo* rotary evaporation (Büchi Rotovapor R-200, Büchi). Dried crystals were resuspended in distilled water (dH_2O) and lyophilized (Freezone® 6 Freeze Dry System, Labconco) to yield a dry powder (Figure 6A).

2.1.3 Preparation of alkaloid-enriched fractions

Alkaloid-enriched fractions were prepared as described by Munari *et al.*[67], with minor modifications to the volumes used. Powder (26.72 g) from the crude extract was acidified with 2% acetic acid (267.2 ml) and agitated on a mechanical shaker for 2 h. Extraction of alkaloids was achieved using liquid-liquid extraction (LLE). Ether (534.4 ml) was added to the acidified mixture, shaken for 20 min and the organic phase siphoned off. This procedure was repeated four more times and all ether fractions combined. The LLE procedure was repeated using chloroform to yield two organic fractions and one aqueous fraction. Both organic fractions were clarified using anhydrous sodium sulphate (10% w/v). The two organic fractions and the aqueous fraction were concentrated through *in vacuo* rotary evaporation and lyophilisation, respectively. The dried crude extract and alkaloid-enriched fractions was then reconstituted in DMSO at 20 mg/ml and stored at 80°C. Yields were determined gravimetrically (Figure 6B).

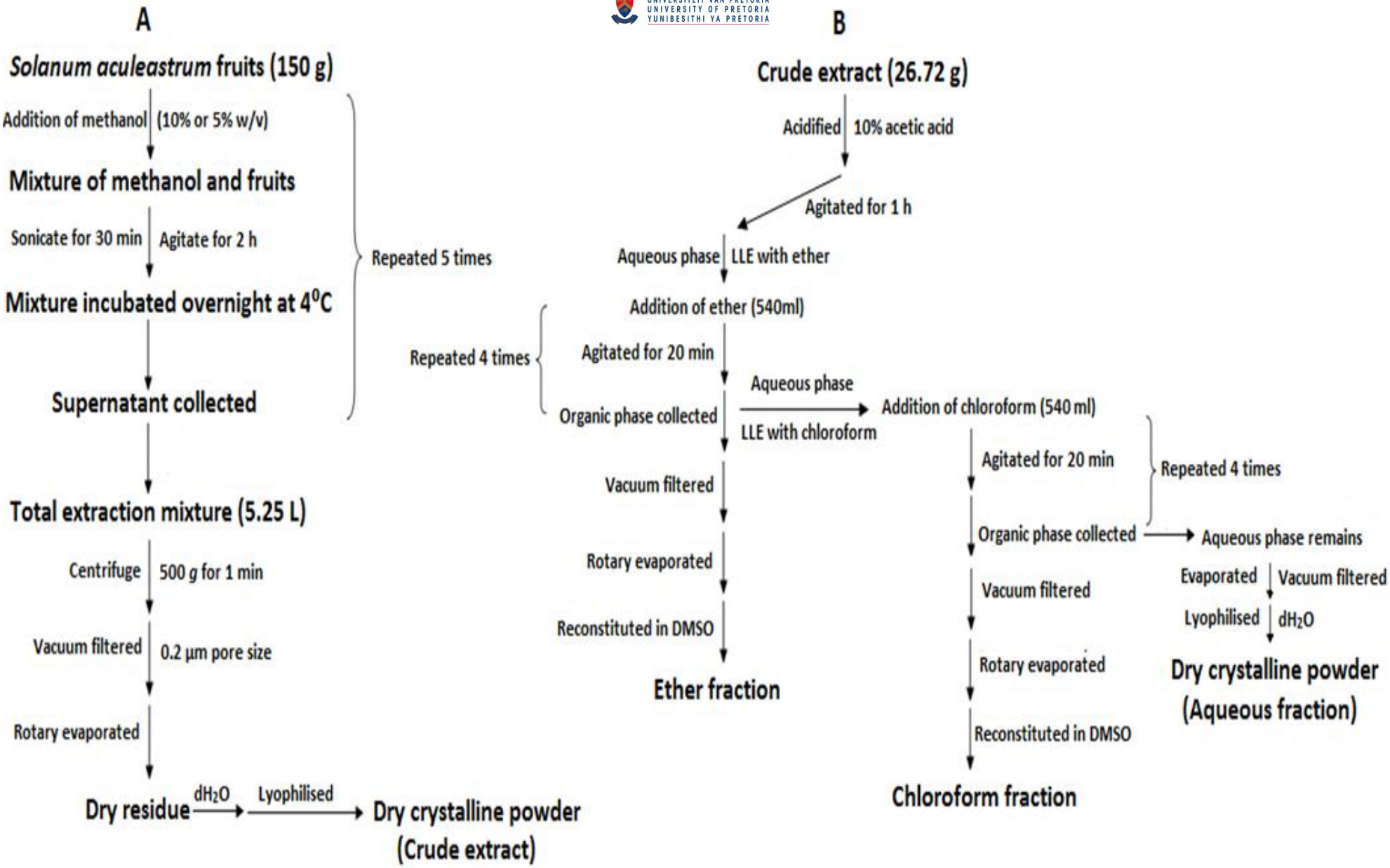

Figure 6: Flow diagram indicating A) crude extraction procedure, and B) alkaloid fractionation procedure.

2.2 Thin-layer chromatography for detection of steroidal alkaloids

Twenty micrograms of each sample was spotted onto a C_{10} silica plate (5 x 10 cm, Agilent Technologies South Africa) and allowed to dry. The thin-layer chromatography (TLC) plate was exposed to a mobile phase consisting of chloroform, acetone and methanol (4:4:2 ratio) in a saturated TLC chamber. The TLC plate was then visualized using ultraviolet light (UV, at 254 and 366 nm), sprayed with Dragendorff's reagent and developed in an oven at 60°C. Under UV at 254 nm, steroidal alkaloids appear as dark areas on a fluorescent background. However, at 366 nm, distinctive dark violet spots are observed.[68] Dragendorff's reagent reacts with secondary and tertiary amines in steroidal alkaloids resulting in an orange colour change.[69]

2.3 Cellular assays

2.3.1 Cellular maintenance and seeding of cells

Cells (Table 4) were propogated in medium supplemented with 10% foetal calf serum (FCS) and 1% penicillin/streptomycin in a humidified incubator at 37°C and 5% CO_2. Cells were grown in 25 cm^3 sterile flasks until 80% confluence was achieved and harvested through trypsination. Harvested cells were centrifuged at 200 *g* for 5 min, counted using the trypan blue exclusion assay and a haemocytometer, and resuspended to the desired concentration in 10% FCS-supplemented medium (HepG2 = 2 x 10^5 cells/ml; 3T3-L1, A2780, C2C12, Caco-2, DU145, EA.hy926, MCF-7, MDA-MB-231, SC-1, Sk-BR-3 and SH-SY5Y = 1 x 10^5 cells/ml). Cells (100 µl) were seeded into clear 96-well plates at the mentioned concentration and allowed to attach for 24 h prior to exposure in a humidified incubator at 37°C and 5% CO_2. Optimal cell densities were determined by the Department of Pharmacology in subsequent experimentation.

Table 4: Cancerous and non-cancerous cell lines used for assessment of cytotoxic activity of the crude extract and alkaloid-enriched fractions.

	Cell type	Concentration (cells/well)	Growth medium
Cancerous cell lines	A2780 ovarian carcinoma (ECACC catalogue no: 93112517)	10 000	RPMI-1640
	Caco-2 colon carcinoma (ATCC: HTB-37)	10 000	EMEM
	DU145 prostate carcinoma (ATCC: HTB-81)	10 000	RPMI-1640
	HepG2 hepatocarcinoma (ATCC: HB-8065)	20 000	EMEM
	MCF-7 breast ductal carcinoma (ATCC: HTB-22)	10 000	DMEM
	MDA-MB-231 breast adenocarcinoma (ATCC: HTB-26)	10 000	DMEM
	SH-SY5Y neuroblastoma (ATCC: CRL-2266)	10 000	Hams-F12
	SK-Br3 breast adenocarcinoma (ATCC: HTB-30)	10 000	RPMI-1640
Non-cancerous cell lines	3T3-L1 pre-adipocytes (ATCC: CL-173)	10 000	DMEM
	C2C12 myoblast (ATCC: CRL-1772)	10 000	DMEM
	EA.hy926 endothelial hybrid (ATCC: CRL-2922)	10 000	DMEM
	SC-1 mouse fibroblast (ATCC: CRL-1404)	10 000	EMEM

DMEM: Dulbecco's Modified Eagle's Medium

EMEM: Eagle's Minimum Essential Medium

Hams-F12: Ham's F12 nutrient medium

RPMI-1640: Roswell Park Memorial Institute 1640

2.3.2 Cytotoxic evaluation of the crude extract and alkaloid-enriched fractions

The effect of the crude extract and fractions were determined using the sulforhodamine B (SRB) colourimetric assay as described by Vichai *et al.*[70] with minor modifications. Trichloroacetic acid-fixed basic protein residues are stained by SRB, which is proportional to cell density.[69] After the 24 h attachment period, cells were exposed to either 100 µl FCS-free medium (negative control [NC]), DMSO (0.5%, vehicle control [VC]), saponin (1%, positive control [PC]), crude extract/alkaloid-enriched fractions (2, 6.4, 20, 64 and 200 µg/ml), or verapamil (0.64, 2, 6.4, 20. 64 and 200 µM) for 24 or 72 h in a humidified incubator at 37°C and 5% CO_2. The DMSO concentration for the crude extract and alkaloid-enriched fractions did not exceed 0.5%. Cells were fixed with 50 µl cold trichloroacetic acid (50%) and incubated overnight at 4°C. Plates were then washed four times with slow-running tap water via plastic tubing and allowed to dry in an oven at 40°C. Cells were stained with 100 µl SRB (0.057% in 1% acetic acid) and incubated at room temperature for 30 min. Excess dye was rinsed with 100 µl acetic acid (1%) thrice and allowed to dry in an oven. The dye was solubilised using 200 µl Tris base solution (10 mM, pH 10.5) and plates agitated on a shaker for 1 h. Absorbance was measured using a microplate reader (ELX800UV, Bio-Tek Instruments, Inc.) at 510 nm (reference 630 nm). Absorbance values were adjusted by subtracting the blank, and percentage cell density determined using the following formula:

$$Cell\ density\ (\%) = \left(\frac{AVS}{AAVNC}\right) \times 100$$

where, AVS = absorbance value of sample, and AAVNC = average absorbance value of negative control

From the cytotoxicity results, two susceptible cancerous cell lines, as well as one resistant and one non-resistant non-cancerous cell line, were selected and used for the remainder of the study. The optimal incubation time (either 24 or 72 h) for further evaluation of cytotoxicity was also based on the above results.

2.3.3 Assessment of P-glycoprotein inhibition for the crude extract and fractions

Rhodamine-123 is a fluorescent dye that accumulates intracellularly, and is a substrate of P-gp. Fluorescence intensity is inversely proportional to the functionality of P-gp. The rhodamine-123 accumulation assay according to Jia and Wasan[71], with minor modifications, was used to assess the P-gp inhibitory activity of the samples against four cell lines (C2C12, EA.hy926, SH-SY5Y, SK-Br3). Cells were seeded as described previously, but allowed to attach for 48 h in white 96-well plates. Wells were exposed to either 100 µl PBS (blank and NC), DMSO (VC, 0.5%), crude extract/alkaloid-enriched fractions (2, 6.4, 20, 64 and 200 µg/ml) or verapamil (PC; 2, 6.4, 20 µM) in PBS, and allowed to incubate at 37°C for 1 h. Thereafter, 40 µl of 10 µM rhodamine-123 was added to each well and allowed to incubate for 1 h. Cells were washed with PBS twice and resuspended in 100 µl PBS. Fluorescence intensity was measured using a fluorescent plate reader (FLUOstar OPTIMA, BMG Labtech) at 485 nm (excitation) and 520 nm (emission) (gain 750). Directly after reading the plate, cell density was assessed using the SRB assay as described in section 2.3.2. Data was blank-excluded, and fluorescence intensity was normalised to the cell density and expressed as a fold change relative to the negative control.

Normalised fluorescence intensity and fold-change in P-gp activity (relative to negative control) was calculated with the use of the following formulas:

$$Normalised\ fluorescent\ value = \left(\frac{FIS}{AVS}\right)$$

$$Fold - change\ in\ P - gp\ activity = \left(\frac{NFIS}{ANFIS}\right)$$

where, FIS = fluorescence intensity of sample, AVS: absorbance value of sample, NFIS = normalized fluorescent intensity of sample and ANFIS = average normalised fluorescent intensity of negative control.

2.3.4 Bioassay-guided fractionation and isolation

2.3.4.1 Bioassay-guided fractionation

A bioassay-guided fractionation (Figure 9A) and isolation method (Figure 9B) was developed in collaboration with Professor Gerda Fouché (Council of Scientific and Industrial Research [CSIR], Biosciences Division, South Africa) to isolate the active component(s) from the most active P-gp inhibitory alkaloid-enriched fraction.

The most active fraction (aqueous fraction) was subjected to High Performance Liquid Chromatography (Agilent 1200 HPLC System, Agilent Technologies South Africa) employing a solvent system consisting of acetonitrile and dH_2O (gradient: 0-10% acetonitrile between 0 and 5 min, to 100% at 30 min, total run time: 35 min) using a Sunfire C_{18} semi-preparative column (150 mm x 10 mm, particle size: 10 µm, Agilent Technologies South Africa) to separate various constituents. Five hundred microlitres of a 25 mg/ml solution (12.5 mg) was repeatedly injected and further fractionated into 11 sub-fractions which was collected every 2 min. Each sub-fraction was reconstituted to the desired concentration in DMSO and assessed for cytotoxic and P-gp inhibitory activity against the SK-Br3 breast carcinoma cell line at 50 µg/ml. Sub-fractions 10 and 11 were shown to be the most active, and thus further assessment focussed on them solely.

2.3.4.2 *Isolation of active constituents by column and solid phase extraction chromatography*

The aqueous alkaloid-enriched fraction and active sub-fractions (10 and 11) were exposed to TLC using a methanol:ethyl acetate:acetone (4:4:2) mobile phase.

Silica gel (65.0 g) was mixed with chloroform and methanol (3:2) and poured into a cotton wool plugged glass column (2.7 x 50.5 cm). The aqueous fraction (2.0 g) was then dissolved in a hydromethanolic solution (10% dH_2O), mixed with silica (1.0 g), left at room temperature to dry and loaded on top of the packed silica gel column. Sub-fractions (20 ml) were collected in glass tubes, monitored with TLC and compared to sub-fractions 10 and 11 as reference. Similar sub-fractions were pooled together (based on purity and complexity).

Pooled sub-fractions were exposed to solid phase extraction (SPE) chromatography using a 20 g ISOLUTE flash C_{18} column (Agilent Technologies South Africa) with a mobile phase of acetonitrile and dH_2O (starting at 100% dH_2O, followed by 5% acetonitrile, then 10%

acetonitrile and increasing to 100% acetonitrile in 10% increments). Major compounds co-eluted at 40% acetonitrile as a white-powder and were separated using preparative TLC (solvent system: methanol, ethyl acetate and acetone; 4:4:2) to afford compound 1 and compound 2.

The identities of the isolated compounds were confirmed using Nuclear Magnetic Resonance (NMR, 600 MHz VNMRS, Varian) and Ultra-Performance Liquid Chromatography Tandem Mass-Spectrometry (Synapt G1 UPLC-TOF-MS system, Microsep) analysis. Compounds were analysed using different NMR techniques such as H-1-NMR, C-13-NMR, Heteronuclear Single Quantum Coherence (HSQC), Heteronuclear Multiple Bond Correlation (HMBC) and correlation spectroscopy (COSY) to accurately determine structural moieties. Mass Lynx 4.1 software was used for analysis of mass spectrometry data and the fragmentation patterns of the isolated compounds were identified using Agilent ChemStation software. All procedures were repeated on multiple occasions for accuracy, repeatability and correct identification of active compounds.

2.3.4.3 UPLC-TOF-MS fingerprinting of the crude extract and alkaloid-enriched fractions

The crude extract and alkaloid-enriched fractions (at 20 mg/ml) were subjected to UPLC-TOF-MS analysis in order to screen for of major constituents. The relative abundance of the major compounds was also compared between samples by equalising the intensity scale between chromatograms of different samples. The highest sample intensity was used as the scale standard for other chromatograms.

2.3.4.4 Assessment of bioactivity for the isolated compounds

Both compound 1 and 2 were assessed for cytotoxic (72 h exposure) potential at 0.32, 1, 3.2, 10, 32 and 50 µg/ml against the C2C12, EA.hy29, SH-SY5Y and SK-Br3 cell lines. P-glycoprotein inhibitory activity was assessed in the SH-SY5Y and EA.hy926 cell lines only. Only the most active compound was subjected to further synergistic studies.

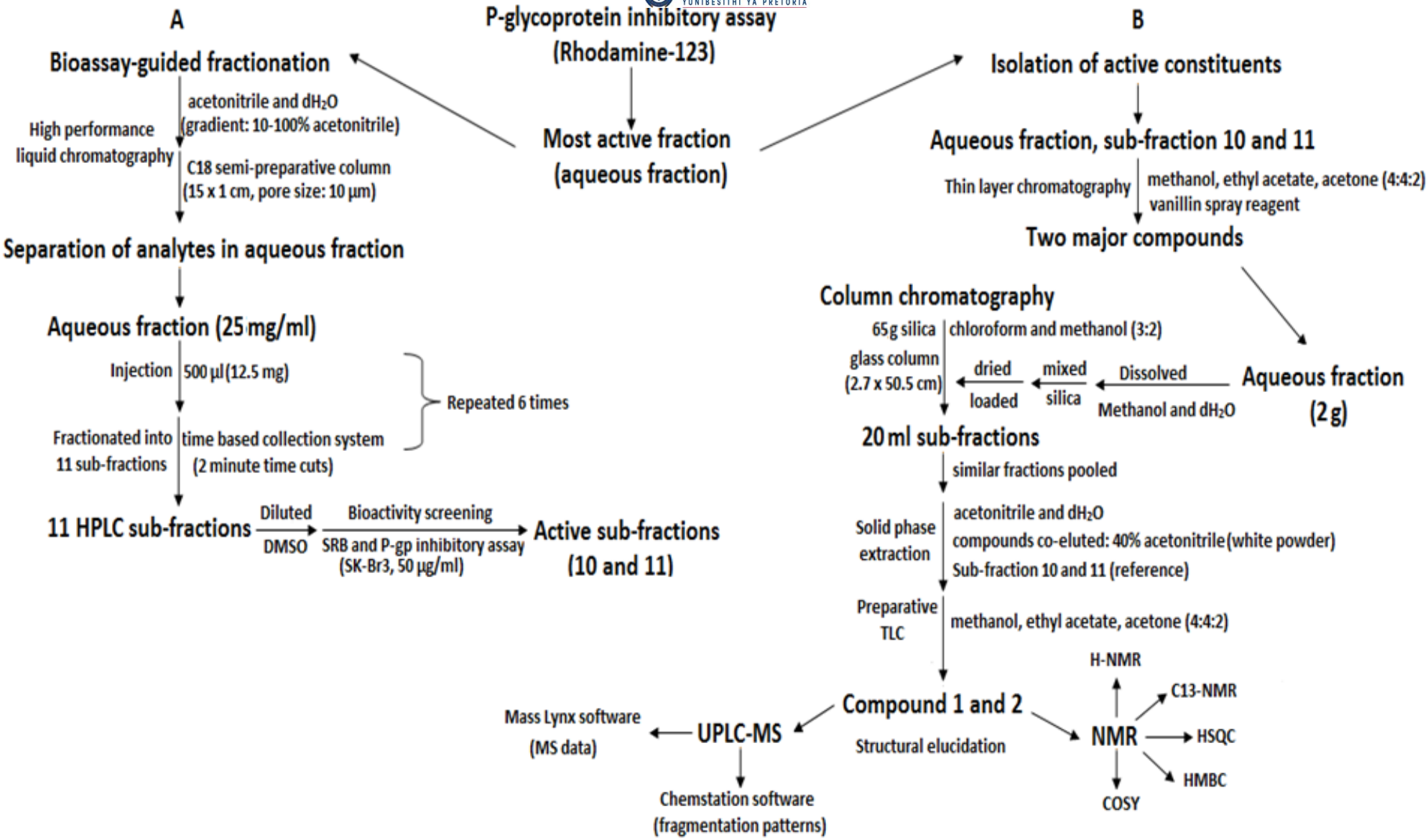

Figure 7: Flow diagram indicating A) bioassay-guided fractionation process, and B) the isolation and structural elucidation process for the active constituents.

2.3.5 Synergistic potential evaluation of the aqueous fraction and active isolated compound(s) in combination with doxorubicin

The synergistic potential of the aqueous alkaloid-enriched fraction and active compound(s) in combination with doxorubicin was assessed as described by Kars *et al*.[72]

Initially, the half maximal inhibitory concentration (IC_{50}) of the aqueous fraction was reassessed (due to cell population differences), as well as the cytotoxicity of doxorubicin against the C2C12, EA.hy29, SH-SY5Y and SK-Br3 cell lines (72 h exposure, using the SRB assay section 2.3.2). The IC_{50} values of the active isolated compounds were obtained from the bioactivity screening done in section *2.3.4.4*. The active isolated compounds, aqueous alkaloid-enriched fraction as well as doxorubicin was assessed at two-, one-, half- and a quarter-times the respective IC_{50} values in a checkerboard fashion (Figure 8).

Interactions between doxorubicin and samples were calculated using the fractional inhibitory concentration (FIC) as follows:

$$FIC(A) = \frac{IC50(A)\ in\ combination}{IC50(A)\ alone}$$

$$FIC(B) = \frac{IC50(B)\ in\ combination}{IC50(B)\ alone}$$

Effects of the combination between doxorubicin and the extract/fractions were given by the fractional inhibitory index:

$$FIX = FIC(A) + FIC(B)$$

<table>
<tr><td></td><td></td><td colspan="3">1 2 3</td><td colspan="3">4 5 6</td><td colspan="3">7 8 9</td><td colspan="3">10 11 12</td></tr>
<tr><td></td><td></td><td colspan="3">1 x S1</td><td colspan="3">1 x S2</td><td colspan="3">1 x S3</td><td colspan="3"></td></tr>
<tr><td>A</td><td>2 x D</td><td colspan="3" rowspan="3">S1</td><td colspan="3" rowspan="3">S2</td><td colspan="3" rowspan="3">S3</td><td rowspan="3">1 x S1 alone</td><td rowspan="3">1 x S2 alone</td><td rowspan="3">1 x S3 alone</td></tr>
<tr><td>B</td><td>1 x D</td></tr>
<tr><td>C</td><td>0.5 x D</td></tr>
<tr><td>D</td><td>0.25 x D</td><td colspan="3">1 x D</td><td colspan="3">PC</td></tr>
<tr><td></td><td></td><td colspan="9">1 x D</td><td colspan="3"></td></tr>
<tr><td>E</td><td>2 x S</td><td colspan="3" rowspan="3">S1</td><td colspan="3" rowspan="3">S2</td><td colspan="3" rowspan="3">S3</td><td colspan="3">VC</td></tr>
<tr><td>F</td><td>1 x S</td><td rowspan="3">1 x D alone</td><td rowspan="3">NC</td><td rowspan="3">B</td></tr>
<tr><td>G</td><td>0.5 x S</td></tr>
<tr><td>H</td><td>0.25 x S</td><td colspan="3">1 x D</td><td colspan="3">PC</td></tr>
</table>

D - Doxorubicin IC_{50} **S** - Sample IC_{50} **NC** - Negative control **PC** - Positive control **VC -** Vehicle control **B -** Blank

Figure 8: Checkerboard assay layout used to assess synergistic potential with doxorubicin.

2.4. Statistics

All experiments were done using both technical and biological replicates on at least three separate occasions (n ≥ 3). Results were compiled in Microsoft Excel (Microsoft) and analysed using GraphPad Prism 5.0 (GraphPad Software). Significance was regarded as $p < 0.05$.

Cytotoxicity**:** The IC_{50} values of all samples were determined using non-linear regression (normalised, variable slope). Outcomes were reported as the mean ± standard error of the mean (SEM).

P-glycoprotein inhibitory potential**:** Significance was assessed with the use of Kruskall-Wallis at a 95% confidence interval. Results were reported as mean fold change values.

Synergism with doxorubicin**:** A FIX value of less than 0.5 is indicative of synergism, between 0.5 – 1 as additive effect, between 1 – 2 as an indifferent effect and > 2 as antagonism. The IC_{50} values of all samples were determined using non-linear regression (normalised, variable slope). Results were reported as mean FIX values.

Chapter 3: Results and discussion

3.1 Extraction yield and steroidal alkaloid screening of crude extract and alkaloid-enriched fractions

S. aculeastrum yielded 17.98% (w/w) dry material following methanol extraction. Sequential LLE yielded 8.98% and 0.15% (w/w) crystalline solution for the ether and chloroform fractions, respectively. During LLE some of the extract was lost due to siphoning, filtration and re-suspension of fractions, which resulted in a 58.42% (w/w) yield for the aqueous fraction. Extraction yield has been shown to be affected by polarity. Fruits of *S. lycocarpum* displayed a higher extraction yield with polar solvents than non-polar solvents, which may explain the lower yield observed after using relatively non-polar solvents.[73] Qualitative assessment of steroidal alkaloids using TLC-based systems identified intense black spots (Figure 9A) and violet spots (Figure 9B) for the crude extract and alkaloid-enriched fractions when viewed under short (254 nm) and long (366 nm)-wave UV light. When exposed to Dragendorff's reagent, orange spots were visible for both the crude extract and alkaloid-enriched fractions (Figure 9C). Retention factor (Rf) values of 0.57 and 0.56 were obtained. The visualisation results and Rf-values are consistent with literature and suggest the presence of steroidal alkaloids.[68, 69]

The majority of *Solanum* steroidal alkaloids only contain one double-bond or possess no chromophores.[74] The latter is the functional group which allows for absorption of wavelengths and results in fluorescence.[75] Due to this, many steroidal alkaloids have low UV sensitivity[74], and larger quantities are needed for detection. Thus a high quantity of 20 µg was used in order to effectively detect steroidal alkaloids.

Assessment of five different *Solanum* spp. revealed that steroidal alkaloid solasodine contributed up to 60 to 80% of the total extract composition.[76] Compounds including solamargine, solasonine and solanine were also shown to be present at varying levels and are known to be present in many *Solanum* species.[76] Isolation studies on *S. aculeastrum*. have also revealed the presence of bioactive steroidal alkaloids.[51] Therefore a positive colour reaction after visualization with UV and Dragendorff's spray reagent was expected for *S. aculeastrum*.

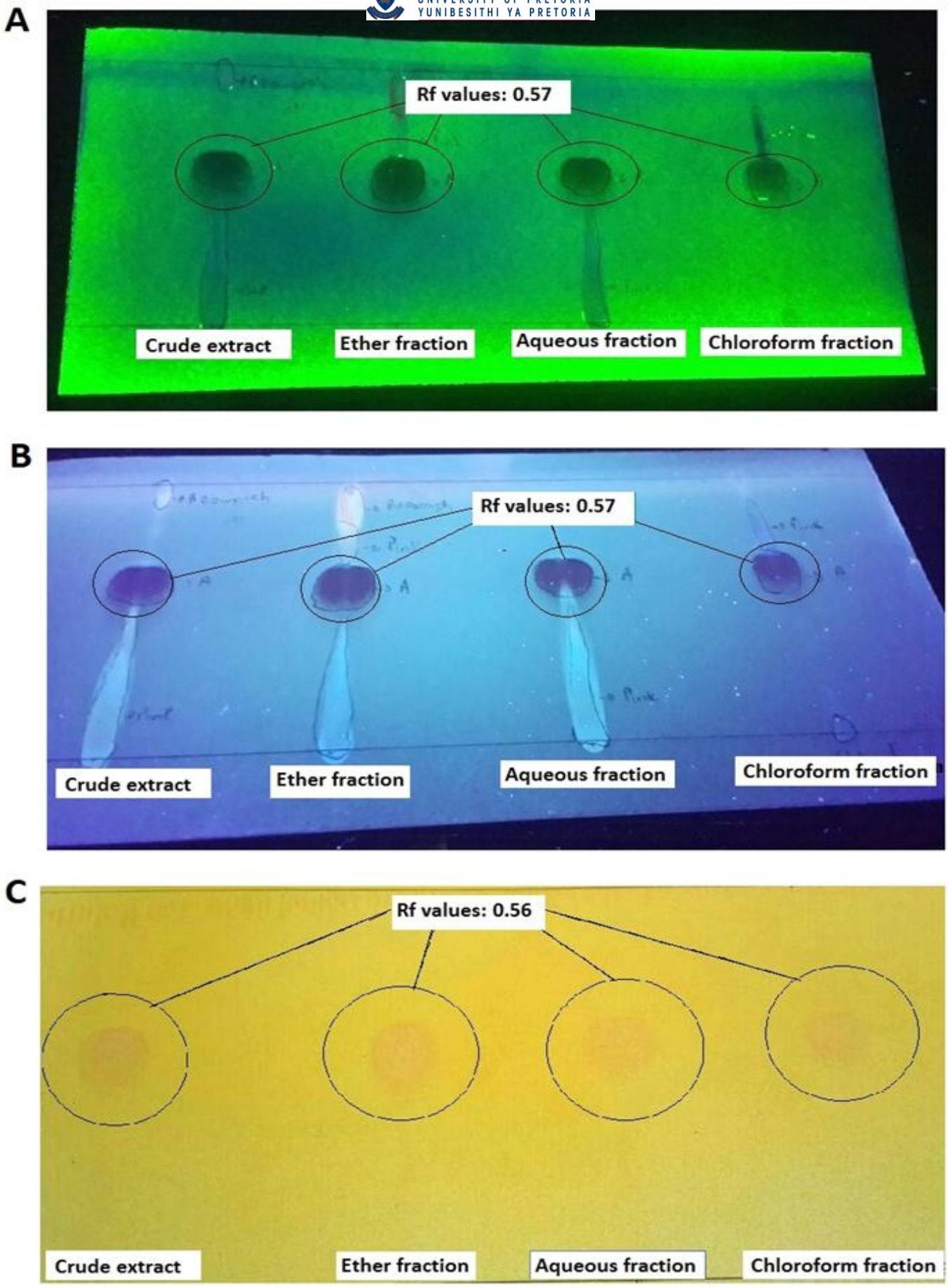

Figure 9: Visualization of steroidal alkaloids A) at 254 nm UV, B) at 366 nm UV and C) after spraying with Dragendorff's reagent.

3.2 Isolation and identification of compounds from the aqueous fraction

3.2.1 HPLC fractionation and bioactivity screening

The aqueous fraction was sub-fractionated into 11 fractions by collecting eluent every 2 min (Figure 9), and pooling similar fractions after repeated injections. In the HPLC profile, a UV fluorescent peak was present in sub-fraction 11 (F-11) but absent in sub-fraction 10 (F-10). TLC analysis of F-10 and F-11 revealed the presence of two major compounds (compound 1 and 2) which were not visible under UV light (Figure 11A and 11B) but were visualized after spraying with vanillin (Figure 11C). F-10 and F-11 were spotted as a reference when isolating (section 3.4.2) compound 1 and 2.

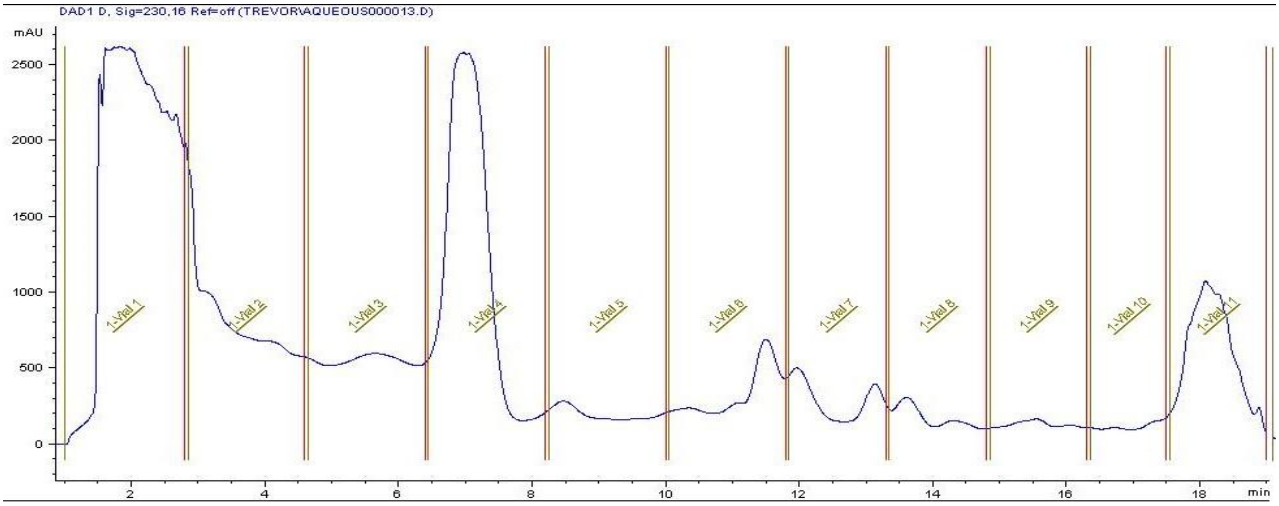

Figure 10: HPLC profile of the aqueous alkaloid-enriched fraction indicating the 11 sub-fractions collected every 2 min.

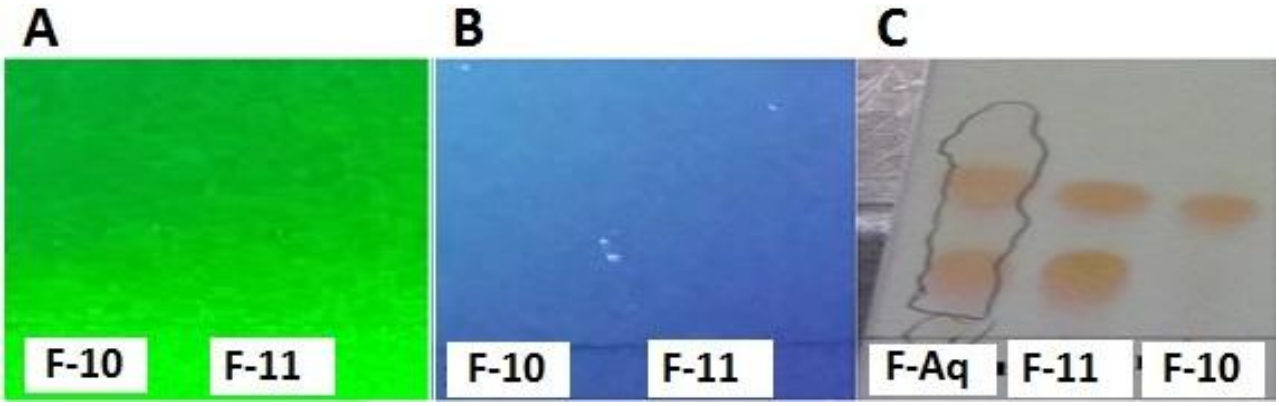

Figure 11: Visualization of compounds in F-10 and F-11 after TLC analysis (methanol:ethyl acetate:acetone, 4:4:2) with A) 254 nm UV, B) 366 nm UV and visualization using C) 1% vanillin spray reagent. F-Aq: Aqueous fraction.

As previously mentioned, compounds such as steroidal alkaloids possess low UV fluorescence due to single double-bond moieties, and thus require high concentrations to be detected. Low amounts of F-10 and F-11 were spotted during TLC analysis, thus no UV detection suggests that major compounds had low fluorescent ability. Vanillin spray reagent is a TLC stain that detects steroid as well as higher functional groups and results in a range of colour changes.[77] Alkaloids such as solasodine and its derivatives are known to have the latter moieties in their structures, which resulted in the positive detection.[78]

3.2.2 Structural elucidation of compound 1

Compound 1 was isolated as white crystals. The structure of compound 1 was identified by H-1-NMR, C-13-NMR, 2-D data analysis (Appendix III-A to III-E) and compared with literature.[60] C-13-NMR revealed that compound 1 possesses an aglycone backbone related to a steroidal spirazolane-type alkaloid.

Four quaternary carbons at chemical shifts (δ_c's) 38.2, δ_c 41.8 ppm including one linked to oxygen and nitrogen at δ_c 99.6 as well as one attached to a double bond at δ_c 142.1, nine methine groups at δ_c's 31.8, 31.8, 42.9, 51.9, 57.9, 64.2, 79.5, 80.5, 122.80, ten methylene groups at δ_c's 22.2, 30.9, 31.1, 32.9, 33.1, 33.4, 38.7, 39.7, 41.2, 48.5 ppm and four methyl groups at δ_c's 15.6, 17.0, 19.91, 19.98 ppm were observed. An ether function with a trisaccharide moiety showing an anomeric carbon at δ_c 100.6 linked to the oxygen of C-3 at δ_c 79.5 was also present. The 1D NMR chemical shifts of the trisaccharide moiety indicated the structure *O*-[α-L-rhamnopyranosyl-(1→2)-*O*-[α-L-rhamnopyranosyl-(1→4)]-β-D-glucopyranoside.

The proton NMR showed four distinctive aglycone methyls at δ_c 0.83 (3H, s), 0.85 (3H, d, *J* [coupling constant] 6.4), 0.97 (3H, d, *J* 7.2) and 1.05 (3H, s). Two multiplets observed at δ_c 1.26 were attributable to 6-deoxyhexose methyls whereas a doublet at δ_c 5.38 with *J* value of 4.6 could be attributed to an olefinic proton at position C-6. Four anomeric H-1-NMR resonances were observed at δ_c 4.34 (1H, m), 4.50 (1H, d, *J* 7.6), 4.84 (1H, s) and 5.21 (1H, s). High Resolution Mass Spectrometry (HRMS) data for compound 1 yielded the molecular formula $C_{45}H_{73}NO_{15}$ with a molecular weight peak at m/z (mass to charge ratio) 868.5077 ($M + H^+$, 100%) (Appendix III-F to III-G) which was identified as the steroidal alkaloid, solamargine (Figure 12).

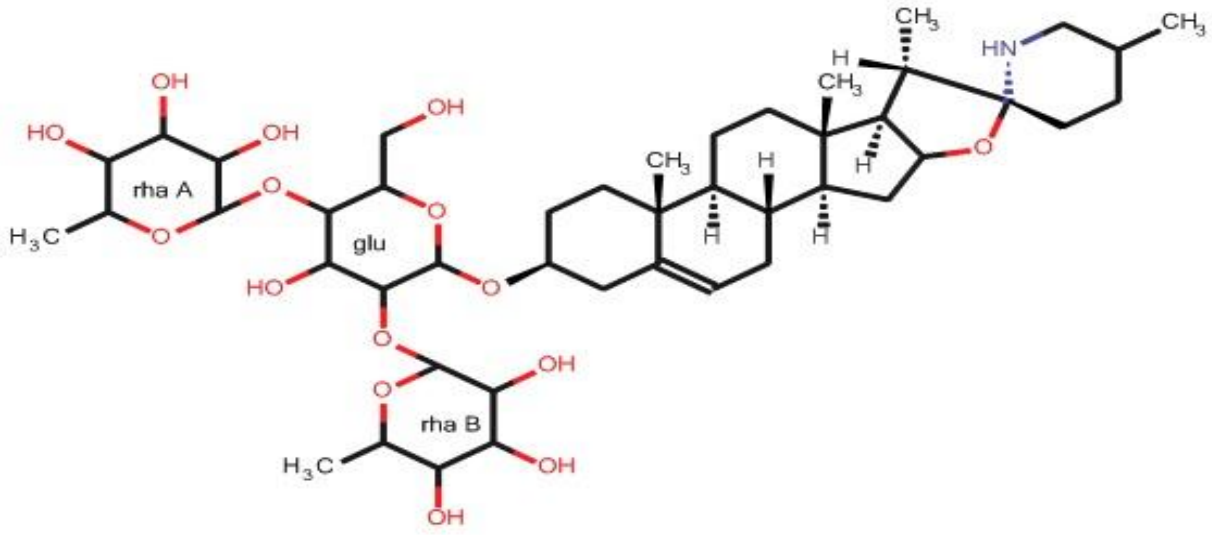

Figure 12: Chemical structure of solamargine.

glu: Glucose; rha A: Rhamnose A; rha B: Rhamnose B

Table 5: H-1-NMR and C-13-NMR resonances of compound 1 compared to solamargine.

		Solamargine (Wanyonyi 2002)[60] (deuterated chloroform and methanol)		Compound 1 (2015) (deuterated methanol)	
	Carbon no (type)	**C13-NMR**	**H-1-NMR (*J* in Hz)**	**C13-NMR**	**H-1-NMR (*J* in Hz)**
Aglycone	C-1 (CH_2)	37.9		38.70	
	C-2 (CH_2)	30.5		31.13	
	C-3 (CH)	79		79.50	
	C-4 (CH_2)	40.4		41.19	
	C-5 (C)	141.1		142.07	
	C-6 (CH)	122.2	5.37 (d, *J* 4.2)	122.78	5.38 (d, *J* 4.6)
	C-7 (CH_2)	32.5		32.94	
	C-8 (CH)	32.1		31.81	
	C-9 (CH)	50.7		51.90	
	C-10 (C)	37.5		38.20	
	C-11 (CH_2)	21.4		22.15	
	C-12 (CH_2)	38.9		39.67	
	C-13 (C)	41.1		41.77	
	C-14 (CH)	57.1		57.90	
	C-15 (CH_2)	30.1		30.90	
	C-16 (CH)	79.7	4.33 (m)	80.45	4.34 (m)
	C-17 (CH)	63.2		64.21	
	C-18 (CH_3)	16.8	0.84 (s)	17.00	0.83 (s)
	C-19 (CH_3)	19.6	1.05 (s)	19.91	1.05 (s)
	C-20 (CH)	42		42.85	
	C-21 (CH_3)	15.4	0.97 (d, *J* 7.0)	15.60	0.97 (d, *J* 7.2)
	C-22 (C)	98.9		99.60	
	C-23 (CH_2)	34.4		33.36	
	C-24 (CH_2)	32.7		33.14	
	C-25 (CH)	31.3		31.81	
	C-26 (CH_2)	47.8	2.6 (m, br)	48.47	2.53 (m)
	C-27 (CH_3)	19.6	0.87 (d, *J* 6.0)	19.98	0.85 (d, *J* 6.4)
Glucose (glu)	C-1' (CH)	99.9	4.48 (d, *J* 7.8)	100.63	4.50 (d, *J* 7.6)
	C-2' (CH)	79.5		80.23	
	C-3'(CH)	77.3		78.19	
	C-4' (CH)	75.7		76.73	
	C-5' (CH)	78.6		79.50	
	C-6' (CH_2)	61.4		62.12	
Rhamnose A (rha A)	C-1'' (CH)	102.4	4.87 (s)	103.16	4.84 (s)
	C-2'' (CH)	71.8		72.60	
	C-3'' (CH)	71.5		72.35	
	C-4'' (CH)	73.3		74.10	
	C-5'' (CH)	69.1		69.94	
	C-6'' (CH_3)	17.7	1.29 (m)	18.11	1.26 (m)
Rhamnose B (rha B)	C-1''' (CH)	101.5	5.23 (s)	102.44	5.21 (s)
	C-2''' (CH)	71.6		72.52	
	C-3''' (CH)	71.3		72.35	
	C-4''' (CH)	73		73.89	
	C-5''' (CH)	70.1		70.85	
	C-6''' (CH_3)	17.6	1.29 (m)	18.01	1.26 (m)

3.2.3 Structural elucidation of compound 2

Extensive evaluation of the similarities in characteristic signals of the H-1-NMR, C-13-NMR and 2-D NMR for compound 2 revealed that it was similar to compound 1 (Appendix IV-A to IV-E). This included an aglycone backbone attached to a trisaccharide moiety. However, differences were present in the trisaccharide sugar moiety in which a *O*-[α-L-rhamnopyranosyl-(1→2)-*O*-[b-glucopyranosyl-(1→3)]-β-D-galactopyranoside structure was observed. The addition of the glucopyranosyl sugar moiety caused an extra hydroxyl group to be present when compared to compound 1. HRMS data for compound 2 yielded the molecular formula $C_{45}H_{73}NO_{16}$ with molecular weight peak at m/z 884.5205 ($M + H^+$, 100%) (Appendix IV-F to IV-G) which was identified as the steroidal alkaloid solasonine (Figure 13) when compared with literature.[79] The mass difference between solasonine and solamargine is consistent with the additional hydroxyl group seen in solasonine's structure.

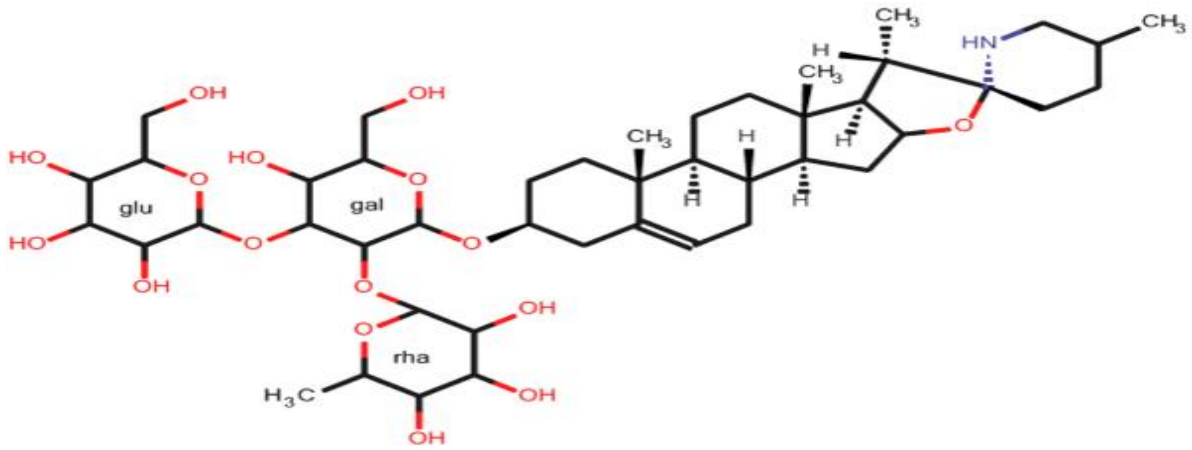

Figure 13: Chemical structure of solasonine.

gal: Galactose; glu: Glucose; rha: Rhamnose

3.2.4 UPLC-TOF-MS fingerprinting

UPLC-TOF-MS analysis of the crude extract and alkaloid-enriched fractions revealed that solamargine and solasonine with m/z's of 868.5 and 884.5 ($M + H^+$, 100%), respectively, were the two major constituents (Appendix V-A to V-D). Although there were similarities in composition between samples, the concentration of major compounds differed. The crude extract and aqueous fraction had a significantly higher abundance of solamargine and solasonine when compared to the chloroform and ether fractions (Figure 14).

Table 6: H-1-NMR and C-13-NMR resonances of compound 2 compared to solasonine.

		Solasonine (Neszmelyi 1987)[79] (deuterated pyridine and methanol)	Compound 2 (2015) (deuterated methanol)
	Carbon no (type)	**C-13-NMR**	**C-13-NMR**
Aglycone	C-1 (CH_2)	37.4	38.74
	C-2 (CH_2)	30.1	30.58
	C-3 (CH)	78.3	78.09
	C-4 (CH_2)	38.8	39.58
	C-5 (C)	140.7	142.16
	C-6 (CH)	121.6	122.69
	C-7 (CH_2)	32.5	32.95
	C-8 (CH)	32.5	33.14
	C-9 (CH)	50.3	49.72
	C-10 (C)	37.1	38.23
	C-11 (CH_2)	21.1	22.15
	C-12 (CH_2)	40.1	41.20
	C-13 (C)	40.6	41.78
	C-14 (CH)	56.7	57.90
	C-15 (CH_2)	31.7	31.13
	C-16 (CH)	78.7	79.13
	C-17 (CH)	63.5	64.22
	C-18 (CH_3)	16.5	17.00
	C-19 (CH_3)	19.3	19.91
	C-20 (CH)	41.5	42.85
	C-21 (CH_3)	15.6	15.60
	C-22 (C)	98.2	99.56
	C-23 (CH_2)	34.6	33.37
	C-24 (CH_2)	31.1	30.86
	C-25 (CH)	31.7	31.82
	C-26 (CH_2)	47.9	48.47
	C-27 (CH_3)	19.7	19.99
Galactose (gal)	C-1' (CH)	100.3	100.96
	C-2' (CH)	76.3	76.10
	C-3'(CH)	84.8	85.82
	C-4' (CH)	70.2	70.39
	C-5' (CH)	74.9	75.81
	C-6' (CH_2)	62.4	62.62
Glucose (glu)	C-1'' (CH)	102	102.36
	C-2'' (CH)	72.4	72.28
	C-3'' (CH)	72.7	72.51
	C-4'' (CH)	74	74.17
	C-5'' (CH)	69.3	69.89
	C-6'' (CH_2)	18.5	18.14
Rhamnose (rha)	C-1''' (CH)	105.7	105.86
	C-2''' (CH)	74.8	75.24
	C-3''' (CH)	78.7	80.45
	C-4''' (CH)	71.4	71.37
	C-5''' (CH)	78.3	78.38
	C-6''' (CH_3)	61.8	62.51

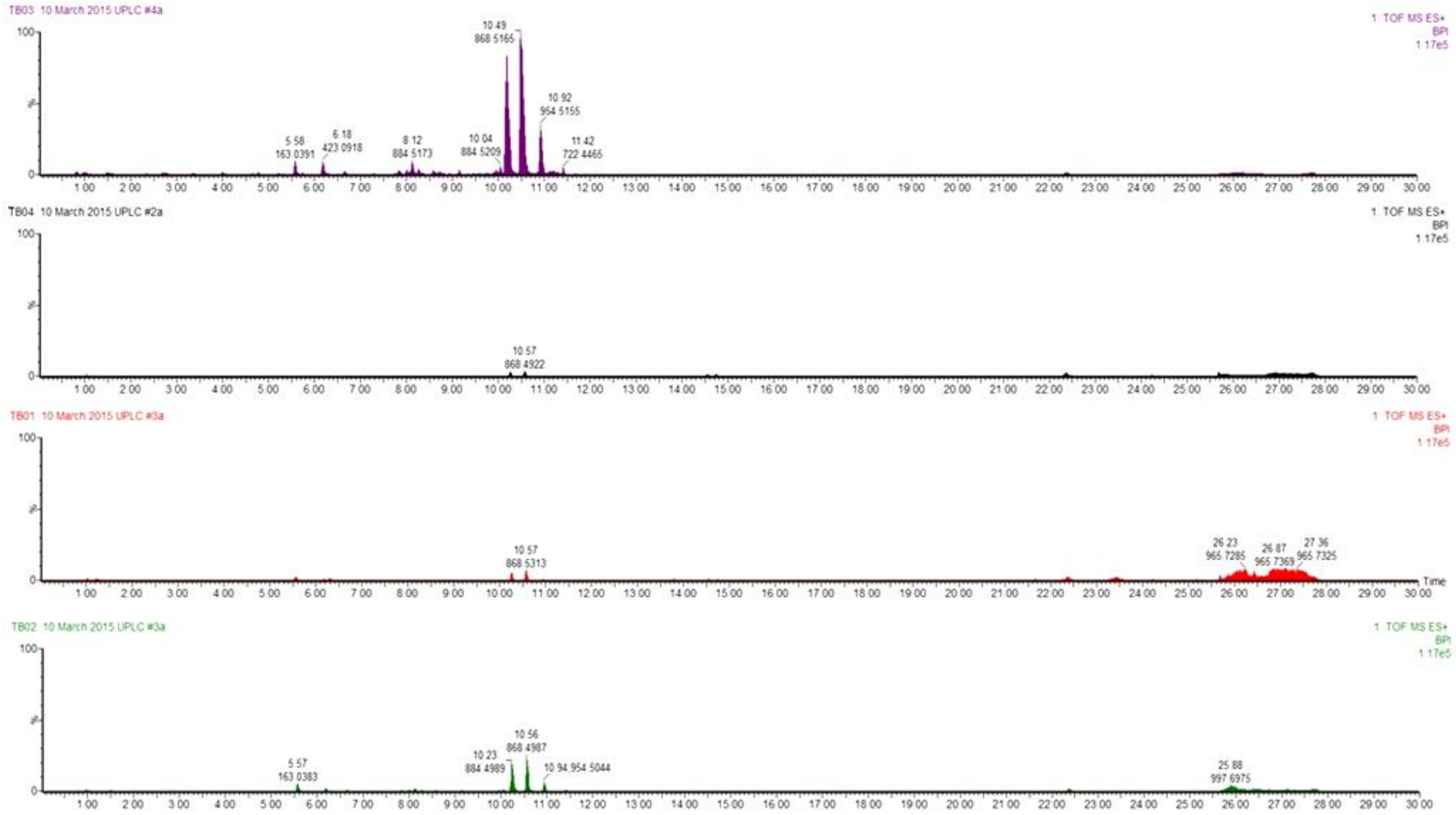

Figure 14: UPLC-TOF-MS stacked chromatogram of the crude extract (TB03), ether fraction (TB04), chloroform fraction (TB01) and aqueous (TB02) fraction of *Solanum aculeastrum* on the same scale.

From literature it is evident that over 100 *Solanum* spp., including *S. aculeastrum*, contain steroidal alkaloids such as solamargine and solasonine which elicit anticancer activity.[80] Other compounds isolated from *S. aculeastrum* include steroidal alkaloids such as solaculine A, solasodine and tomatidine.[51,60] Alkaloids such as solanopubamine and solanidine have also been noted in other *Solanum* spp.(Table 7).[81,82] Although no studies have isolated non-alkaloidal compounds from *S. aculeastrum*, the genus is known to contain other phytochemicals that may incur biological effects.[83] Examples include flavonoids such as astragalin and biochanin A, as well as phenolic compounds including ferulic acid and gallic acid.[84,85] Saponins, such as methyl-protodioscin and indioside D, have been described, which possess cytotoxic, cytoprotective and antioxidant bioactivity.[83,86] Phytochemicals such as tannic acid and several terpenoids, including aromadendrene and caryophyllene, have also been isolated.[87,88]

Table 7: Phytochemical classes and compounds isolated from the *Solanum* genus.

Phytochemical class	Compound	Species isolated from
Alkaloids	Solamargine[82]	*S. aculeastrum*
	Solasonine[82]	
	Solaculine A[62]	
	Solasodine[53]	
	Tomatidine[53]	
	Solanopubamine[83]	*S. schimperianum*
	Solanidine[84]	*S. tuberosum*
Flavonoids	Astragalin[86]	*S. crinitum*
	Biochanin[86]	
	Kaempferol[86]	
	4-hydroxybenzoic acid[86]	
Phenols	Ferulic acid[87]	*S. melongena*
	Gallic acid[87]	
	Salicyclic acid[87]	
Saponins	Methyl-protodioscin[69]	*S. incanum* and *S. heteracanthum*
	Indioside D[88]	
	Dioscin[88]	
	Protodioscin[88]	
Tannins	Tannic acid[89]	*S. trilobatum*
Terpenoids	Aromadendrene[90]	*S. stipulaceum*
	Caryophyllene[90]	

3.3 Bioactivity of the crude extract, fractions and isolated steroidal alkaloid (s)

3.3.1 Cytotoxicity

Cytotoxic activity was observed in both cancerous (A2780, Caco-2, DU-145, HepG2, MCF-7, MDA-MB-231, SH-SY5Y and SK-Br3) and non-cancerous (3T3-L1, C2C12, EA.hy.926 and SC-1) cell lines (Table 8). The crude extract and aqueous alkaloid-enriched fraction displayed noteworthy (<30 µg/ml) and moderate-to-low cytotoxicity (>30 µg/ml) after 72 h exposure (Table 8). In the majority of cell lines, cytotoxicity was induced within 24 h by the crude extract and aqueous alkaloid-enriched fraction, which either plateaued or decreased (1-to-2-fold increase) during the 72 h exposure. This suggests a mixture of concentration- and time-dependent cytotoxic effects, which showed a modicum of cell-specificity. A slightly lower IC_{50} was obtained in the SC-1 cell line after 24 h incubation compared to a 72 h incubation period, however, this may be within experimental error. Variable cytotoxicity towards the non-cancerous cell lines was observed, with IC_{50} values ranging from 3.88 to 93.41 µg/ml (24 h) and 2.79 to 91.18 µg/ml (72 h), respectively. The chloroform and ether fractions had negligible cytotoxic effects with IC_{50} values ≥100 µg/ml after 24 h, and ≥73.54 µg/ml after 72 h on all cell lines tested.

The aqueous alkaloid-enriched fraction had potent dose-dependent effect on the SH-SY5Y (IC_{50} = 17.21 µg/ml, Figure 15), Sk-Br3 (IC_{50} = 18.81 µg/ml, Figure 16) and HepG2 (IC_{50} = 20.66, Table 8) cancerous cell lines, and displayed low cytotoxicity towards the C2C12 (IC_{50} = 62.00 µg/ml, Figure 17, Table 8) non-cancerous cell line after 72 h exposure. The EA.hy926 cell line (Figure 18) was most susceptible to the aqueous fraction with an IC_{50} of 9.35 µg/ml after 72 h.

The crude extract and aqueous alkaloid-enriched fraction induced similar cytotoxic profiles across all cell lines. A small concentration difference was noted when eliciting a 90% decrease in cell density and compared to a 0% decrease, which highlights a narrow cytotoxicity range. This narrow cytotoxic range led to ambiguity when predicting the IC_{50} in several cell lines.

Literature is scarce with regards to *S. aculeastrum* cytotoxicity. A previous study by Koduru *et al.*[56] indicated that a methanolic fruit extract also had a narrow range between non-cytotoxic and toxic concentrations. In contrast, the greatest cytotoxic effect was observed

against the MCF-7 cell line (when compared to HeLa cervix adenocarcinoma and HT29 colon adenocarcinoma cell lines) with an IC_{50} of 17.8 µg/ml. The slightly higher IC_{50} (10.14 µg/ml) calculated during the present study may be dependent on geographical location, seasonal variation or extraction procedure.[89] An ethanol extract from *S. nigrum* fruits, also known to possess steroidal alkaloids such as solamargine, was shown to induce autophagy and apoptosis in HepG2 hepatocarcinoma cell line.[90] The latter was evident with increases in p-JNK, Bax, release of cytochrome c and the activation of caspase-3.[90] The results illustrate apoptosis as a possible mechanism by which *Solanum spp.* extracts elicit anticancer activity.

According to the criterion of the National Cancer Institute, a plant extract or fraction with an IC_{50} ≤20 µg/ml is regarded as a favourable anticancer agent.[91] The latter indicates that the crude extract and aqueous fraction possess notable anticancer activity towards the HepG2, SH-SY5Y and SK-Br3 cell lines and should be considered for further development, although the non-cancerous cytotoxicity may prove difficult to overcome. In contrast, the ether and chloroform fractions were inactive across all cell lines.

The increase in cell density observed at lower concentrations of the ether and chloroform alkaloid-enriched fractions may be due to a hormetic effect. Hormesis refers to a biphasic dose response where low doses of a cytotoxic agent cause cell proliferation while higher concentrations cause growth inhibition. Agents elicit this effect through cell survival as well as oxidative stress response pathways (including MAPK/ERK1/2 and PI3K/AKT) and cause 30 to 60% cell proliferation relative to the negative control.[92]

Table 8: Cytotoxicity of the crude extract and alkaloid-enriched fractions as described by their IC_{50} values in a panel of cancerous and non-cancerous cell lines. Values in bold indicate extracts with noteworthy activity at 72 h.

	IC_{50} ± SEM											
Extract/fraction[a]	**Cancerous cell lines**								**Non-cancerous cell lines**			
	A2780	Caco-2	DU-145	HepG2	MCF-7	MDA-MB-231	SH-SY5Y	SK-Br3	3T3-L1	C2C12	EA.hy.926	SC-1
Crude 24 h	34.73 ± 1.07	36.46 ± 1.20	74.33 ± 1.14	**9.44 ± 1.11**	44.35 ± 1.06	26.87 ± *	**19.10 ± 1.07**	**33.25 ± 1.10**	37.24 ± 1.34	**93.41 ± 1.08**	3.88 ± 1.07	28.73 ± 1.09
Crude 72 h	32.88 ± *	24.40 ± 1.13	47.11 ± 1.18	**7.04 ± 1.08**	27.94 ± 1.11	24.00 ± *	**12.97 ± 1.07**	**20.11 ± 1.08**	19.55 ± 1.23	**91.18 ± 1.13**	2.79 ±1.55	23.07 ± 1.10
Chloroform 24 h	> 100	> 100	> 100	> 100	> 100	> 100	> 100	> 100	> 100	> 100	> 100	> 100
Chloroform 72 h	> 100	> 100	> 100	> 100	> 100	> 100	> 100	> 100	> 100	> 100	> 100	> 100
Ether 24 h	> 100	> 100	> 100	> 100	> 100	> 100	> 100	> 100	> 100	> 100	> 100	> 100
Ether 72 h	> 100	> 100	> 100	> 100	73.54 ± 1.19	> 100	> 100	> 100	> 100	> 100	> 100	> 100
Aqueous 24 h	31.45 ± *	50.37 ± 1.26	46.53 ± 1.21	**40.02 ± 1.08**	31.91 ± 1.06	28.05 ± *	**29.11 ± ***	**29.24 ± ***	21.95 ± 1.50	**> 100**	16.45 ± 1.06	**19.89 ± 1.09**
Aqueous 72 h	29.81 ± *	25.21 ± 1.12	34.08 ± *	**20.66 ± 1.10**	25.49 ± 1.13	26.11 ± *	**17.21 ± 1.15**	**18.81 ± 1.14**	12.89 ± 1.23	**62.00 ± 1.22**	9.35 ± 1.08	**21.10 ± 1.08**
Anticancer agent[b]												
Verapamil 24 h	93.48 ± 1.05	> 100	> 100	18.72 ± 1.08	> 100	> 100	> 100	> 100	> 100	> 100	31.55 ± 1.12	> 100
Verapamil 72 h	65.75 ± 1.06	> 100	> 100	8.34 ± 1.08	46.76 ± 1.14	47.5 ± 1.09	> 100	41.92 ± 1.09	79.22 ± 1.21	> 100	5.69 ± 1.11	60.01 ± 1.16

*: Ambiguity in data points (GraphPad 5.0 software could not predict SEM due to steepness of dose-response curve)
a: presented in µg/ml
b: presented in µM

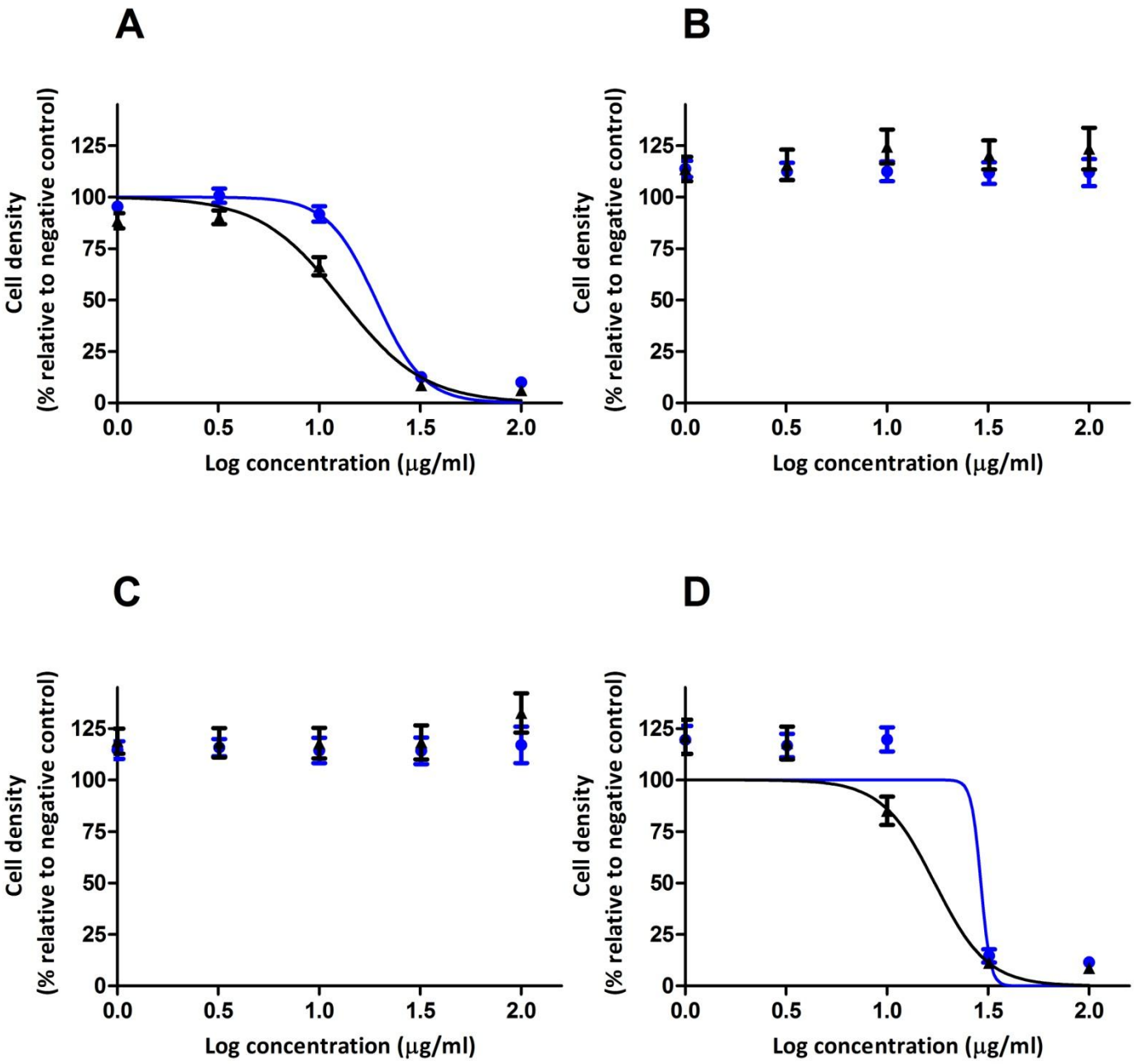

Figure 15: The effect on cell density in the SH-SY5Y neuroblastoma cell line when exposed to the A) crude extract, B) ether fraction, C) chloroform fraction and D) aqueous fraction. Blue line: 24 h exposure and black line: 72 h exposure.

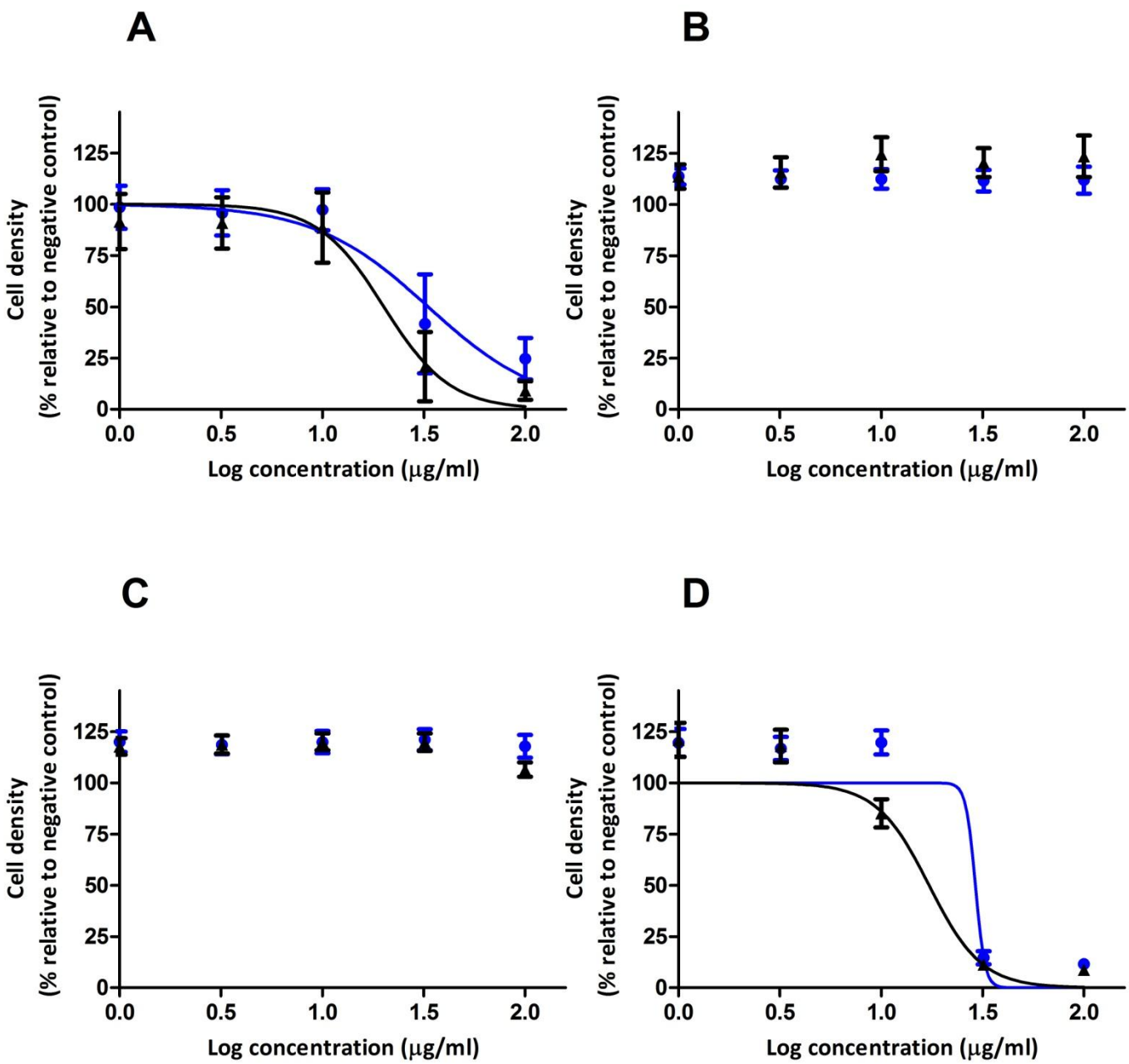

Figure 16: The effect on cell density in the SK-Br3 breast carcinoma cell line when exposed to the A) crude extract, B) ether fraction, C) chloroform fraction and D) aqueous fraction. Blue line: 24 h exposure and black line: 72 h exposure.

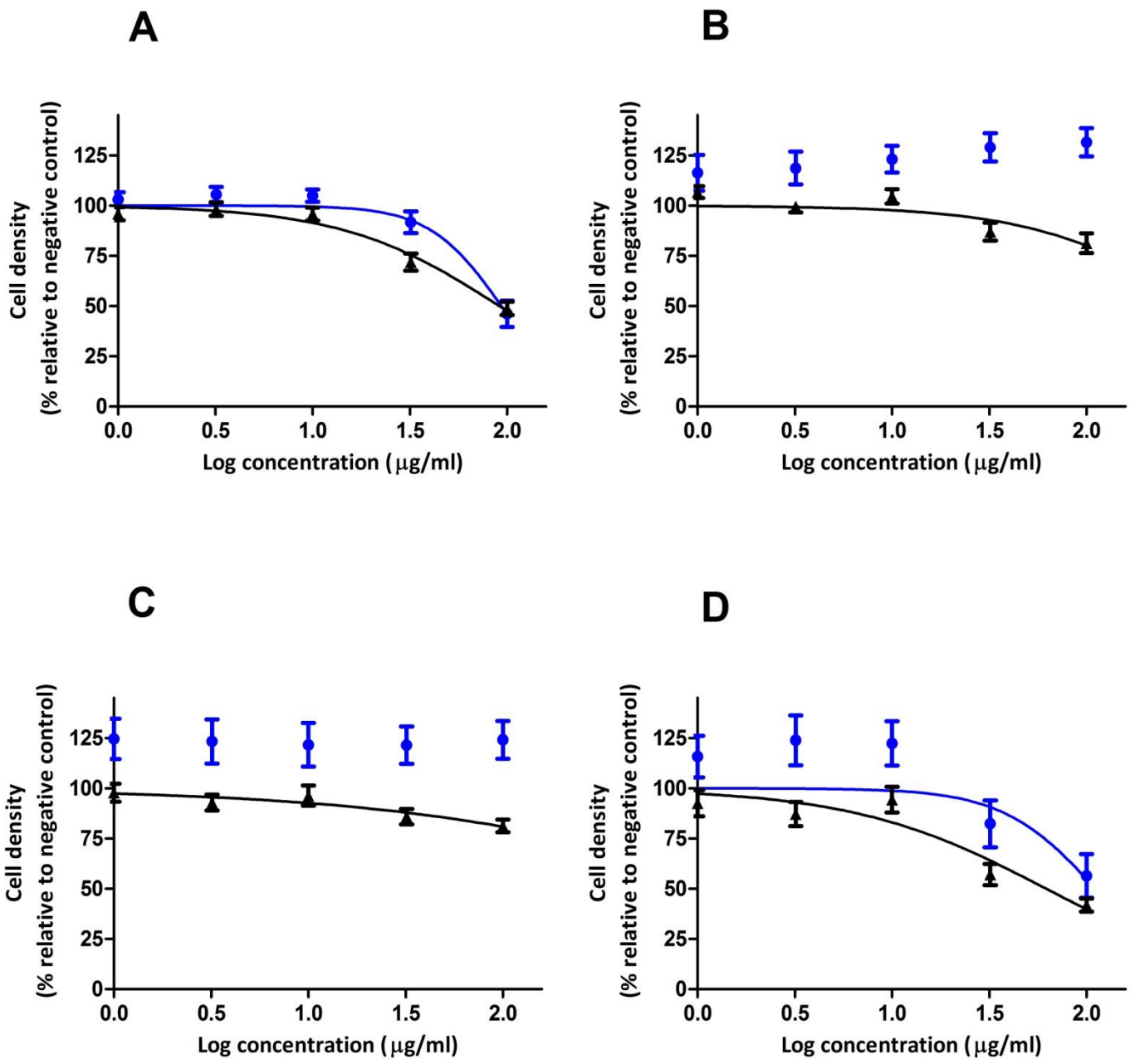

Figure 17: The effect on cell density in the C2C12 myoblast cell line when exposed to the A) crude extract, B) ether fraction, C) chloroform fraction and D) aqueous fraction. Blue line: 24 h exposure and black line: 72 h exposure.

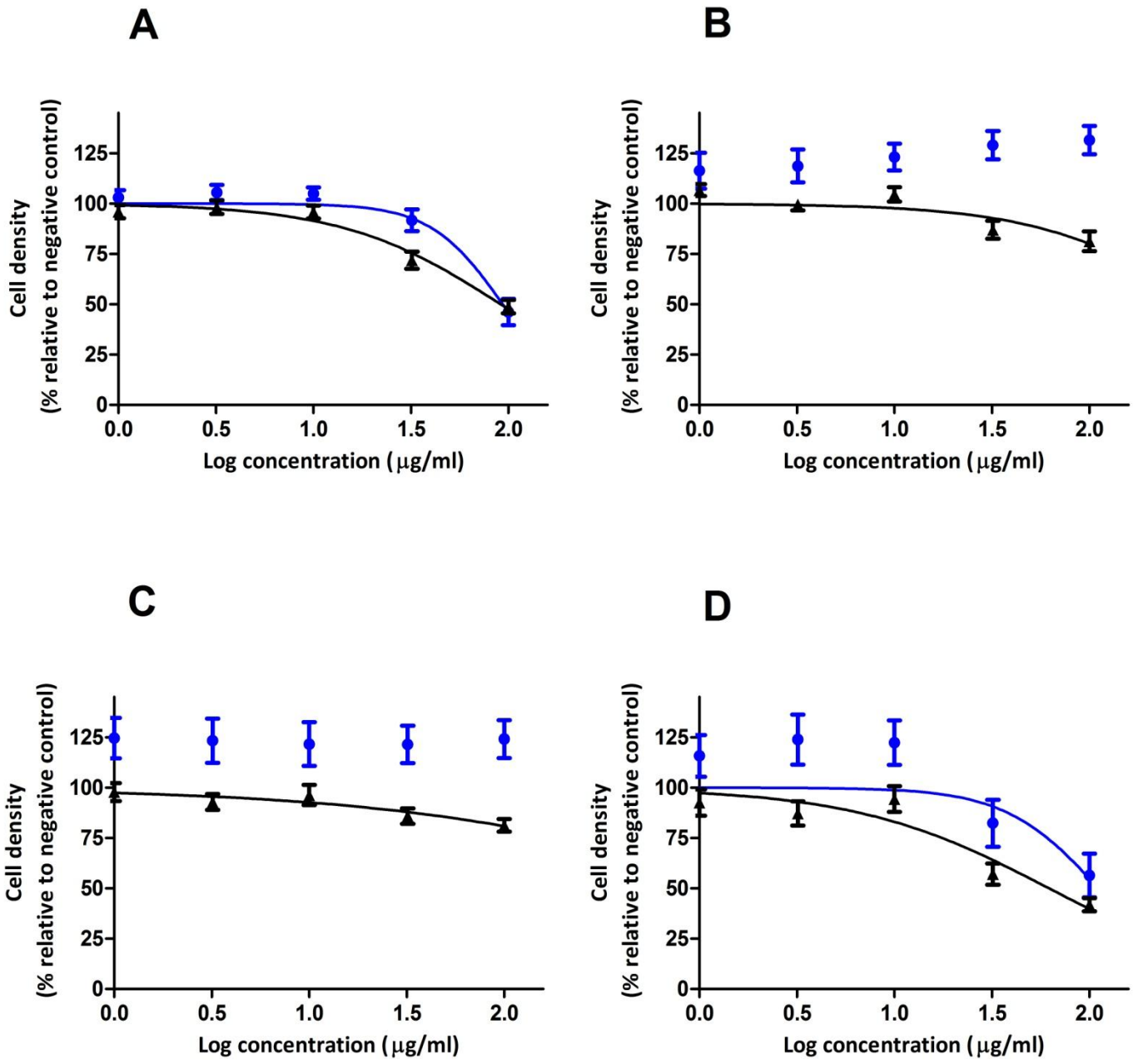

Figure 18: The effect on cell density in the EA.hy926 cell line when exposed to the A) crude extract, B) ether fraction, C) chloroform fraction and D) aqueous fraction. Blue line: 24 h exposure and black line: 72 h exposure.

After HPLC fractionation of the aqueous fraction, bioactivity screening was done using the SRB assay, to assist in isolation of the bioactive component(s). F-10 and F-11 were found to be the most active and had potent cytotoxicity at 50 µg/ml towards the SK-Br3 cell line with a cell density reduction of 91.06% and 91.72%, respectively. Sub-fractions 1 to 9 (F-1 to F-9) elicited a medium to low cytotoxic effect (Figure 19).

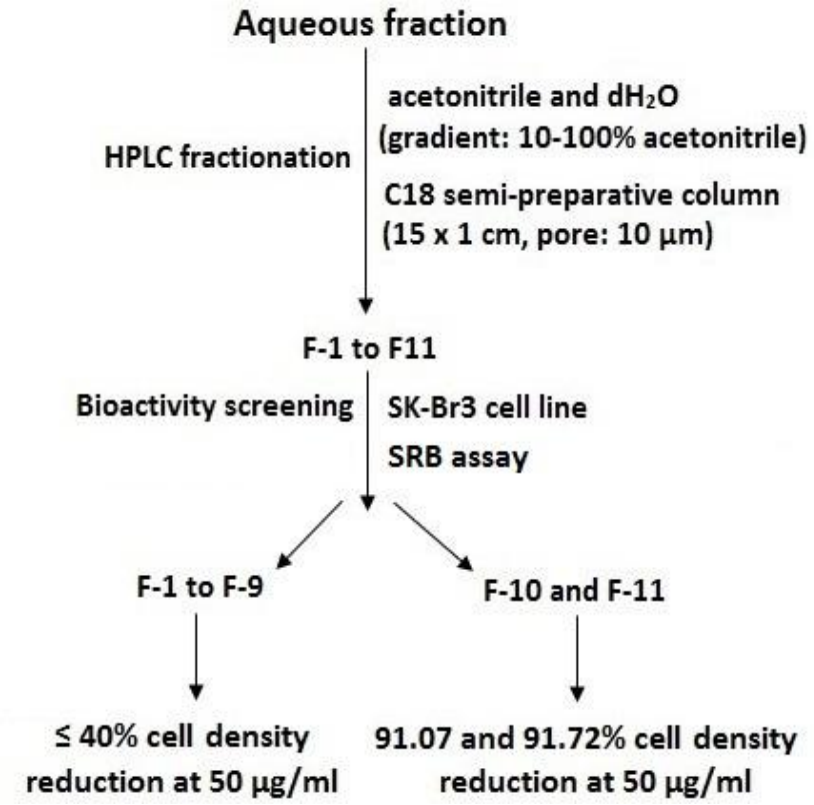

Figure 19: Flow diagram indicating the HPLC fractionation process for the aqueous fraction and subsequent bioactivity screening.

As previously stated, steroidal alkaloids are the proposed anticancer components of *S. aculeastrum*.[59,60] This is supported by the findings in the current study where bioactivity-guided fractionation and isolation procedures identified solamargine as the bioactive constituent. Solamargine induced a dose-dependent cytotoxic effect in both SH-SY5Y and SK-Br3 cell lines with IC_{50} values of 15.62 µM (13.54 µg/ml) and 18.59 µM (16.12 µg/ml) after 72 h incubation, respectively (Table 9). Munari *et al.*[67] evaluated the antiproliferative potential of solamargine from *S. lycocarpum* against murine melanoma (B16F10), colon carcinoma (HT29), breast adenocarcinoma (MCF-7), cervical adenocarcinoma (HeLa), hepatocarcinoma (HepG2), glioblastoma cells (MO59J, U343, U251). Growth inhibition was

observed across all cell lines with IC_{50}'s ranging from 5.28 to 21.03 µM (4.58 to 18.23 µg/ml).[67]

The IC_{50} of solamargine was slightly lower than the aqueous fraction in the cancerous cell lines, by approximately ~3.20 µg/ml. Although this may suggest a greater cytotoxic effect when used as a singular compound instead of an extract mixture, this difference may be regarded as insignificant. However, in the non-cancerous cell lines (Table 9) solamargine presented with higher cytotoxicity, illustrating an increased cytotoxicity upon isolation. Due to a complex phytochemical matrix, it is possible that interactions alter the cytotoxic potential of an extracts or fractions compared to an isolated compound.[93] Antagonistic interactions in the aqueous fraction as well as cellular variation may account for the increased toxicity observed.[93,94]

Kuo *et al.*[95] reported changes in cellular structure induced by solamargine, as well as chromatin condensation, DNA fragmentation and an increased sub-G1 peak in hepatoma (Hep3B) cells, suggesting a pro-apoptotic effect.[95] Apoptosis was further illustrated by Shiu *et al.*[63], with upregulation of Fas receptors (Fas), tumour necrosis factor receptor I (TNFR I), Fas-associated death domain (FaDD) and TNFR-I-associated death domain (TRADD) in breast cancer cells. This lead to the initiation of intrinsic and extrinsic apoptotic pathways mediated by cytochrome c release, as well as caspase-3, -8 and -9 activation in breast cancer cells.[63] These results correlate with the pro-apoptotic activity of numerous *Solanum* spp.[63], which may be the anticancer mechanism elicited in the present study.

In contrast, the IC_{50} of solasonine was greater than the highest concentration tested (56.63 µM or 50 µg/ml) in both cancerous and non-cancerous cell lines (Table 9), suggesting a lack of bioactivity. Solasonine, isolated from *S. crinitum* (Lam), displayed low cytotoxic potential against the K562 leukaemia and Ehrlich carcinoma cell lines, yielding IC_{50} values of 76.90 µM (67.90 µg/ml) and 74.20 µM (65.65 µg/ml).[53] The aglycone, solasodine, from *S. crinitum* was shown to possess low cytotoxicity when compared to solasonine, suggesting that the additional sugar moiety in solasonine's structure enhances growth inhibition.[53] Other investigations have shown that solasonine possesses notable cytotoxicity with IC_{50}'s ≤30 µM, which indicates that the compound has variable cytotoxicity.[67,74] Slight conformational changes in solasonine's molecular structure could account for the significant cytotoxicity results.[96]

Table 9: Cytotoxicity of solamargine and solasonine as described by their IC_{50} values in a panel of cancerous and non-cancerous cell lines.

Compound	IC_{50} (µM) ± SEM			
	SH-SY5Y	SK-Br3	C2C12	EA.hy926
Solamargine	15.62 ± 1.45	18.59 ± 1.13	20.25 ± 1.08	8.30 ± 1.12
Solasonine	> 56.63	> 56.63	> 56.63	> 56.63

Differences in cytotoxicity between studies involving solamargine and solasonine could also be due to assay differences, cell line origin, cell line passage number and the software used to calculate IC_{50}'s. The latter leads to high variability in *in vitro* studies.[97]

Although notable anticancer activity was present after exposure to the crude extract, aqueous alkaloid-enriched fraction and solamargine, major decreases in cell density were also noted for the non-cancerous cell lines. Similar results were observed by Munari *et al.*[67], where an ethanol extract from *S. lycocarpum* fruits, as well as solamargine, had an antiproliferative effect towards the human (GM07492A, IC_{50}'s: 25.39 and 30.74 µM) and Chinese hamster lung (V79, IC_{50}'s: 37.60 and 19.31 µM) fibroblast cell lines.[67] This cytotoxicity indicates that the crude extract, aqueous alkaloid-enriched fraction and solamargine were non-selective towards cancerous cells and would therefore not be ideal candidates for further drug development, unless structural alterations were carried out to improve its cancer-selectivity.

3.3.2. P-glycoprotein inhibition

The crude extract and the aqueous alkaloid-enriched fraction had potent dose-dependent P-gp inhibition of 2.87 to 21.2-fold at 100 µg/ml for the various cell lines (Figure 20A/D to 23A/D). The chloroform and ether fraction elicited poor P-gp inhibition of 1.12 to 1.63-fold at the highest concentration tested (Figure 20B/C to 23B/C).

The ether, chloroform and aqueous alkaloid-enriched fractions showed the greatest inhibitory potential towards the SH-SY5Y cell line (Figure 20B to 20D) with 1.26, 1.64 and 21.21-fold at 100 µg/ml, respectively. The fractions exhibited the lowest activity towards the C2C12 cell line with inhibitory values of 1.13, 1.27 and 2.87-fold at 100 µg/ml, respectively. The aqueous fraction (Figures 20D to 23D) displayed inhibitory activity across all cell lines, with values of 2.82 to 21.21-fold at 100 µg/ml ($p < 0.001$). The amount of inhibition exhibited by the aqueous fraction was similar to the crude extract, which had P-gp inhibitory values of 5.89 to 18.88-fold at 100 µg/ml ($p < 0.001$) against all tested cell lines.

Significant ($p < 0.05$ and 0.001), but low P-gp inhibition was observed for the chloroform fraction against in the SH-SY5Y cancerous cell line (Figure 20C) with an inhibitory value of 1.64–fold, at 100 µg/ml. A dose-dependent effect was not as apparent as significance ($p < 0.05$ and 0.001) was noted for four out of the five concentrations tested (Figure 20C). The ether fraction displayed low but significant ($p < 0.01$) inhibition in the EA.hy926 cell line (Figure 23B) of 1.47-fold at 100 µg/ml. No significant activity was noted for the other cell lines. As the aqueous alkaloid-enriched fraction exhibited the greatest activity, sub-fractionation was focussed on this fraction.

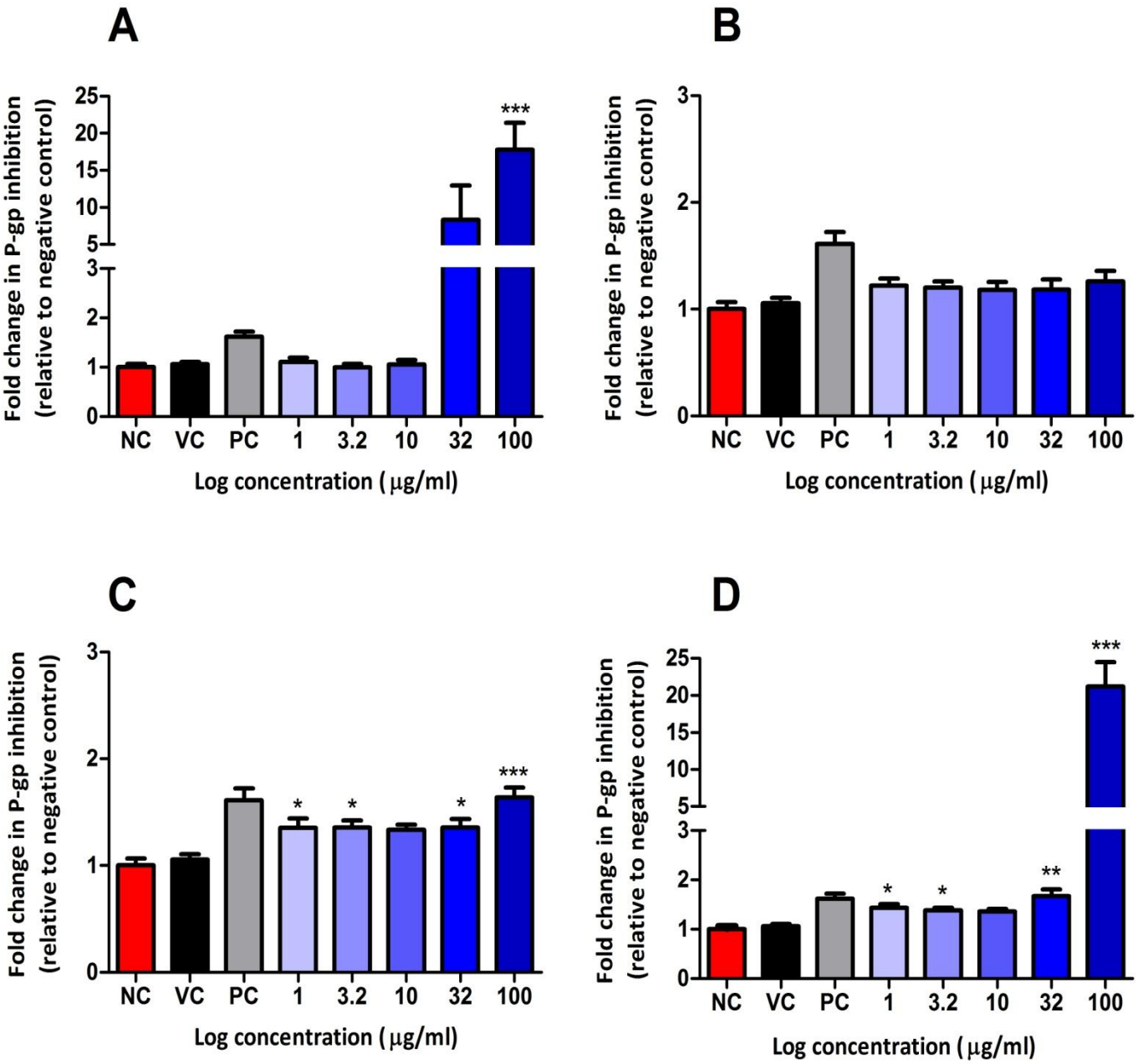

Figure 20: P-gp inhibitory potential in the SH-SY5Y neuroblastoma cell line when exposed to the A) crude extract, B) ether fraction, C) chloroform fraction and D) aqueous fraction. PC: verapamil (1 µM). * $p < 0.05$, ** $p < 0.01$, *** $p < 0.001$.

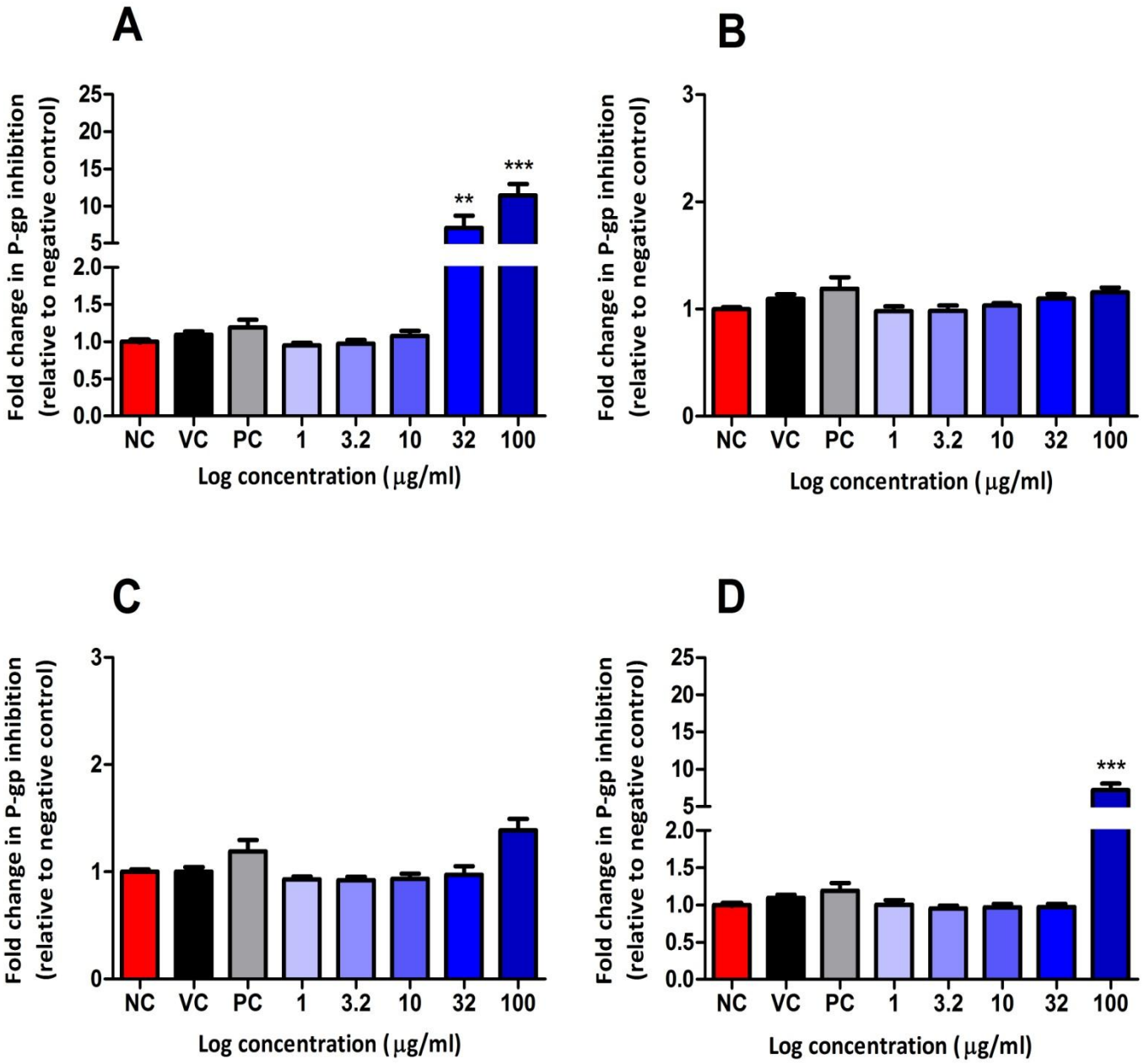

Figure 21: P-gp inhibitory potential in the SK-br3 breast carcinoma cell line when exposed to the A) crude extract, B) ether fraction, C) chloroform fraction and D) aqueous fraction. PC: verapamil (1 µM). ** $p < 0.01$, *** $p < 0.001$.

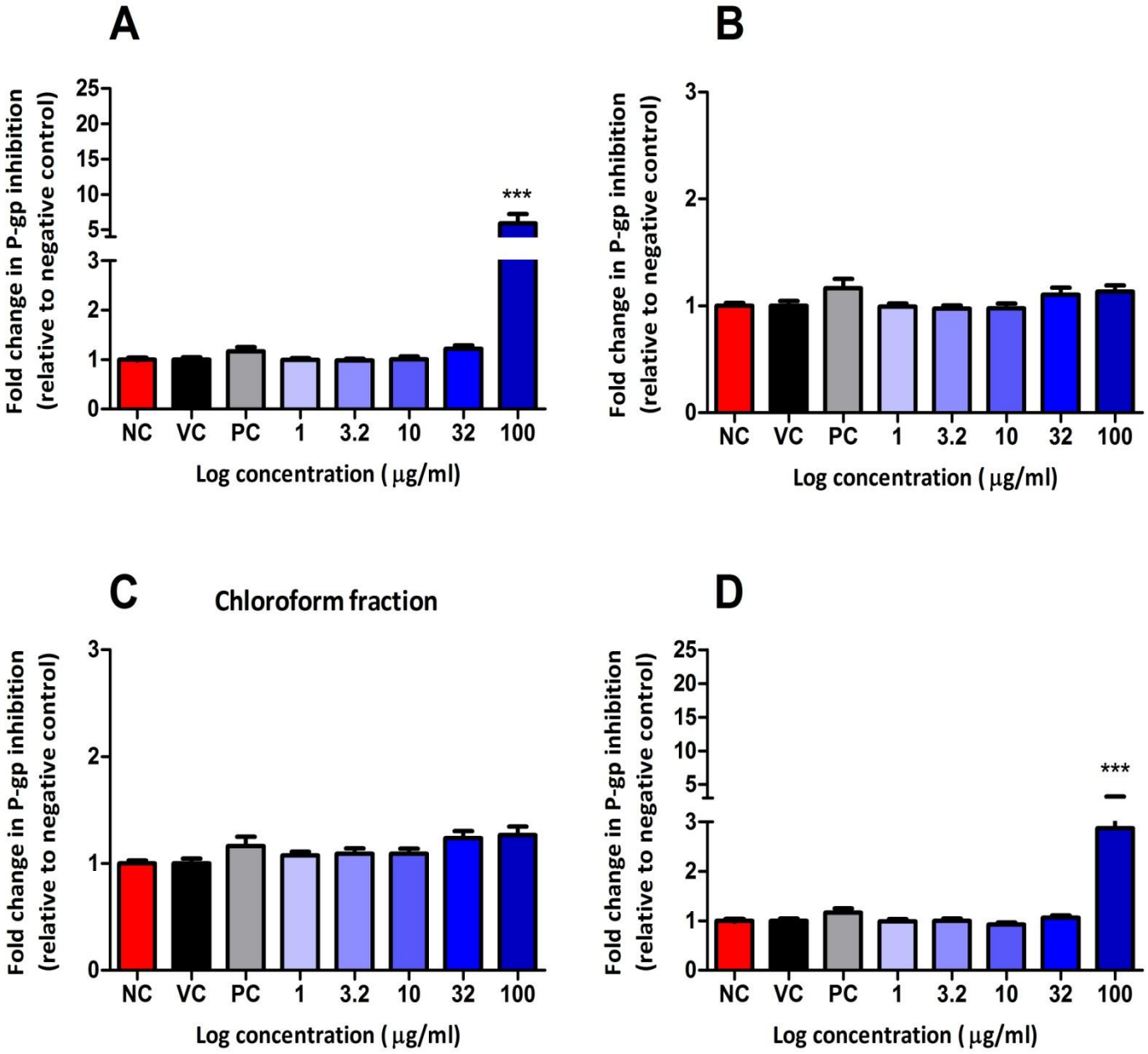

Figure 22: P-gp inhibitory potential in the C2C12 myoblast cell line when exposed to the A) crude extract, B) ether fraction, C) chloroform fraction and D) aqueous fraction. PC: verapamil (1 µM). *** $p < 0.001$.

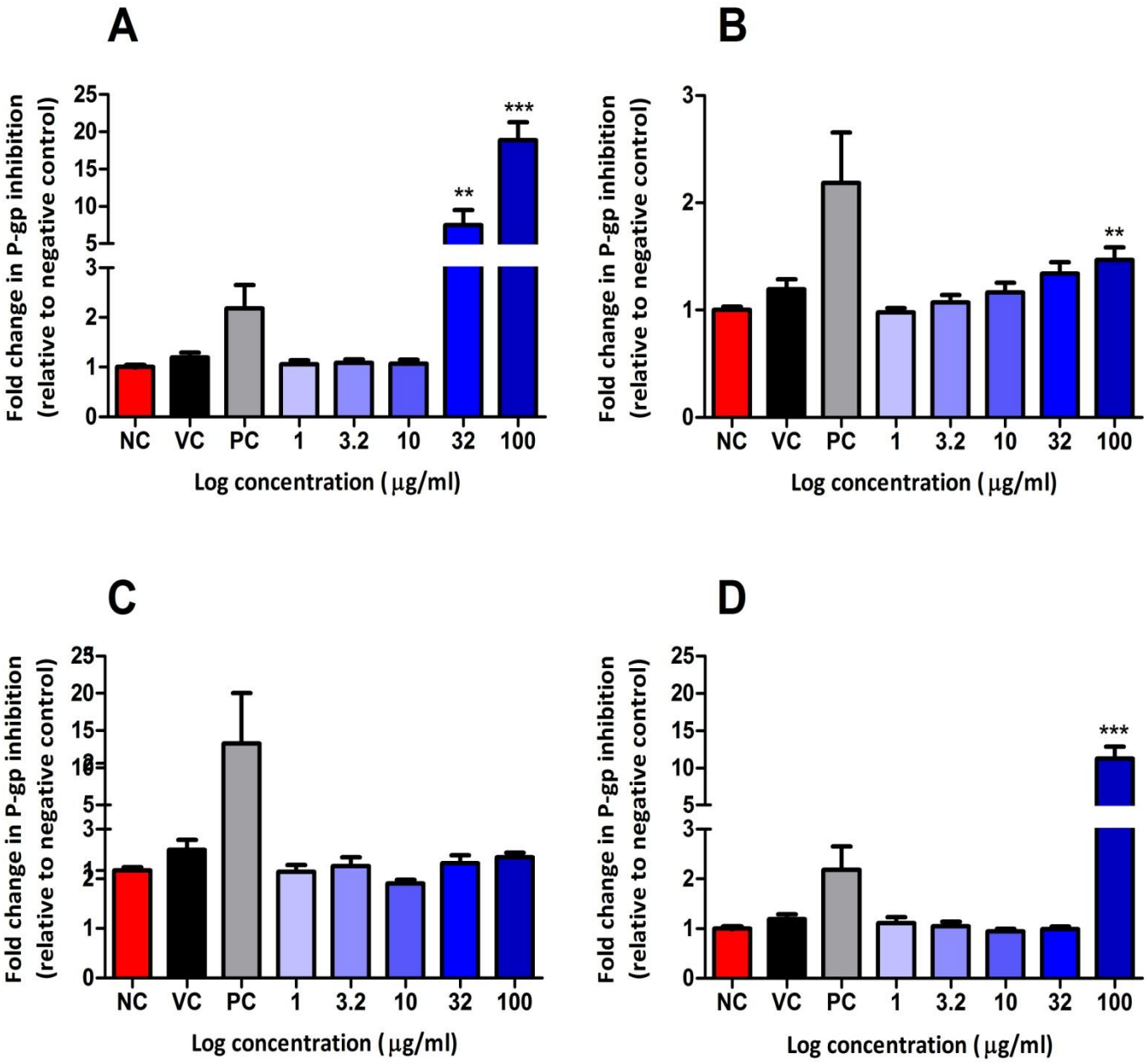

Figure 23: P-gp inhibitory potential in the EA.hy926 endothelial hybrid cell line when exposed to the A) crude extract, B) ether fraction, C) chloroform fraction and D) aqueous fraction. PC: verapamil (1 µM). ** $p < 0.01$, *** $p < 0.001$.

Junyaprasert *et al.*[98] evaluated the P-gp inhibitory potential of extracts made from various plants in Thailand using HPLC and a rhodamine-123 assay. An ethanol extract from *S. trilobatum* was found to induce significant ($p < 0.05$) inhibition when compared to verapamil.[98] However, the inhibitory effect was only evident at 300 µg/ml, which falls into the cytotoxic concentration range. This particular species is also known to possess high levels of steroidal alkaloids including solamargine and solasodine which are known to disrupt P-gp activity.[99]

In the present study, the isolated steroidal alkaloids yielded similar results when compared to the cytotoxic effect. Solamargine showed a significant ($p < 0.05$ and $p < 0.001$) dose-dependent P-gp inhibition in the SH-SY5Y cancerous cell line (Figure 24A) with 5.07-fold activity at 36.9 µM (32 µg/ml) and 9.10-fold activity at 57.7 µM (50 µg/ml). However, the effect was 3.95-fold less when compared to the aqueous alkaloid-enriched fraction (13.05-fold) at 50 µg/ml (Figure 24A). Solamargine elicited greater P-gp inhibition towards the EA.hy926 (13.81-fold) non-cancerous cell line when compared to the SH-SY5Y (9.05-fold) cancerous cell line (Figure 24C) at 57.70 µM (50 µg/ml). Solasonine did not inhibit P-gp activity at any of the concentrations tested. To the knowledge of the author, this study is the first to evaluate the P-gp inhibitory potential of solasonine. The P-gp results of the active fractions and solamargine further illustrate the non-selectivity towards cancerous cells.

Solamargine induced a dose-dependent decrease in MDR1 mRNA expression in the MDR K562/A02 leukaemia cell line.[100] MDR1 encodes P-gp and is therefore linked to the transporter expression.[101] The latter was further illustrated by flow cytometry, where reductions in P-gp expression of 41.7% at 7.50 µM (6.50 µg/ml), 38.8% at 5.00 µM (4.34 µg/ml) and 11.2% at 3.75 µM (3.25 µg/ml) after a 12 h exposure period was observed.[99] Western blot analysis showed a decrease in the Bcl-2 anti-apoptotic protein and increases in the Bax pro-apoptotic protein. Immunofluorescence also revealed that solamargine disrupted the cellular cytoskeleton and caused decreases in actin expression.[100] Both apoptosis as well as P-gp expression have been linked to the cellular structure and actin in MDR cells.[100] The study suggests that the apoptotic mechanism of action elicited by solamargine is linked to a down regulation of MDR1 and P-glycoprotein.[100]

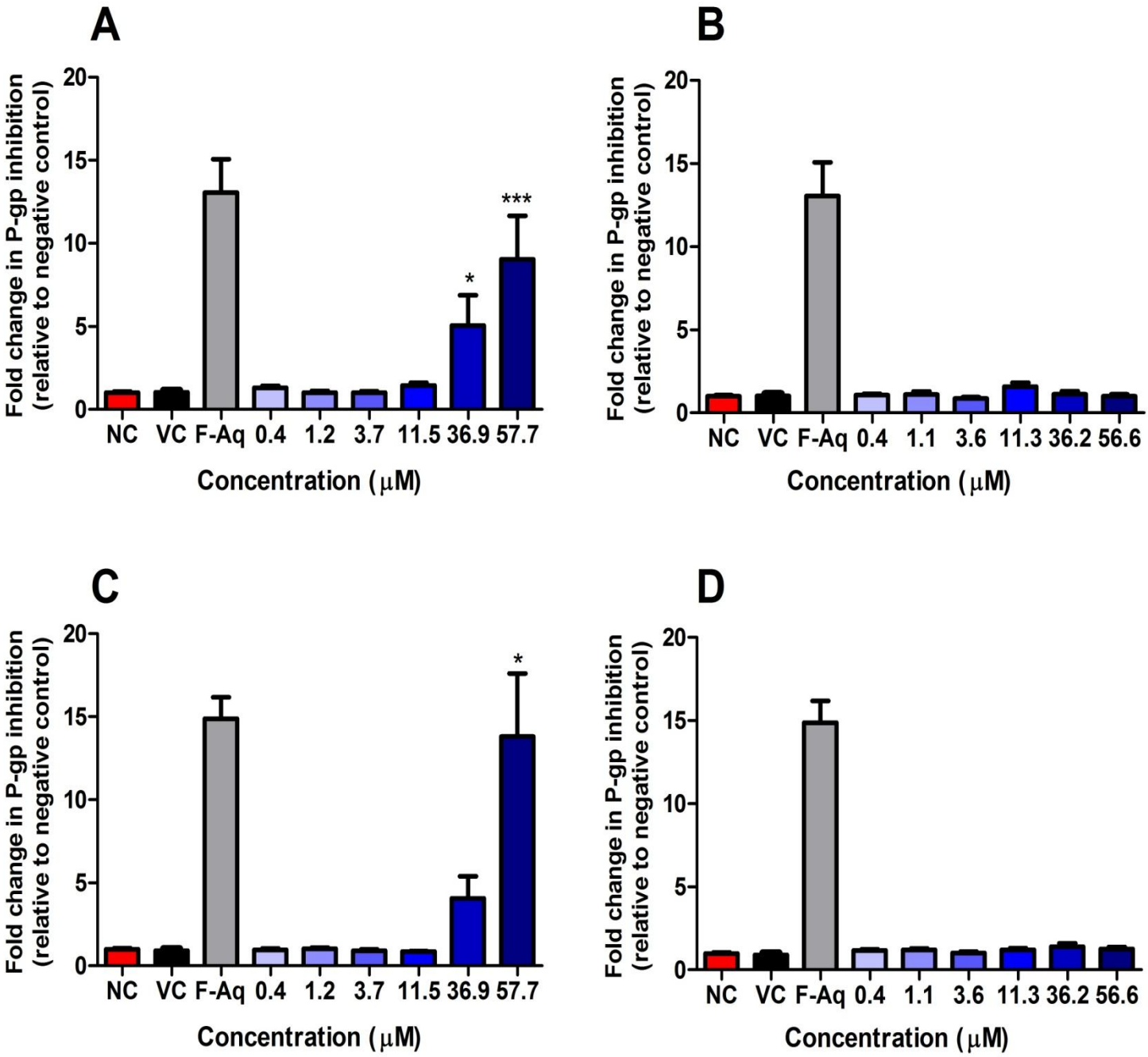

Figure 24: P-gp inhibitory potential of solamargine (A, C) and solasonine (B, D) against the SH-SY5Y neuroblastoma (A,B) and EA.hy926 endothelial hybrid cell lines (C, D). * $p < 0.05$, *** $p < 0.001$.

Other steroidal alkaloids such as tomatidine and cyclopamine have also been shown to possess potent P-gp inhibition.[102] Another proposed mechanism is that steroidal alkaloids act as non-competitive inhibitors. P-gp is known to actively transport compounds across the cellular membrane via two distinct sites (H and R) in the transmembrane region which are

responsible for drug binding and interactions.[103] Steroidal alkaloids are miniscule compounds, possess nitrogen and have a planar structure which allows rapid diffusion into cells. Thus interactions between the isolated compounds and these regions may occur.[103]

3.3.3 Synergistic potential of the aqueous alkaloid-enriched fraction and solamargine with doxorubicin

During experimentation, it was observed that the IC_{50} values were slightly changed during the study period. As cells of different passages were utilised, it appeared that a phenotypic shift was occurring. Due to the latter, cytotoxicity re-evaluation was done for the aqueous fraction prior the synergistic assay. Slight shifts of 2.05 and 0.89 µg/ml were observed against the EA.hy926 and SK-Br3 cell lines whereas a larger variation of 48.30 and 9.29 µg/ml in cytotoxicity was noted for the C2C12 and SH-SY5Y cell lines.

A dose-dependent decrease in cell density was observed when all four cell lines were exposed to doxorubicin. The most pronounced effect was observed in the SH-SY5Y cell line with an IC_{50} of 56.60 nM after 72 h exposure. A greater cytotoxic effect towards cancerous cells was seen compared to non-cancerous cells (Table 10).

No synergistic interaction was detected in any of the tested cell lines after exposure to the aqueous alkaloid-enriched fraction and solamargine in combination with doxorubicin (Table 10). An additive effect was observed in the SH-SY5Y cell line when exposed to both combinations (aqueous alkaloid-enriched fraction FIX value = 0.71; solamargine FIX value = 0.51). In contrast, the combination elicited an antagonistic effect in the C2C12 cell line (aqueous alkaloid-enriched fraction FIX value = 2.10; solamargine FIX value = 2.53). Additive effects were observed in the SK-Br-3 and EA.hy926 cell lines when exposed to the combination with solamargine (FIX value = 0.66) and the aqueous alkaloid-enriched fraction (FIX value = 0.94), respectively. Indifferent effects were noted when the SK-Br-3 and EA.hy926 cell lines were exposed to the combination with the aqueous alkaloid-enriched fraction and solamargine, respectively. (FIX values: > 1 but < 2).

Table 10: Synergistic potential of solamargine and the aqueous fraction as described by their FIX values in a panel of cancerous and non-cancerous cell lines.

Cell type	**Cancerous**				**Non-cancerous**			
Cell line	**SH-SY5Y**		**SK-Br3**		**C2C12**		**EA.hy926**	
Compound/Fraction	**Solamargine**	**Aqueous fraction**	**Solamargine**	**Aqueous fraction**	**Solamargine**	**Aqueous fraction**	**Solamargine**	**Aqueous fraction**
IC_{50} of (A) [IC_{50} sample + doxorubicin (µM or µg/ml)]	3.4	7.39	4.3	11.18	30.77	15.7	5.5	2.62
IC_{50} of (B) [IC_{50} doxorubicin + sample (nM)]	16.27	24.22	40.83	47.48	149.9	140.7	213.4	220
IC_{50} (A) [Solamargine (µM) or aqueous alone (µg/ml)]	15.62	26.5	18.59	19.7	20.25	13.7	8.3	7.3
IC_{50} (B) [doxorubicin alone (nM)]	56.6	56.6	94.1	94.1	148.5	148.5	381.6	381.6
FIC (A)	0.22	0.28	0.23	0.57	1.52	1.15	0.66	0.36
FIC (B)	0.29	0.43	0.43	0.5	1.01	0.95	0.56	0.58
FIX value	**0.51**	**0.71**	**0.66**	**1.07**	**2.53**	**2.1**	**1.22**	**0.94**
Result	**Additive effect**	**Additive effect**	**Additive effect**	**Indifferent effect**	**Antagonistic effect**	**Antagonistic effect**	**Indifferent effect**	**Additive effect**

Additive interactions involve the targeting of the same pathway or effect the same target directly or indirectly.[104] Induction of apoptosis is a proposed death pathway for both doxorubicin and the samples. Simultaneous exposure of the combination could thus potentiate the apoptotic effect leading to an additive cytotoxic effect. Conversely an antagonistic interaction involves conflicting mechanisms on the same pathway, which includes binding at the same site (interference) or contradicting effects at different targets.[104] The latter two mechanisms may be why antagonism was noted in the current study. Tai *et al.*[105] investigated combinations of an aqueous extract of *S. nigrum* with various anticancer agents including docetaxel, doxorubicin, 5-fluorouracil and cisplatin against two colon cancer cell lines (DLD-1 and H29).[105] The extract acted synergistically in both cell lines when combined with all anticancer agents. The chemotherapeutics used by the author are known to induce apoptosis via a caspase-3 death pathway. Extract combination was found to lead to the activation of the latter and autophagy through accumulation of death marker LC-3. They attributed enhancement in cytotoxicity to the activation of multiple pathways and potentiation of the caspase-3 apoptotic pathway.[105] A methanol extract from *S. nigrum* was also shown to increase doxorubicin's cytotoxicity in a synergistic manner against the T47D breast carcinoma cells when combined at 4:4, 6:4, 18:1.5 and 18:4 (extract (µg/ml):doxorubicin (nM)). However, antagonism was also observed against T47D cells with FIX values >2, at combinations of 6:1.5, 6:2, 12:2 and 6:6.[106] Activity by *S. nigrum* has been attributed to major phytochemical constituents such as steroidal alkaloid solamargine.[107] Although no studies other than the current study have evaluated the synergistic potential of purified solamargine and doxorubicin, the phytochemical is known to enhance the antitumor effects of many chemotherapeutics.[105]

Liang *et al.*[108] evaluated the effect of solamargine in combination with cisplatin on the cisplatin-resistant A549 lung adenocarcinoma cell line.[108] Cisplatin is known to induce apoptosis in cancerous cells by activating caspase-3 which further regulates caspase-8 and -9 via death receptors.[108] From their results it was evident that cisplatin alone increased activities of caspase-3, -9 as well as -8 by 3.7, 2.6 and 3.0-fold, respectively. Combination with solamargine yielded greater fold change values of 6.9, 3.9 and 4.6.[108] Solamargine has been shown to down regulate HER-2/neu expression in the ZR-75-1 breast cancer cells as well as enhance the efficacy of commonly used anticancer agents (5-fluorouracil,

methotrexate and cisplatin) for treatment.[109] Overexpression of HER-2/neu receptor on breast cancer cells often leads to treatment failure and drug resistance.[109] Findings from the above studies indicate show that solamargine has the potential to potentiate the anticancer effects of known chemotherapeutics and elicit MDR reversal. Furthermore, down regulation of HER-2/neu receptors illustrates another mechanism by which *Solanum* spp. extracts possessing solamargine (such as the berries of *S. aculeastrum* in this study) may elicit an ethnomedicinal effect.

Friedman *et al.*[110] illustrated the effect of combining steroidal alkaloids chaconine and solanine against a panel of cancerous cell lines (including the HepG2 hepatocarcinoma and AGS gastric cancer).[110] Synergism was observed in the HepG2 cell line at combinations of 1:9, 3:7 and 1:1 while antagonism was noted at 9:1. For the AGS cell line additive effects were noted at 1:9, 3:7, 1:1 and 9:1, while antagonism was noted at 7:3.[110] The variations in results imply that molecular interactions are both cell line and combination specific.

P-gp inhibitors have also been shown to enhance the anticancer activity of known chemotherapeutics against resistant cell lines.[111] An MDR modulating drug known as 1416, which is an analogue of verapamil, was reported to significantly increase the cytotoxic effect of verapamil towards the resistant K562 cell line but not in the susceptible equivalent.[113] The effect of 1416 was further illustrated by an accumulation of rhodamine-123 in P-gp over expressed MDR K562 cells.[111] Compounds including limonin and hesperidin, isolated from two *Citrus* species have been shown to cause dose-dependent P-gp inhibition in a MDR CEM/ADR500 leukemia cell line.[112] Following addition of 20 µM limonin, the doxorubicin resistant Caco-2 cell line was made susceptible by increasing doxorubicins cytotoxicity by 2.98-fold, which illustrated MDR reversal.[112]

From the results of the present study, solamargine was shown to enhance the cytotoxic effect of doxorubicin in both SH-SY5Y as well as the SK-Br3 cancerous (possess HER-2/neu receptors) cell lines.[113] This potentiated response was not observed in non-cancerous cell lines, indicating selectivity and suggesting that solamargine may be effective in improving treatment regimens for both brain and breast cancers. The variable combination effects observed by Friedman *et al.*[110] may explain differences across cell lines when combining the aqueous fraction or solamargine with doxorubicin in the current study. Although inhibition

of P-gp activity has been shown to enhance efficacy against MDR cancers, studies reveal that no significant differences in P-gp activity are present in susceptible cell lines.[110] In the present study, P-gp inhibition was only evident at cytotoxic concentrations. Thus enhancement of doxorubicin cytotoxic effects through P-gp inhibition seems improbable, and a separate mechanism is thus at play.

Chapter 4: Conclusion

Aims of the investigation included evaluating the *in vitro* P-gp inhibitory potential of alkaloid-enriched fractions from *S. aculeastrum* berries and the synergistic potential with doxorubicin. Lack of knowledge regarding the proposed bioactive component, the mechanism by which the berries elicit bioactivity during ethnomedicinal use and that steroidal alkaloids cause MDR reversal via P-gp modulation, formed the basis for further evaluation. During the study, phytochemical screening yielded fluorescent spots and orange bands across all samples. According to literature, this indicates the presence of steroidal alkaloids. Further assessment revealed that the crude extract as well as the aqueous fraction possessed notable cytotoxicity and P-gp inhibition towards both cancerous and non-cancerous cell lines. The ether and chloroform fractions were shown to be inactive.

Bioactivity guided fractionation lead to the isolation of steroidal alkaloids solamargine and solasonine which are known to be present in many *Solanum* spp. Solasonine was found to be inactive throughout and had variable activity when compared to previous studies. Variability may be due to slight conformational changes in the molecular structure as well as cell line, assay and IC_{50} predicting differences. Solamargine was shown to be the bioactive compound responsible for potent, non-selective cytotoxicity and P-gp inhibition in *S. aculeastrum* fruits. Variable quantities of solamargine in the crude extract and alkaloid-enriched fractions contribute to the differences in activity. Literature states that solamargine induces either an autophagic or apoptotic mode of cell death and down regulates HER2/neu receptors on breast cancer cells. These mechanisms may explain the mechanism of bioactivity of *S. aculeastrum* fruits during ethnomedicinal usage.

Furthermore, solamargine and the aqueous fraction were also shown to enhance doxorubicin through additive effects in select cell lines as well as indifferent and antagonistic responses in others. P-gp inhibition only occurred at the higher concentration ranges which make this mechanism of enhancement unlikely. Potentiating of activity could be due to the combination targeting the same pathway simultaneously, whereas antagonistic interactions may be due to interference when binding to similar sites. Further studies are needed to elucidate the exact mechanism.

Chapter 5: Limitations of study and recommendations

Experiments which were not done that would have supported or given more insight into the study finding is one possible limitation. It is recommended that the mechanisms behind the cytotoxic and synergistic effects be evaluated further by flow cytometric analysis, as this may elucidate the death pathway which *S. aculeastrum* extracts and solamargine targets. To further explain the latter, the use of fluorescence spectroscopy and confocal microscopy is recommended to identify structural changes of cells after exposure.

Berries collected from different locations and times of the year (seasons) may provide different results due to varying steroidal alkaloid concentrations and should be tested. As cell lines undergo phenotypic shifts, it is recommended that evaluation of cytotoxicity should be confined to low passage numbers to be reliable.

Due to the non-selectivity of *S. aculeastrum* extracts and solamargine, careful dose selection is recommended for future *in vivo* studies. The derivitization or synthesis of analogues with similar structure to solamargine may be an effective way to identify compounds which are more selective towards various cancer types. Further crystallography is recommended to assess the orientation (alpha or beta) or conformation of solamargine and solasonine as this could possibly clarify the differences in activity noted between studies.

Chapter 6: Summary

Cancer is one of the most life threatening groups of diseases. Due to the prevalence of multi-drug resistance, novel treatment methods are sought. *Solanum aculeastrum* Dunal, also known as the goat apple, is used ethnomedicinally to treat cancer, in the Eastern Cape. Literature is scarce concerning the plants bioactivity but steroidal alkaloids, such as solasodine and solamargine, are the proposed bioactive components. The study aim was to assess the anticancer and P-glycoprotein inhibitory potential of alkaloid-enriched fractions from *S. aculeastrum* fruits as well as its synergistic potential with doxorubicn *in vitro*.

A crude extract was made from *S. aculeastrum* fruits via ultrasonic maceration followed by fractionation to yield ether, chloroform and aqueous fractions. Bioactivity regarding cytotoxicity as well as P-gp inhibition was assessed with the use of the sulphorhodamine B and rhodamine-123 assays. After screening, the most active fraction was subjected to further fractionation and isolation procedures. Furthermore, the isolated bioactive component (s) as well as the active fraction was assessed for their potential to enhance doxorubicins efficacy using a checkerboard combination layout.

The crude extract and aqueous fraction were shown to possess potent activity with regard to cytotoxicity and P-gp inhibition, however this was non-selective towards cancerous cells. The ether and chloroform fractions were inactive. Subsequent fractionation of the aqueous fraction, isolation procedures as well as structural elucidation yielded steroidal alkaloids solamargine and solasonine. Bioactivity evaluation revealed solasonine was inactive which varied from previous studies and could be due assay as well as conformation differences. Solamargine was the bioactive component responsible for the activity elicited by *S. aculeastrum*. Both solamargine and the aqueous fraction enhanced doxorubicin through additive effects in select cell lines as well as indifferent and antagonistic responses in others. Another process may be present here.

S. aculeastrum elicited non-selectivity towards different cancer cell lines. Although P-gp inhibition was present concurrently with cytotoxicity, it is not the proposed mechanism of the enhanced effect. The exact mechanism needs to be elucidated.

Chapter 7: References

1 Siegel R, DeSantis C, Virgo K, Stein K, Marlotto A, Smith Y, *et al*. Cancer treatment and survivorship statistics, 2012. CA Cancer J Clin. 2012; 62:220-41.

2. Globocan.irac.fr [Internet]. Cancer fact sheets., [updated 2013, accessed 2014 May]. Available from: http://globocan.iarc.fr/Pages/fact_sheets_cancer.aspx

3. Wcrf.org [Internet]. Worldwide., [updated 2013; accessed 2014 May]. Available from: http://www.wcrf.org/cancer_statistics/world_cancer_statistics.php.

4. Iarc.fr [Internet]. Latest cancer statistics., [updated 2013 December; accessed 2014 May]. Available from: http://www.iarc.fr/en/media-centre/pr/2013/pdfs/pr223_E.pdf.

5. Cansa.org [Internet]. South African cancer statistics., [updated 2012 May; accessed 2014 May]. Available from: http://www.cansa.org.za/south-african-cancer-statistics/.

6. Zuckerman V, Wolyniec K, Sionov RV, Haupt S, Haupt Y. Tumour suppression by p53: the importance of apoptosis and cellular senescence. J Pathol. 2009; 219:3-15.

7. Hanahan D, Weinberg RA. Hallmarks of Cancer: The Next Generation. Cell Dev Biol. 2011; 144:646-74.

8. Discoverymedicine.com [Internet]. The Immune System: Taming and Unleashing Cancer., [updated 2014, accessed 2014 May]. Available from: http://www.discoverymedicine.com/Antoine-Tesniere/2009/07/28/the-immune-system-taming-and-unleashing-cancer/.

9. Meropol NJ, Schrag D, Smith TJ, Mulwey TM, Langdon RM, Blum D, *et al*. American society of clinical oncology guidance statement: the cost of cancer care. J Clin Oncol. 2009; 27:3868-74.

10. Royal S, Smeaton L, Avery AJ, Hurwitz B, Sheikh A. Interventions in primary care to reduce medication related adverse effects and hospital admissions: systematic review and meta-analysis. Qual Saf Health Care. 2006; 15:23-31.

11. Cancer.org [Internet]. Chemotherapy principles, [updated 2013 July; accessed 2014 May]. Available from:

http://www.cancer.org/treatment/treatmentsandsideeffects/treatmenttypes/chemotherapy/how-chemotherapy-drugs-work.

12. da Rocha AB, Lopes RM, Schwartsmann G. Natural products in anticancer therapy. Curr Opin Pharmacol. 2001; 1:364-9.

13. Kreeger PK, Lauffenburger DA. Cancer systems biology: a network modeling perspective. Carcinogenesis. 2010; 31:2-8.

14. Schwartz GK, Shah MA. Targeting the cell cycle: A new approach to cancer therapy. J Clin Oncol. 2005; 23:9408-21.

15. Edinger AL, Thompson CB. Death by design: apoptosis, necrosis and autophagy. Curr Opin Cell Biol. 2004; 16:663-9.

16. Wikipedia.org [Internet]. Necrosis., [updated 2013; accessed 2014 May]. Available from: http://en.wikipedia.org/wiki/Necrosis.

17. Bock C, Lengauer T. Managing drug resistance in cancer: lessons from HIV therapy. Nat Rev Cancer. 2012; 12:494-501.

18. Conde J, de la Fuente JM, Baptista PV. Nanomaterials for reversion of multidrug resistance in cancer: a new hope for an old idea?. Front Pharmacol. 2013; 4:2-5.

19. Wilson TR, Johnston P G, Longley DB. Anti-apoptotic mechanisms of drug resistance in cancer. Curr Cancer Drug Targets. 2009; 9:307-19.

20. Liu FS. Mechanisms of chemotherapeutic drug resistance in cancer therapy--a quick review. Taiwan J Obstet Gynecol. 2009; 48:239-44.

21. Thomas H, Coley HM. Overcoming multidrug resistance in cancer: An update on the clinical strategy of inhibiting P-glycoprotein. Cancer Control. 2003; 10:159-65.

22. Rautio J, Humphreys JE, Webster LO, Balakrishnan A, Keogh JP, Kunta JR, *et al*. In-vitro P-glycoprotein inhibition assays for assessment of clinical drug interaction potential of new drug candidates: A recommendation for probe substrates. Drug Metab Dispos. 2006; 34:786-92.

23. Polli JW, Wring SA, Humphreys JE, Huang L, Morgan JB, Webster LO, *et al*. Rational use of in vitro P-glycoprotein assays in drug discovery. J Pharmacol Exp Ther. 2001; 299:620-8.

24. Borst P, Oude Elferink R. Mammalian ABC Transporters and Disease. Annu. Rev. Biochem. 2002; 71:537-92.

25. Ijhg.com [Internet]. Indian journal of human genetics., [accessed 2014 May]. Available from: http://www.ijhg.com/articles/2011/17/4/images/IndianJHumGenet_2011_17_4_12_80353_f3.jpg.

26. Drugdevelopment-technology.com [Internet]. Tesmilifene-Chemopotentiator for Cancer., [Updated 2014, accessed 2014 May]. Available from: http://www.drugdevelopment-technology.com/projects/tesmilifene/tesmilifene2.html.

27. Pusztai L, Wagner P, Ibrahim N, Rivera E, Theriault R, Booser D, *et al*. Phase two study of Tariquidar, a selective P-glycoprotein inhibitor, in patients with chemotherapy-resistant, advanced breast carcinoma. Cancer. 2005; 104:682-91.

28. Bergson P, Lipkind G, Lee SP, Duban ME, Hanck DA. Verapamil Block of T-Type Calcium Channel. Mol Pharmacol. 2011; 79:411-9.

29. Iannetti P, Spali.ce A, Parisi P. Calcium-channel blocker Verapamil administration in prolonged and refactory status epilepticus. Epilepsia. 2005; 46:967-9.

30. Pauli-magnus C, Richter OV, Burk O, Zieger A, Mettang T, Eichelbaum M, *et al*. Characterization of the major metabolite of verapamil as substances and inhibitors of P-glycoprotein. J Pharmacol Exp Ther. 2000; 293:376-82.

31. Bozic I, Reiter JG, Allen B, Antal T, Chatterjee K, Shah P, *et al*. Evolutionary dynamics of cancer in response to targeted combination therapy. Elife. 2013; 25;2:e00747.

32. Kerbel RS, Kamen BA. The anti-angiogenic basis of metronomic chemotherapy. Nat Rev Cancer. 2004; 4:423-36

33. O'Shaughnessy J, Miles D, Vukelja S, Moiseyenko V, Ayoub JP, Cervantes G, *et al*. Superior survival with capecitabine plus docetaxel combination therapy in anthracycline-

pretreated patients with advanced breast cancer: phase III trial results. J Clin Oncol. 2002; 20:2812-23.

34. Jacquin JP, Chargari C, Thorin J, Mille D, Mélis A, Orfeuvre H, *et al*. Phase II trial of pegylated liposomal doxorubicin in combination with gemcitabine in metastatic breast cancer patients. Am J Clin Oncol. 2012; 35:18-21.

35. Thorn CF, Oshiro C, Marsh S, Hernandez-Boussard T, McLeod H, Klein TE, *et al*. Doxorubicin pathways: pharmacodynamics and adverse effects. Pharmacogenet Genomics. 2011; 21:440-6.

36. Aghaee F, Islamian JP, Baradaran B, Mesbahi A, Mohammadzadeh M, Jafarabadi MA. Enhancing the Effects of Low Dose Doxorubicin Treatment by the Radiation in T47D and SKBR3 Breast Cancer Cells. J Breast Cancer. 2013; 16:164-70.

37. Monteiro Lde S, Bastos KX, Barbosa-Filho JM, de Athayde-Filho PF, Diniz Mde F, Sobral MV. Medicinal Plants and Other Living Organisms with Antitumor Potential against Lung Cancer. Evid Based Complement Alternat Med. 2014; 2014:1-15.

38. Cuellar N, Aycock T, Cahill B, Ford J. Complementary and alternative medicine (CAM) use by African American (AA) and Caucasian American (CA) older adults in a rural setting: a descriptive, comparative study. BMC Complement Altern Med. 2003; 3:8-14.

39. Tascilar M, de Jong FA, Verweij J, Mathijssen RHJ. Complementary and alternative medicine during cancer treatment: beyond innocence. Oncologist. 2006; 11:732-41.

40. Molassiotis A, Fernadez-Ortega P, Pud D, Ozden G, Scott JA, Panteli V, *et al*. Use of complementary and alternative medicine in cancer patients: a European survey. Ann Oncol. 2005; 16:655-63.

41. Kaur R, Kapoor K, Kaur H. Plants as a source of anticancer agents. J Nat Prod Plant Resour. 2011, 1:119-24.

42. Shu L, Cheung KL, Khor TO, Chen C, Kong AN. Phytochemicals: cancer chemoprevention and suppression of tumour onset and metastasis. Cancer Metastasis Rev. 2010; 29:483-502.

43. Miele E, Spinelli GP, Miele E, Tomao F, Tomao S. Albumin-bound formulation of paclitaxel (Abraxane ABI-007) in the treatment of breast cancer. Int J Nanomedicine. 2009; 4:99-105.

44. Defelice MS. The Black Nightshades, *Solanum nigrum* L. *et al*.—Poison, Poultice, and Pie. Weed Technol. 2003; 17:421-7.

45. Olmstead RG, Sweere JA, Sprangler RE, Bohs L, Palmer JD. Phylogeny and provisional classification of the Solanaceae based on chloroplast DNA. Lester RN, Jessop JP,editors. Royal Botanical Gardens, Kew; 1999. 111-137 p.

46. Giorgetti M, Negri G. Plants from Solanaceae family with possible anxiolytic effect reported on 19th century's Brazilian medical journal. Rev Bras Farmacogn. 2011; 21:772-80

47. Ikeda O, Egami H, Ishiko T, Ishikawa S, Kamohara H, Hidaka H, *et al*. Expression of proteinase-activated receptor-2 in human pancreatic cancer: a possible relation to cancer invasion and induction of fibrosis. Int J Oncol. 2003; 22:295-300.

48. Grace MH, Saleh MM. Hepatoprotective effect of daturaolone isolated from *Solanum arundo*. Pharmazie. 1996; 51:593-5.

49. Vieira G, Ferreira PM, Matos LG, Ferreira EC, Rodovalho W, Ferri PH, *et al*. Anti-inflammatory effect of *Solanum lycocarpum* fruits. Phytother Res. 2003; 17:892-6.

50. Ibarrola DA, Hellión-Ibarrola MC, Montalbetti Y, Heinichen O, Alvarenga N, *et al*. Isolation of hypotensive compounds from *Solanum sisymbriifolium* Lam. J Ethnopharmacol. 2000; 70:301-7.

51. Koduru S, Jimoh FO, Grierson DS, Afolayan AJ. Antioxidant activity of two steroid alkaloids extract from *Solanum aculeastrum*. J Toxicol Pharmacol. 2007; 2:160-7.

52. Gupta AK, Ganguly P, Majumder UK, Ghosal S. Improvement of lipid and antioxidant status in hyperlipidaemic rats treated with steroidal saponins of *Solanum nigrum* and *Solanum xanthocarpum*. Pharmacologyonline. 2009; 1:1-14.

53. Esteves-Souza A, da Silva TMS, Alves CCF, de Carvalho MG, Braz-Filho R, Aurea E. Cytotoxic activities against Ehrlich carcinoma and human k562 leukaemia of alkaloids and flavonoid from two *Solanum* species. Braz Chem Soc. 2002; 13:838-42.

54. Smith SW, Giesbrecht E, Thompson M, Nelson LS, Hoffman RS. Solanaceous steroidal glycoalkaloids and poisoning by *Solanum torvum*, the normally edible susumber berry. Toxicon. 2008; 52:667-76.

55. Maruo VM, Soares MR, Bernardi MM, Spinosa HS. Embryotoxic effects of *Solanum lycocarpum* St. Hill fruits consumption during preimplantation and organogenesis in rats. Neurotoxicol Teratol. 2003; 25:627-31.

56. Koduru S, Grierson DS, Afolayan AJ. Antimicrobial activity of *Solanum aculeastrum*. Pharm Biol. 2006; 44:283-6.

57. Hutchings A, Scott AH, Lewis G, Cunningham AB. Zulu medicinal plants, an inventory. Pietermaritzburg; 1996. 45 p.

58. Agnew ADQ, Agnew S. Upland Kenya Wild Flowers: A Flora of the Ferns and Herbaceous Flowering Plants of Upland Kenya. Nairobi; 1994. 475 p.

59. Drewes FE, van Staden J. Aspects of the extraction and purification of solasodine from *Solanum aculeastrum* tissues. Phytochem Anal. 1995; 6:203-6.

60. Wanyonyi AW, Sumesh CC, Gerld M, Udo E, Wilson MN. Bioactive steroidal alkaloid glycosides from *Solanum aculeastrum*. Phytochemistry. 2002; 59:79-84.

61. Papamichael D. The use of thymidylate synthase inhibitors in the treatment of advanced colorectal cancer. Curr Status Stem Cells. 2000; 3:166-75.

62. Lavie Y, Harel-Orbital T, Gaffield W, Liscovitch M. Inhibitory effect of steroidal alkaloids on drug transport and multidrug resistance in human cancer cells. Anticancer Res. 2001; 21:1189-94.

63. Shiu LY, Chang LC, Liang CH, Huang YS, Sheu HM, Kuo KW. Solamargine induces apoptosis and sensitizes breast cancer cells to cisplatin. Food Chem Toxicol. 2007; 45:2155-64.

64. Shiu LY, Liang CH, Chang LC, Sheu HM, Tsai EM, Kuo KW. Solamargine induces apoptosis and enhances susceptibility to trastuzumab and epirubicin in breast cancer cells with low or high expression levels of HER2/neu. Biosci Rep. 2009; 29:35-45.

65. Li X, Zhao Y, Ji M, Liu SS, Cui M, Lou HX. Induction of actin disruption and downregulation of P-glycoprotein expression by solamargine in multidrug-resistant K562/A02 cells. Chin Med J. 2011; 124:2038-44.

66. plantzafrica.com [Internet]. *Solanum aculeastrum*., [accessed 2014 May]. Available from: http://www.plantzafrica.com/plantqrs/solanacul.htm

67. Munari CC, de Oliveira PF, Campos JCL, Martins SP, Da Costa JC, Bastos JK, *et al*. Antiproliferative activity of *Solanum lycocarpum* alkaloidic extract and their constituents, solamargine and solasonine, in tumor cell lines. J Nat Med. 2014; 68:236-41.

68. Flieger J. Alkaloids/thin-layer (planar) chromatography. Wilson ID, editor. Encyclopedia of Separation Science. New York: Academic Press; 2000. p. 1956–73.

69. Sreevidya N, Mehrotra S. Spectrophotometric method for estimation of alkaloids precipitable with Dragendorff's reagent in plant materials. J AOAC Int. 2003; 86:1124-7.

70. Vichai V, Kirtikara K. Sulforhodamine B colorimetric assay for cytotoxicity screening. Nat Protoc. 2006; 1:1112-6.

71. Jia JX, Wasan KM. Effects of monoglycerides on rhodamine 123 accumulation, estradiol 17 beta-D-glucuronide bidirectional transport and MRP2 protein expression within Caco-2 cells. J Pharm Pharm Sci. 2008; 11:45-62.

72. Kars MD, Gündüz U, Üney K, Baş AL. Exploring a natural MDR reversal agent: potential of medical food supplement *Nerium oleander* leaf distillate. Asian Pac J Trop Biomed. 2013; 3:644-9.

73. Martins GZ, dos Santos AN, Vilela RR, de Carvalho Ferreira M, de Oliveira P, Moreira RR, *et al*. Optimization of Extraction Conditions and Antioxidant Activity of *Solanum lycocarpum* Fruits. J Appl Sci. 2013; 13:147-53.

74. Al Sinani SS, Eltayeb EA, Kamal YT, Khan MS, Ahmad S. Variations in the cytotoxic glycoalkaloids solamargine and solasonine in different parts of the *Solanum incanum* plant during its growth and development in Oman. J Taibah Univ Sci. doi:10.1016/j.jtusci.2014.11.013

75. Halsall CJ. Environmental Organic Chemistry. Harrison RM, editor. Principles of Environmental Chemistry. Illustrated ed. Great Britain: Royal Society of Chemistry; 2007. p. 279–308.

76. Mohy-ud-Din A, Khan ZU, Ahmad M, Kashmiri MA. Chemotaxonomic value of alkaloids in *Solanum nigrum* complex. Pak J Bot. 2010; 42:653-60.

77. Selvameenal L, Radhakrishnan M, Balagurunathan R. Antibiotic pigment from desert soil actinomycetes; biological activity, purification and chemical screening. Indian J Pharm Sci. 2009; 71:499.

78. Abdel-Sattar E, Farag MA, Mahrous EA. Chemical Constituents from *Solanum glabratum* Dunal var. sepicula. Rec Nat Prod. 2015; 9:94-104.

79. Neszmelyi A, Machytka D, Shabana MM. ^{13}C NMR spectroscopy of solasodine glycosides from *Solanum laciniatum*. Phytochemistry. 1988; 27:603-5.

80. Blankemeyer JT, Mc-Williams ML, Rayburn JR, Weissenberg M, Friedman M. Developmental toxicology of solamargine glycoalkaloids in frog embryos. Food Chem Toxicol. 1998; 36:383-9.

81. Nikolic NC, Stankovic MZ. Solanidine hydrolytic extraction and separation from the potato (*Solanum tuberosum* L.) vines by using solid-liquid-liquid systems. J Agric Food Chem. 2003; 51:1845-9.

82. Al-Rehaily AJ, Ahmad MS, Mustafa J, Al-Oqail MM, Hassan WH, Khan SI, *et al*. Solanopubamine, a rare steroidal alkaloid from *Solanum schimperianum*: synthesis of some new alkyl and acyl derivatives, their anticancer and antimicrobial evaluation. J Saudi Chem Soc. 2013; 17:67-76.

83. Chinedu SN, Olasumbo AC, Eboji OK, Emiloju OC, Arinola OK, Dania DI. Proximate and phytochemical analyses of *Solanum aethiopicum* L. and *Solanum macrocarpon* L. fruits. Res J Chem Sci. 2011; 1:63-71.

84. Cornelius MT, Carvalho MG, Silva T, Alves CC, Siston AP, Alves KZ, *et al*. Other chemical constituents isolated from *Solanum crinitum* Lam.(Solanaceae). J Braz Chem Soc. 2010; 21:2211-9.

85. Basha SA, Sarma BK, Singh KP, Singh UP. Variation in Biochemical Composition among Indian Isolates of *Sclerotinia sclerotiorum*. Mycobiology. 2006; 34:114-9.

86. Manase MJ, Mitaine-Offer AC, Pertuit D, Miyamoto T, Tanaka C, Delemasure S, *et al*. *Solanum incanum* and *S. heteracanthum* as sources of biologically active steroid glycosides: Confirmation of their synonymy. Fitoterapia. 2012; 83:1115-9.

87. Doss A, Mubarack HM, Dhanabalan R. Antibacterial activity of tannins from the leaves of *Solanum trilobatum* Linn. Indian J Sci Technol. 2009; 2:41-3.

88. Osorio A, Silva TM, Duarte LP, Ferraz VP, Pereira MT, Mercadante-Simões MO, *et al.* Essential Oil from Flowers of *Solanum stipulaceum*: Composition, Effects of γ-Radiation, and Antileukemic Activity. J Braz Chem Soc. 2015; 26:2233-40.

89. Qusti SY, Abo-khatwa AN, Lahwa MB. Screening of antioxidant activity and phenolic content of selected food items cited in the Holly Quran. Eur J Biol Sci. 2010; 2:40-51.

90. Lin HM, Tseng HC, Wang CJ, Chyau CC, Liao KK, Peng PL, *et al*. Induction of autophagy and apoptosis by the extract of *Solanum nigrum* Linn in HepG2 cells. J Agric Food Chem. 2007; 55:3620-8.

91. Abdel-Hameed ES, Salih A, Bazaid SA, Shohayeb MM, El-Sayed MM, El-Wakil EA. Phytochemical studies and evaluation of antioxidant, anticancer and antimicrobial properties of *Conocarpus erectus* L. growing in Taif, Saudi Arabia. Eur J Med Plants.2012;2:93–112.

92. Bao J, Huang B, Zou L, Chen S, Zhang C, Zhang Y, *et al*. Hormetic effect of berberine attenuates the anticancer activity of chemotherapeutic agents. PloS one. 2015; 10:1-13.

93. Rasoanaivo P, Wright CW, Willcox ML, Gilbert B. Whole plant extracts versus single compounds for the treatment of malaria: synergy and positive interactions. Malar J. 2011; 10:1-12.

94. McKim J, James M. Building a tiered approach to in vitro predictive toxicity screening: a focus on assays with *in vivo* relevance. Comb Chem High Throughput Screen. 2010; 1:188-206.

95. Kuo KW, Hsu SH, Li YP, Lin WL, Liu LF, Chang LC, *et al*. Anticancer activity evaluation of the *Solanum* glycoalkaloid solamargine: triggering apoptosis in human hepatoma cells. Biochem Pharmacol. 2000; 60:1865-73.

96. Nekooki-Machida Y, Kurosawa M, Nukina N, Ito K, Oda T, Tanaka M. Distinct conformations of *in vitro* and *in vivo* amyloids of huntingtin-exon1 show different cytotoxicity. Proc Natl Acad Sci USA. 2009; 106:9679-84.

97. Volpe DA, Hamed SS, Zhang LK. Use of different parameters and equations for calculation of IC_{50} values in efflux assays: potential sources of variability in IC50 determination. AAPS J. 2014; 16:172-80.

98. Junyaprasert VB, Soonthornchareonnon N, Thongpraditchote S, Murakami T, Takano M. Inhibitory effect of thai plant extracts on P-glycoprotein mediated efflux. Phytother Res. 2006; 20:79-81.

99. Sahu J, Rathi B, Koul S, Khosa RL. *Solanum trilobatum* (Solanaceae)-an overview. J Nat Remedies. 2013; 13:76-80.

100. Li X, Zhao Y, Ji M, Liu SS, Cui M, Lou HX. Induction of actin disruption and downregulation of P-glycoprotein expression by solamargine in multidrug-resistant K562/A02 cells. Chin Med J. 2011; 124:2038-44.

101. Fung KL, Pan J, Ohnuma S, Lund PE, Pixley JN, Kimchi-Sarfaty C, *et al*. MDR1 synonymous polymorphisms alter transporter specificity and protein stability in a stable epithelial monolayer. Cancer Res. 2014; 74:598-608.

102. Lavie YA, Harel-Orbital TO, Gaffield WI, Liscovitch MO. Inhibitory effect of steroidal alkaloids on drug transport and multidrug resistance in human cancer cells. Anticancer Res. 2001; 21:1189-94.

103. Shapiro AB, Ling V. Positively cooperative sites for drug transport by P-glycoprotein with distinct drug specificities. Eur J Biochem. 1997; 250:130-7.

104. Jia J, Zhu F, Ma X, Cao ZW, Li YX, Chen YZ. Mechanisms of drug combinations: interaction and network perspectives. Nat Rev Drug Discov. 2009; 8:111-28.

105. Tai CJ, Wang CK, Tai CJ, Lin YF, Lin CS, Jian JY, *et al*. Aqueous extract of *Solanum nigrum* leaves induces autophagy and enhances cytotoxicity of cisplatin, doxorubicin, docetaxel, and 5-fluorouracil in human colorectal carcinoma cells. Evid Based Complement Alternat Med. 2013; 2013:1-12.

106. Anindyajati S, Putri DD, Hermawan A, Meiyanto E. Combination of *Solanum nigrum* L. Herb Ethanolic Extract and Doxorubicin Performs Synergism on T47D Breast Cancer Cells. Indones J chemoprev. 2010; 1:78-84.

107. Ding X, Zhu FS, Li M, Gao SG. Induction of apoptosis in human hepatoma SMMC-7721 cells by solamargine from *Solanum nigrum* L. J Ethnopharmacol. 2012; 139:599-604.

108. Liang CH, Liu LF, Shiu LY, Huang YS, Chang LC, Kuo KW. Action of solamargine on TNFs and cisplatin-resistant human lung cancer cells. Biochem Biophys Res Commun. 2004; 322:751-8.

109. Shiu LY, Liang CH, Huang YS, Sheu HM, Kuo KW. Downregulation of HER2/neu receptor by solamargine enhances anticancer drug-mediated cytotoxicity in breast cancer cells with high-expressing HER2/neu. Cell Biol Toxicol. 2008; 24:1-10.

110. Friedman M, Lee KR, Kim HJ, Lee IS, Kozukue N. Anticarcinogenic effects of glycoalkaloids from potatoes against human cervical, liver, lymphoma, and stomach cancer cells. J Agric Food Chem. 2005; 53:6162-9.

111. Xu Y, Zhi F, Xu G, Tang X, Lu S, Wu J, Hu Y. Overcoming multidrug-resistance *in vitro* and in vivo using the novel P-glycoprotein inhibitor 1416. Biosci Rep. 2012; 32:559-66.

112. El-Readi MZ, Hamdan D, Farrag N, El-Shazly A, Wink M. Inhibition of P-glycoprotein activity by limonin and other secondary metabolites from Citrus species in human colon and leukaemia cell lines. Eur J Pharmacol. 2010; 626:139-45.

113. Singh JK, Farnie G, Bundred NJ, Simões BM, Shergill A, Landberg G, *et al*. Targeting CXCR1/2 significantly reduces breast cancer stem cell activity and increases the efficacy of inhibiting HER2 via HER2-dependent and-independent mechanisms. Clin Cancer Res. 2013; 19:643-56.

Appendix I: Ethical approval letter for study

The Research Ethics Committee, Faculty Health Sciences, University of Pretoria complies with ICH-GCP guidelines and has US Federal wide Assurance.
- FWA 00002567, Approved dd 22 May 2002 and Expires 20 Oct 2016.
- IRB 0000 2235 IORG0001762 Approved dd 22/04/2014 and Expires 22/04/2017.

UNIVERSITEIT VAN PRETORIA
UNIVERSITY OF PRETORIA
YUNIBESITHI YA PRETORIA

Faculty of Health Sciences Research Ethics Committee

28/05/2015

Approval Certificate
New Application

Ethics Reference No.: 167/2015

Title: In vitro p-glycoprotein activity of alkaloid-enriched fractions from Solanum aculeastrum and its synergistic potential with doxorubicin

Dear Mr Trevor Burger

The **New Application** as supported by documents specified in your cover letter dated 22/04/2015 for your research received on the 22/04/2015, was approved by the Faculty of Health Sciences Research Ethics Committee on its quorate meeting of 27/05/2015.

Please note the following about your ethics approval:
- Ethics Approval is valid for 2 years
- Please remember to use your protocol number (**167/2015**) on any documents or correspondence with the Research Ethics Committee regarding your research.
- Please note that the Research Ethics Committee may ask further questions, seek additional information, require further modification, or monitor the conduct of your research.

Ethics approval is subject to the following:
- The ethics approval is conditional on the receipt of 6 monthly written Progress Reports, and
- The ethics approval is conditional on the research being conducted as stipulated by the details of all documents submitted to the Committee. In the event that a further need arises to change who the investigators are, the methods or any other aspect, such changes must be submitted as an Amendment for approval by the Committee.

We wish you the best with your research.

Yours sincerely

*** Kindly collect your original signed approval certificate from our offices, Faculty of Health Sciences, Research Ethics Committee, H W Snyman South Building, Room 2.33 / 2.34.*

Dr R Sommers; MBChB; MMed (Int); MPharMed.
Deputy Chairperson of the Faculty of Health Sciences Research Ethics Committee, University of Pretoria

The Faculty of Health Sciences Research Ethics Committee complies with the SA National Act 61 of 2003 as it pertains to health research and the United States Code of Federal Regulations Title 45 and 46. This committee abides by the ethical norms and principles for research, established by the Declaration of Helsinki, the South African Medical Research Council Guidelines as well as the Guidelines for Ethical Research: Principles Structures and Processes 2004 (Department of Health).

☎ 012 354 1677 🖷 0866516047 deepeka.behari@up.ac.za http://www.healthethics-up.co.za
✉ Private Bag X323, Arcadia, 0007 - 31 Bophelo Road, HW Snyman South Building, Level 2, Room 2.33, Gezina, Pretoria

Appendix II: Reagent list

Acetone, chloroform, dimethyl sulphoxide and methanol

Acetone, chloroform, dimethyl sulphoxide and methanol was attained from Merck (Pty) Ltd (Modderfontein, South Africa) as liquid, used undiluted and stored at room temperature till use.

Acetonitrile

Acetonitrile was obtained from Sigma-Aldrich (Pty) Ltd (Kempton Park, South Africa) as a liquid, used undiluted and stored at room temperature till use.

Basic bismuth nitrate

Basic bismuth nitrate was acquired from from Merck (Pty) Ltd (Modderfontein, South Africa) in powder form and stored at room temperature till use.

Deuterated methanol

Deuterated methanol was attained from Sigma-Aldrich (Pty) Ltd (Kempton Park, South Africa) as a liquid, used undiluted and stored at 4^{o}C till use.

Diethyl ether

Diethyl ether was obtained from Saarchem (Pty) Ltd (Krugersdorp, South Africa) as a liquid, used undiluted and stored at room temperature till use.

Doxorubicin hydrochloride

Doxorubicin hydrochloride was acquired from Sigma-Aldrich (Pty) Ltd (Kempton Park, South Africa) in powder form. Doxorubicin hydrochloride was prepared by dissolving 2 mg in 1 ml DMSO yielding a 3.68 mM stock, which was then aliquoted and stored in plastic 1.5 ml tubes at -80^{o}C till use. Initially the stock was further diluted to 200 µM by dissolving 5 µl (3.68 mM) in 87 µl DMSO, then to a working concentration of 2 µM by dissolving 1 µl (200 µM) in 99 µl of the appropriate media.

Dragendorff's spray reagent

Dragendorffs spray reagent was prepared by combining 0.17 g basic bismuth nitrate, 2ml acetic acid, 4 g potassium iodide and 8ml dH_2O which was stored in a foil covered plastic tube at room temperature till use. One millilitre of the above mixture was then further diluted to a working concentration using 2 ml acetic acid and 10 ml dH_2O.

Dulbecco's Modified Eagle's Medium (DMEM)

DMEM was attained from Sigma-Aldrich (Pty) Ltd (Kempton Park, South Africa) in powder form. DMEM was prepared by dissolving 5 g in 500 ml of sterilised (using an autoclave) dH_2O, supplemented with 3.7 g/L sodium bicarbonate. The mixture was then further filter (0.22 µm) sterilized and stored in a sterile 500 ml clear glass bottle at 4^oC till use.

Eagle's Minimum Essential Medium (EMEM)

EMEM was obtained from Sigma-Aldrich (Pty) Ltd (Kempton Park, South Africa) in powder form. EMEM was prepared by dissolving 4.8 g in 500 ml of sterilised (using an autoclave) dH_2O, supplemented with 2.2 g/L sodium bicarbonate. The mixture was then further filter (0.22 µm) sterilized and stored in a sterile 500 ml clear glass bottle at 4^oC till use.

Ethyl acetate

Ethyl acetate was acquired from Sigma-Aldrich (Pty) Ltd (Kempton Park, South Africa) as a liquid, used undiluted and stored at room temperature till use.

Foetal calf serum

FCS was attained from Sigma-Aldrich (Pty) Ltd (Saint Louis, USA) as a liquid, used undiluted and stored at 4^oC till use. FCS was heat inactivated before addition.

Glacial Acetic acid

Acetic acid was obtained from Saarchem (Pty) Ltd (Krugersdorp, South Africa) and Sigma-Aldrich (Pty) Ltd (Kempton Park, South Africa) as a liquid. Ten millilitres of acetic acid was dissolved in 990 ml of dH_2O and stored in clear glass container at room temperature till use.

Hams F12 nutrient media (F12)

F12 was acquired from Sigma-Aldrich (Pty) Ltd (Kempton Park, South Africa) in powder form. F12 was prepared by dissolving 5.35 g in 500 ml of sterilised (using an autoclave) dH_2O, supplemented with 1.2 g/L sodium bicarbonate. The mixture was then further filter (0.22 µm) sterilized and stored in a sterile 500 ml clear glass bottle at 4^oC till use.

Phosphate buffered saline

PBS was attained from Becton, Dickinson and Company (New Jersey, USA) in powder form. PBS was prepared by dissolving 4.115 g in 500 ml of dH_2O and then stored in a 500 ml plastic container at 4^oC till use.

Potassium iodide

Potassium iodide was obtained from Merck (Pty) Ltd (Modderfontein, South Africa) in powder form and then stored at room temperature till use.

Rhodamine-123

Rhodamine-123 was acquired from Sigma-Aldrich (Pty) Ltd (Kempton Park, South Africa) in powder form. Rhodamine-123 was prepared by dissolving 1 mg to 1 ml DMSO which yielded a 2.63 mM stock, which was then aliquoted and stored in plastic 1.5 ml tubes at -80^oC till use. The stock was further diluted to a working concentration of 40 µM by dissolving 4 µl in 259 µl in PBS.

Roswell Park Memorial Institute-1640 (RPMI)

RPMI was attained from Sigma-Aldrich (Pty) Ltd (Kempton Park, South Africa) in powder form. RPMI was prepared by dissolving 5.2 g in 500 ml sterilised dH_2O, supplemented with 2 g/L sodium bicarbonate. The mixture was then further filter (0.22 µm) sterilized and stored in a sterile 500 ml clear glass bottle at 4^oC till use.

Saponin

Saponin was obtained from Sigma-Aldrich (Pty) Ltd (Kempton Park, South Africa) in powder form. Saponin was prepared by dissolving 6.66 g in 15 ml of the desired medium which was then sonicated, syringe filtered and stored in a sterile clear 15 ml plastic tube at 4^oC till use.

Silica gel

Silica gel was acquired from Sigma-Aldrich (Pty) Ltd (Kempton Park, South Africa) in powder form and then stored at room temperature till use.

Sodium sulphate

Sodium sulphate was attained from Saarchem (Pty) Ltd (Krugersdorp, South Africa) in powder form and then stored at room temperature till use.

Sulforhodamine B

SRB was obtained from Sigma-Aldrich (Pty) Ltd (Kempton Park, South Africa) in powder form. SRB was prepared by dissolving 285 mg in 500 ml of 1% acetic acid and then stored in a 500 ml foil covered clear plastic container until use.

Trichloroacetic acid

Trichloroacetic acid was acquired from Merck (Pty) Ltd (Modderfontein, South Africa) in powder form. Trichloroacetic acid (250 g) was dissolved in dH_2O to give a total volume of 500 ml and stored in 500 ml clear glass container at 4^{o}C till use.

Tris-base solution

Tris-base was attained from Research Organics Inc (Cleveland, USA) in powder form. Tris base (600 mg) was dissolved in 500 ml dH_2O, adjusted to pH 10.5 and stored in 500 ml clear plastic container at room temperature till use.

Trypan blue

Trypan blue was obtained from BDH Laboratory Supplies (Dorset, England) in powder form in 20 g black plastic container. Trypan blue was prepared by dissolving 200 mg in 50 ml PBS and then stored in a 50 ml plastic foil covered tube at room temperature till use.

Trypsin

Trypsin (2.5% w/v) was acquired from Sigma-Aldrich (Pty) Ltd (Kempton Park, South Africa) as a solution, used undiluted and stored in a sterile 15 ml plastic tube at 4^{o}C till use.

Verapamil hydrochloride

Verapamil hydrochloride was attained from Sigma-Aldrich (Pty) Ltd (Kempton Park, South Africa) in powder form. Verapamil hydrochloride was prepared by dissolving 10 mg in 1 ml DMSO yielding a 20 mM stock, which was then aliquoted and stored in plastic 1.5 ml tubes at -80^{o}C till use. The stock was further diluted to working concentration of 200 µM by dissolving 1 µl in 99 µl of the appropriate medium.

Appendix III

A: H-1-NMR spectra for solamargine

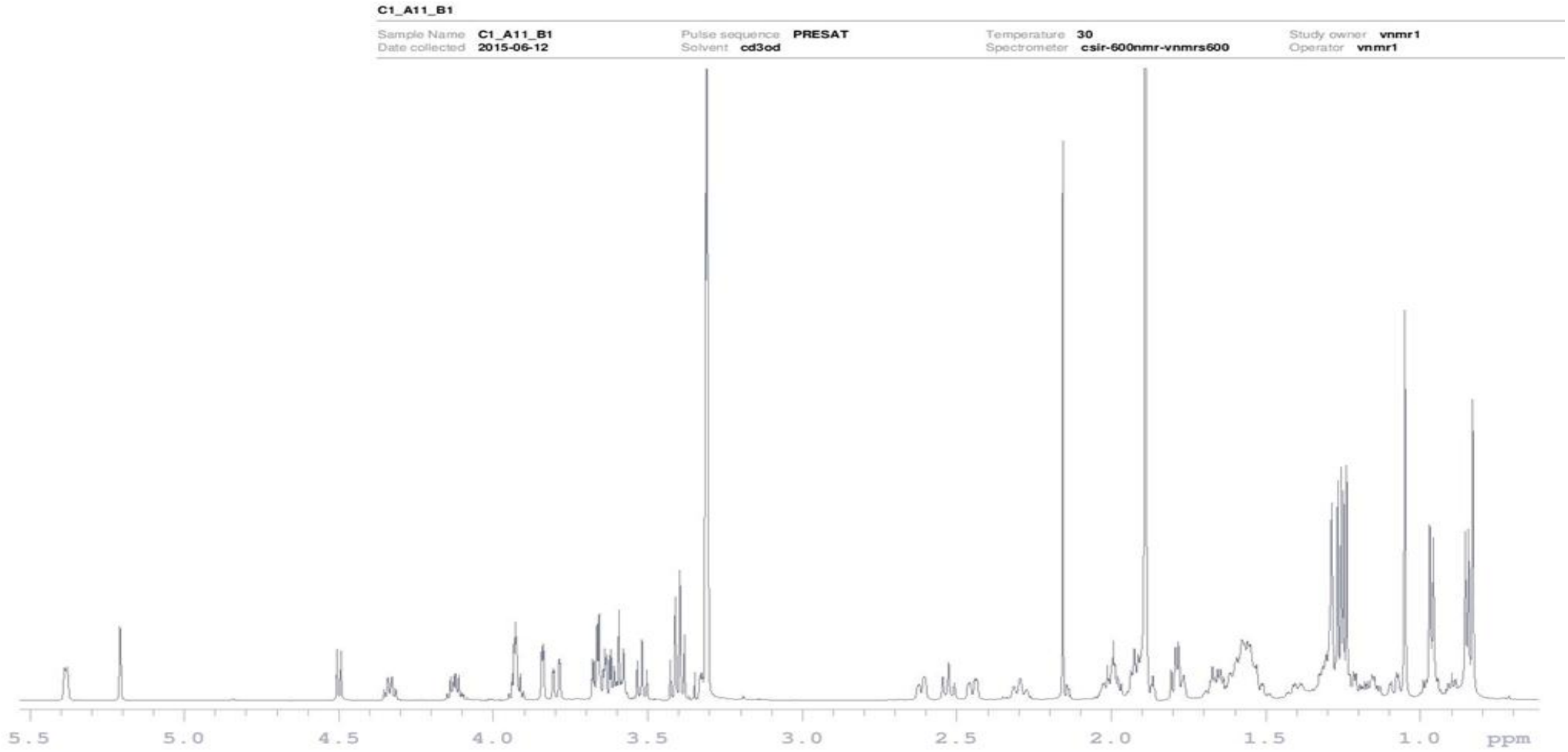

B: C-13-NMR for solamargine

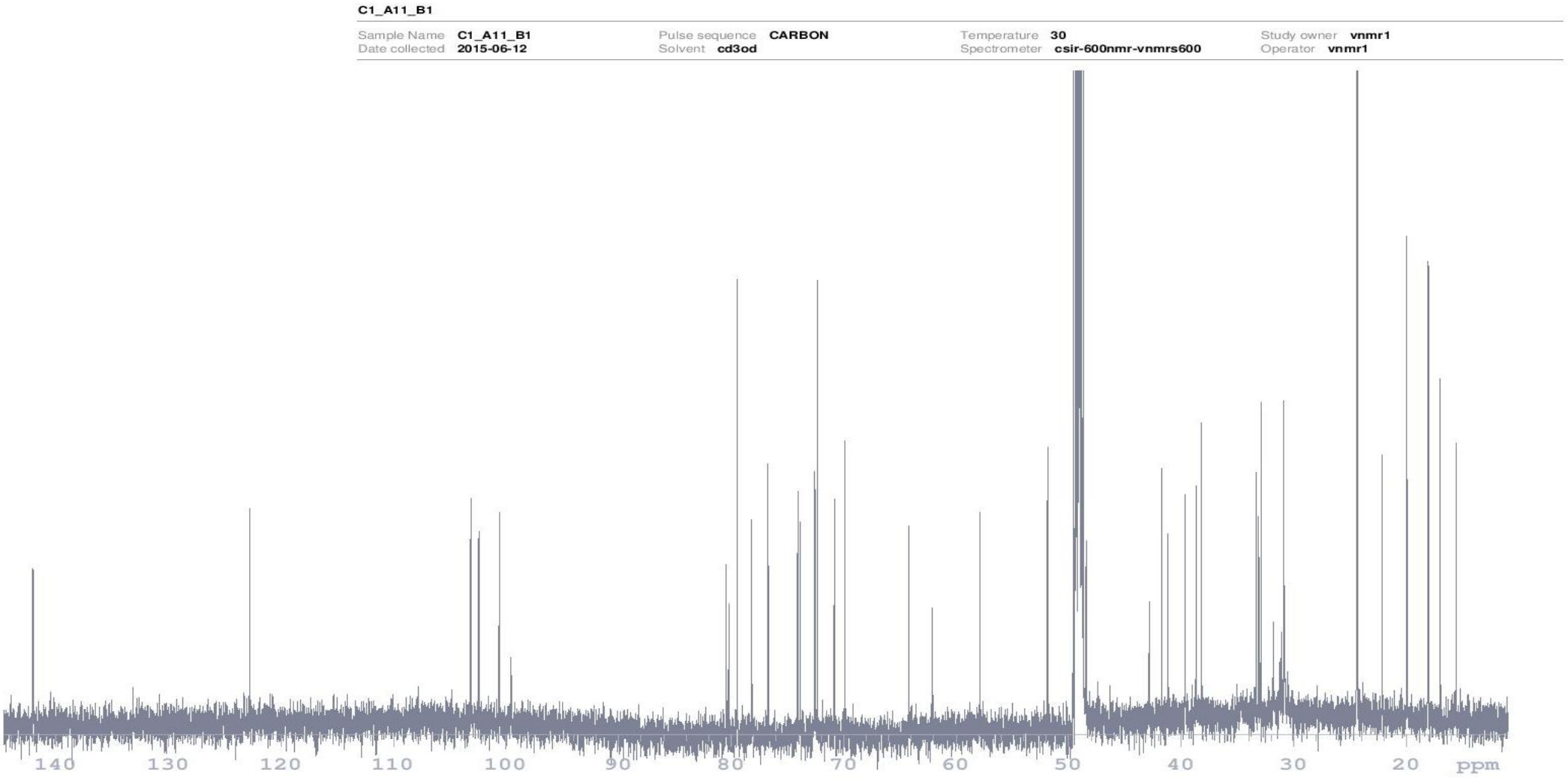

C: HSQC for solamargine

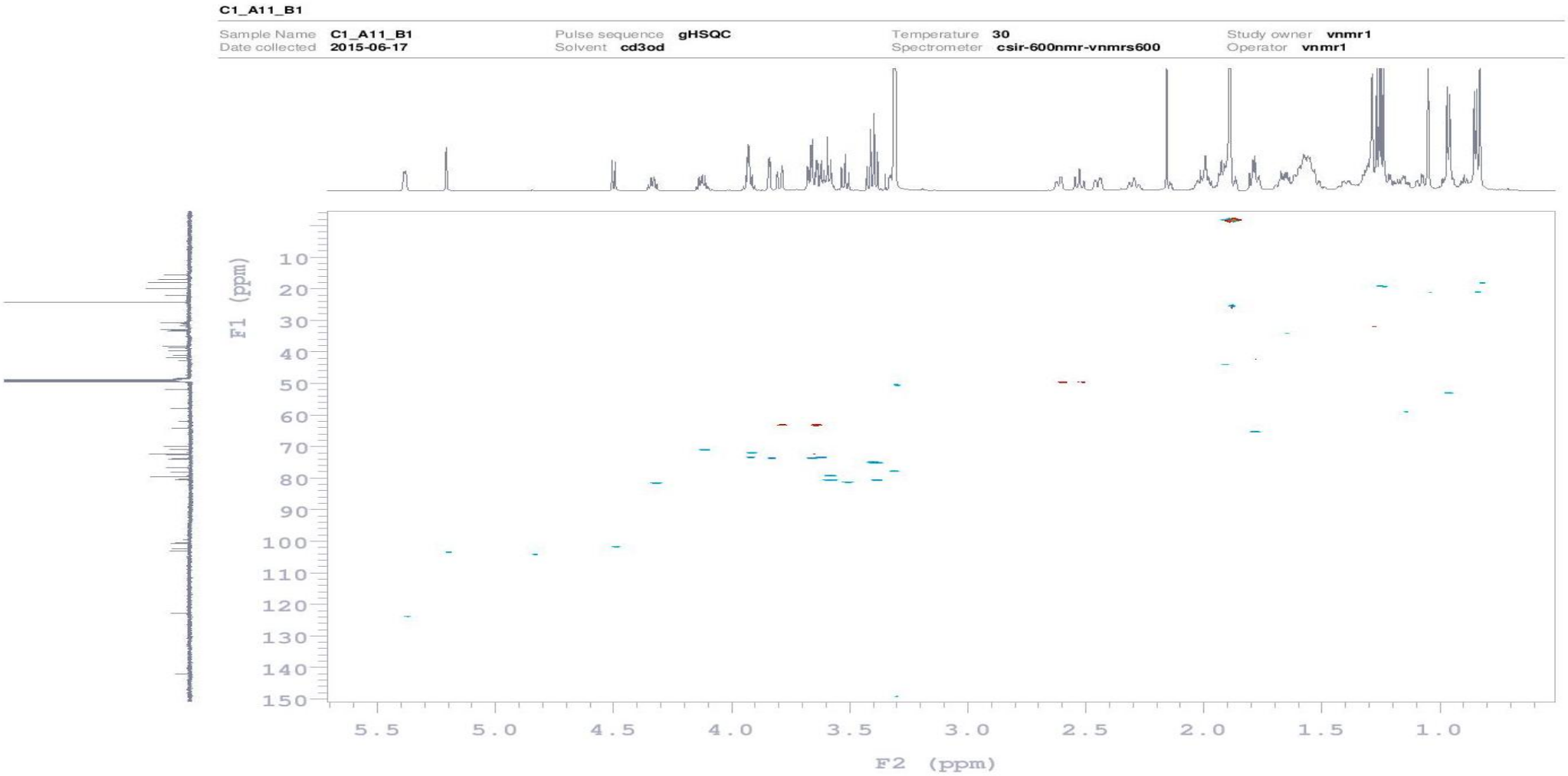

D: HMBC for solamargine

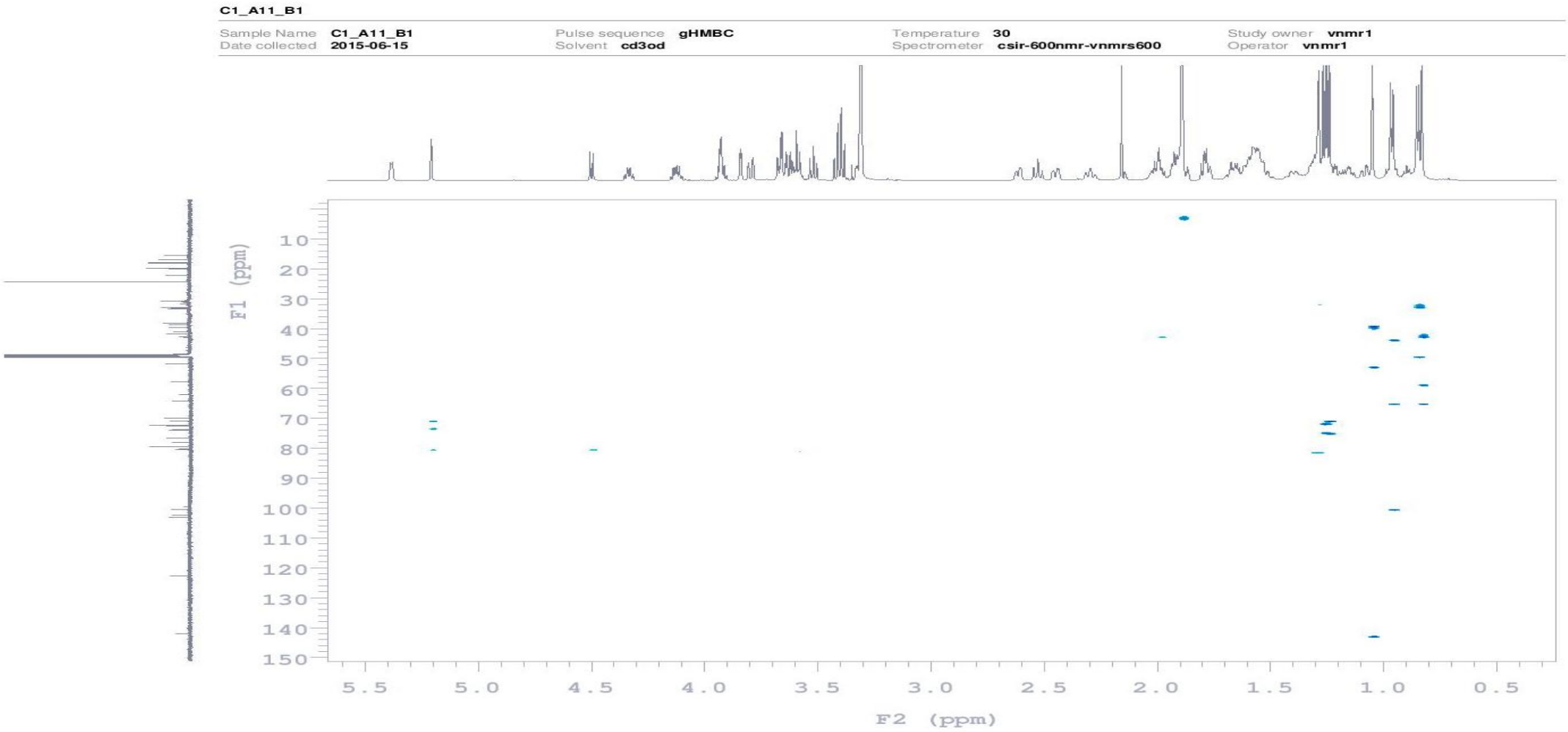

E: COSY for solamargine

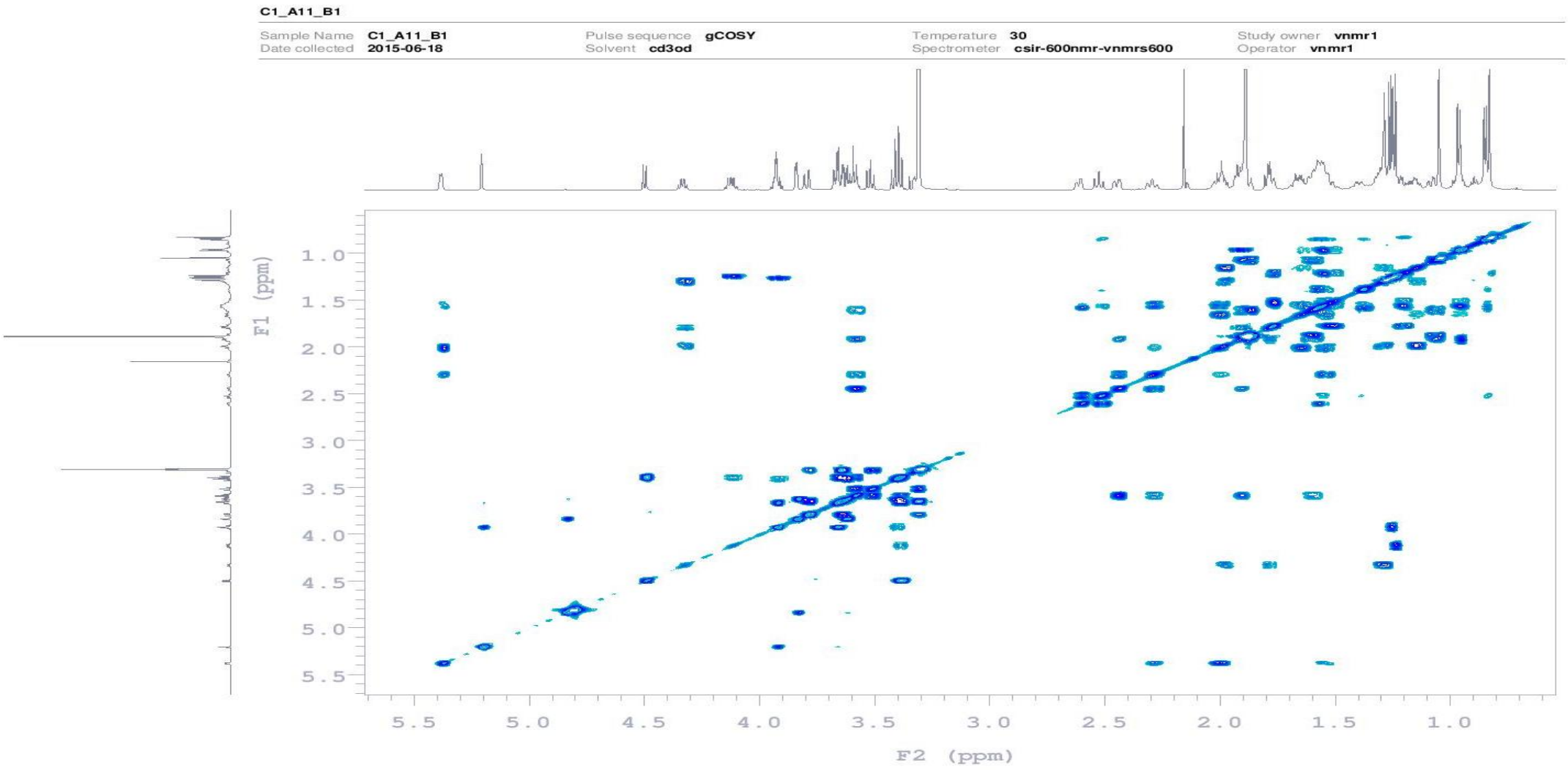

F: UPLC-TOF-MS chromatogram and fragmentation pattern for solamargine

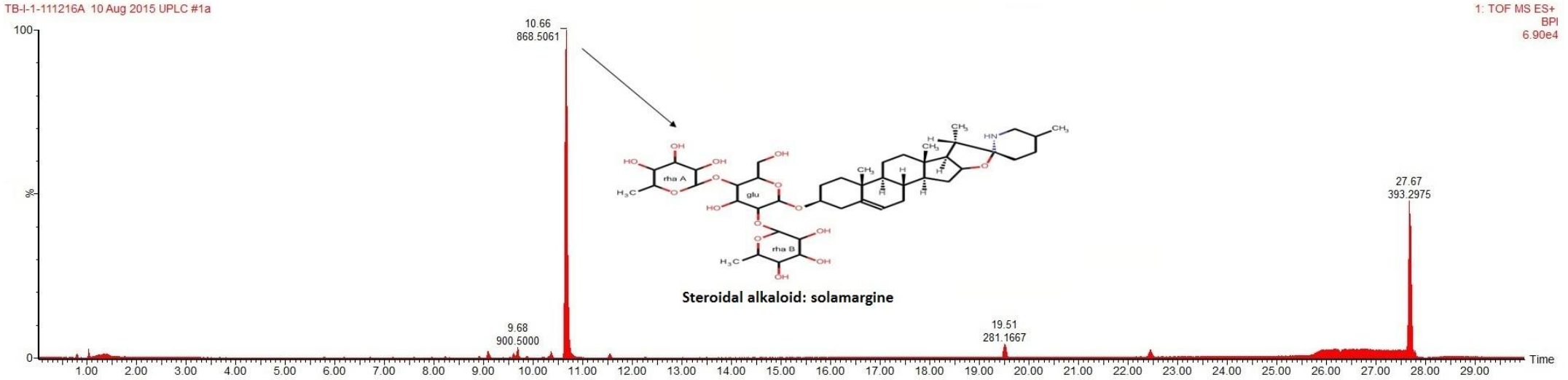

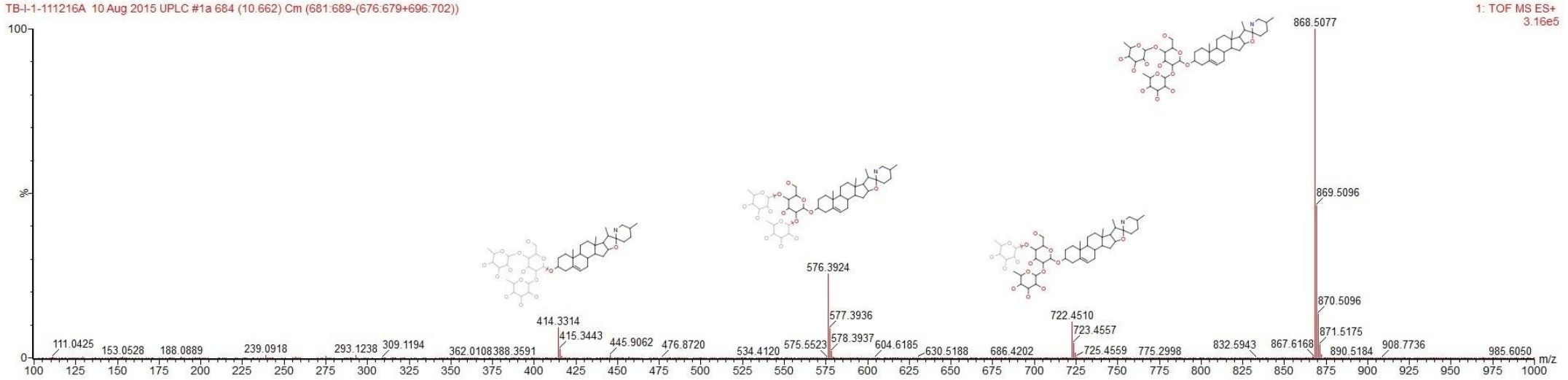

G: UPLC-TOF-MS empirical formula calculation for solamargine

Elemental Composition Report

Single Mass Analysis

Tolerance = 6.0 mDa / DBE: min = -1.0, max = 100.0
Element prediction: Off
Number of isotope peaks used for i-FIT = 4

Monoisotopic Mass, Even Electron Ions
4 formula(e) evaluated with 1 results within limits (up to 50 closest results for each mass)
Elements Used:
C: 45-46 H: 1-100 N: 1-1 O: 15-16

ESIPos VTOF 98%A2:02%B2 @ 0.4 60C SYNAPT HDMS G1
TB-I-1-111216A 10 Aug 2015 UPLC #1a 684 (10.662) Cm (684:689-(677:681+693:698)) 1: TOF MS ES+
1.81e+005

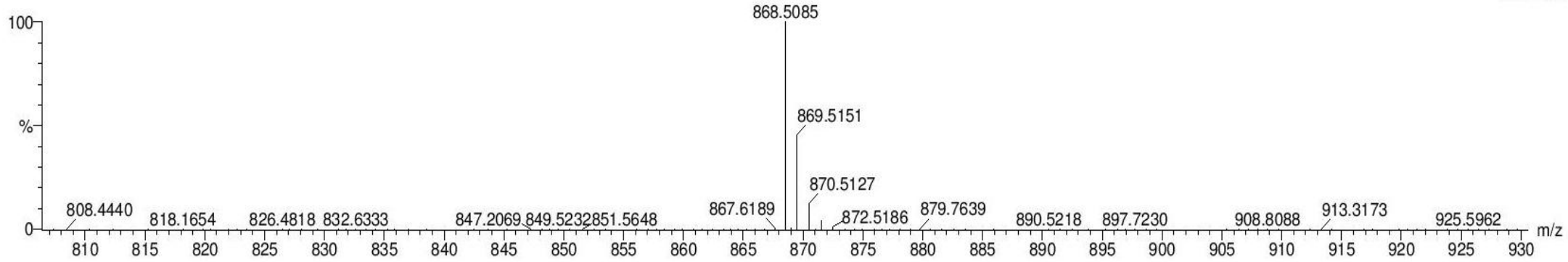

Mass	Calc. Mass	mDa	PPM	DBE	i-FIT	i-FIT (Norm)	Formula
Minimum:				-1.0			
Maximum:		6.0	10.0	100.0			
868.5085	868.5058	2.7	3.1	9.5	65.5	0.0	C45 H74 N O15

Appendix IV

A: H-1-NMR spectra for solasonine

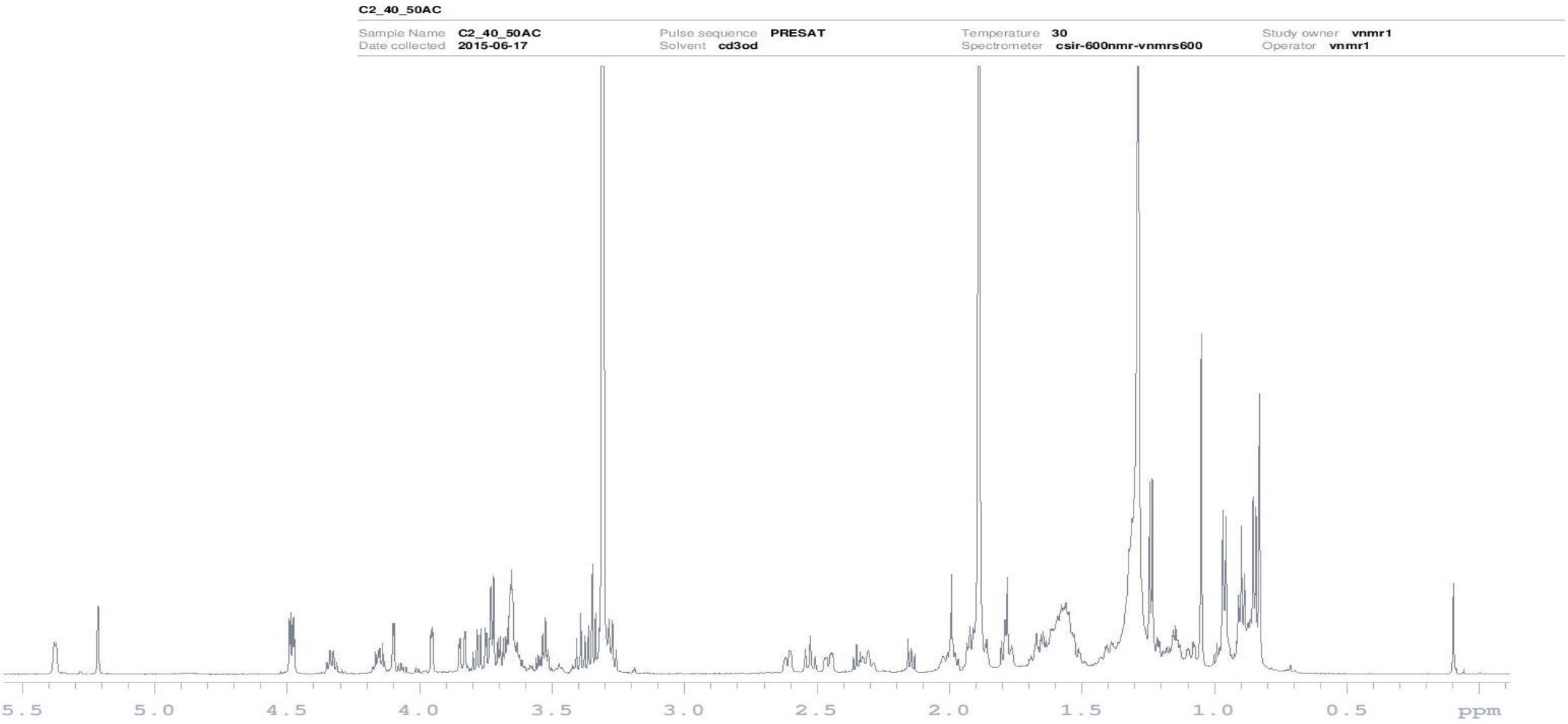

B: C-13-NMR for solasonine

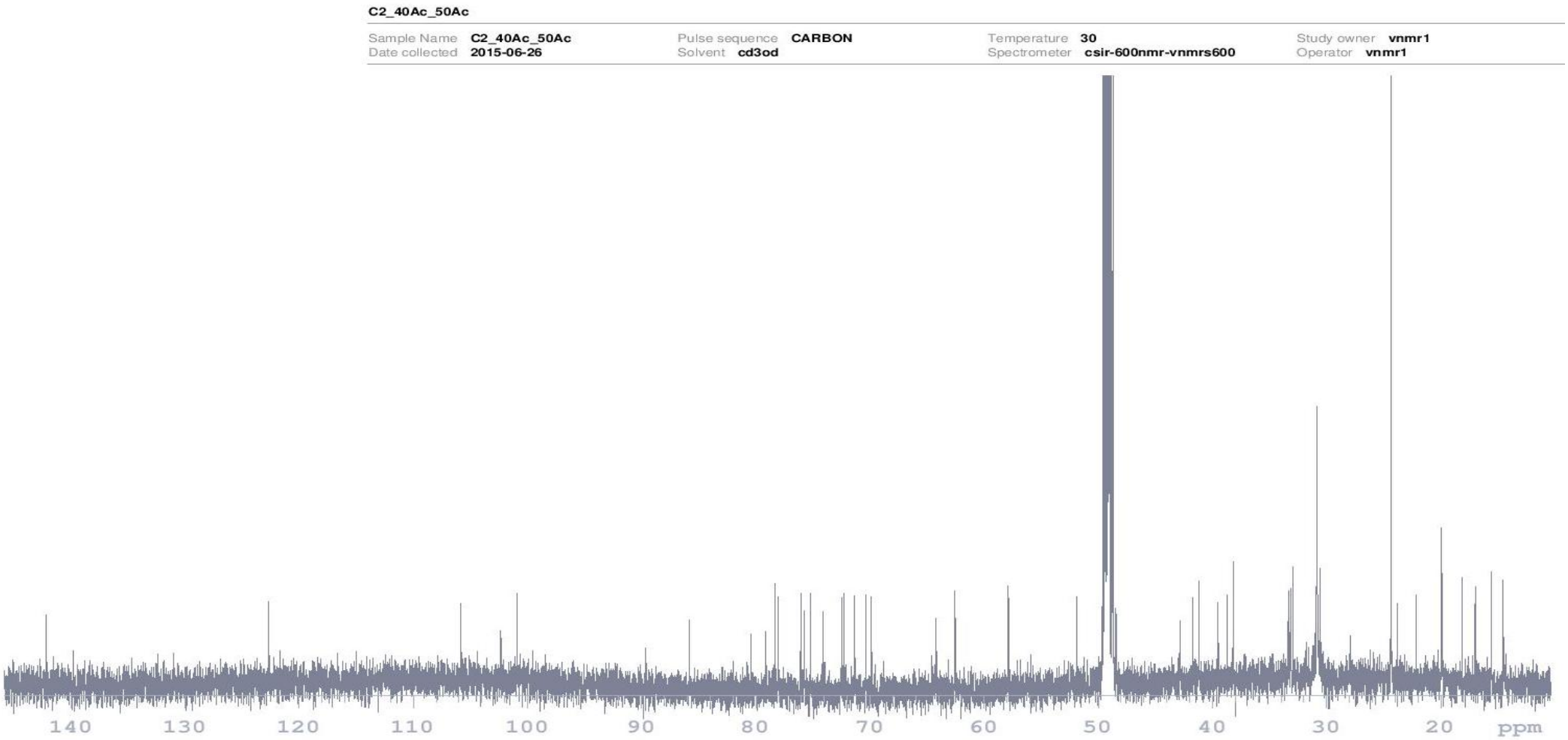

C: HSQC for solasonine

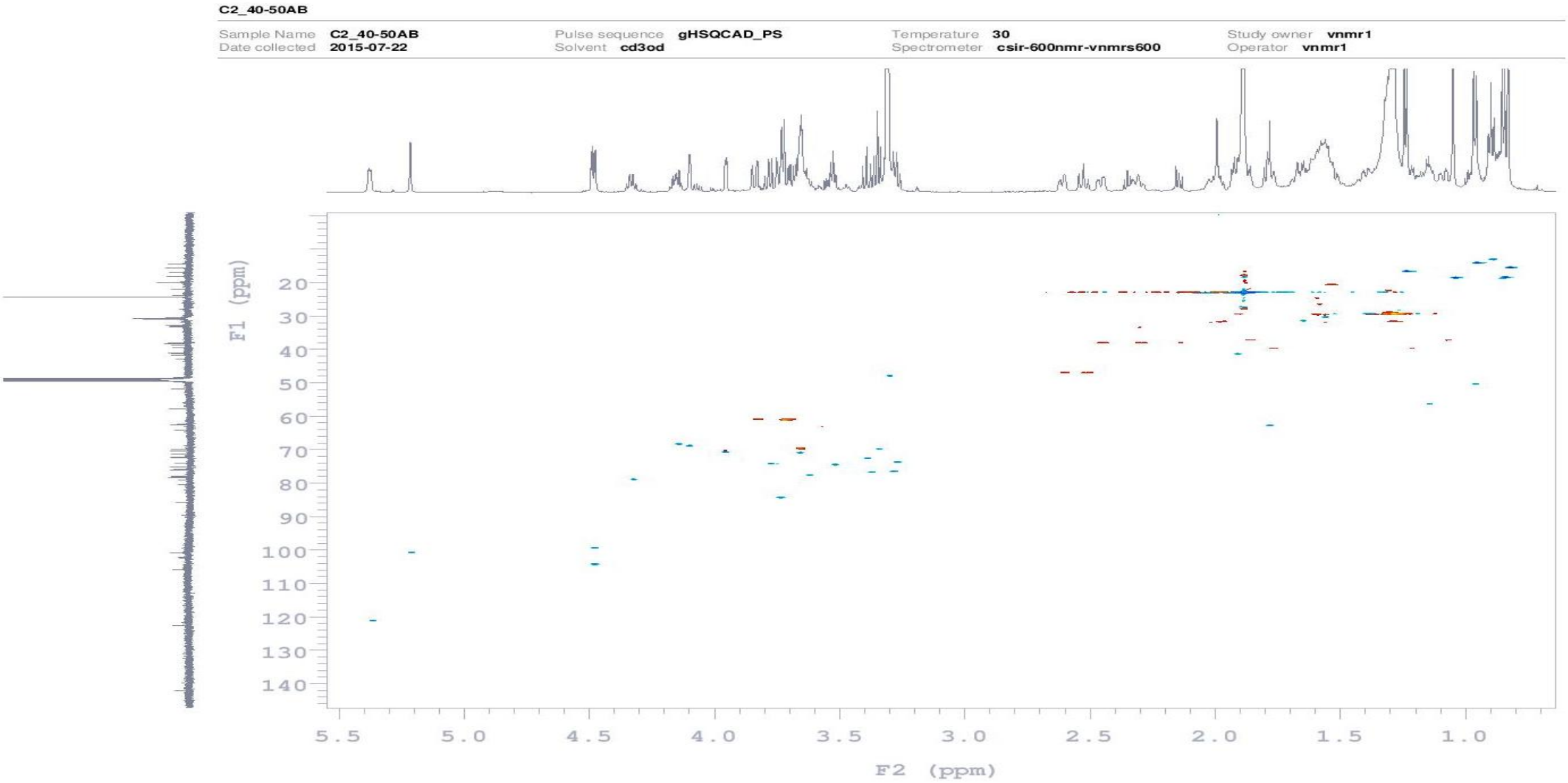

D: HMBC for solasonine

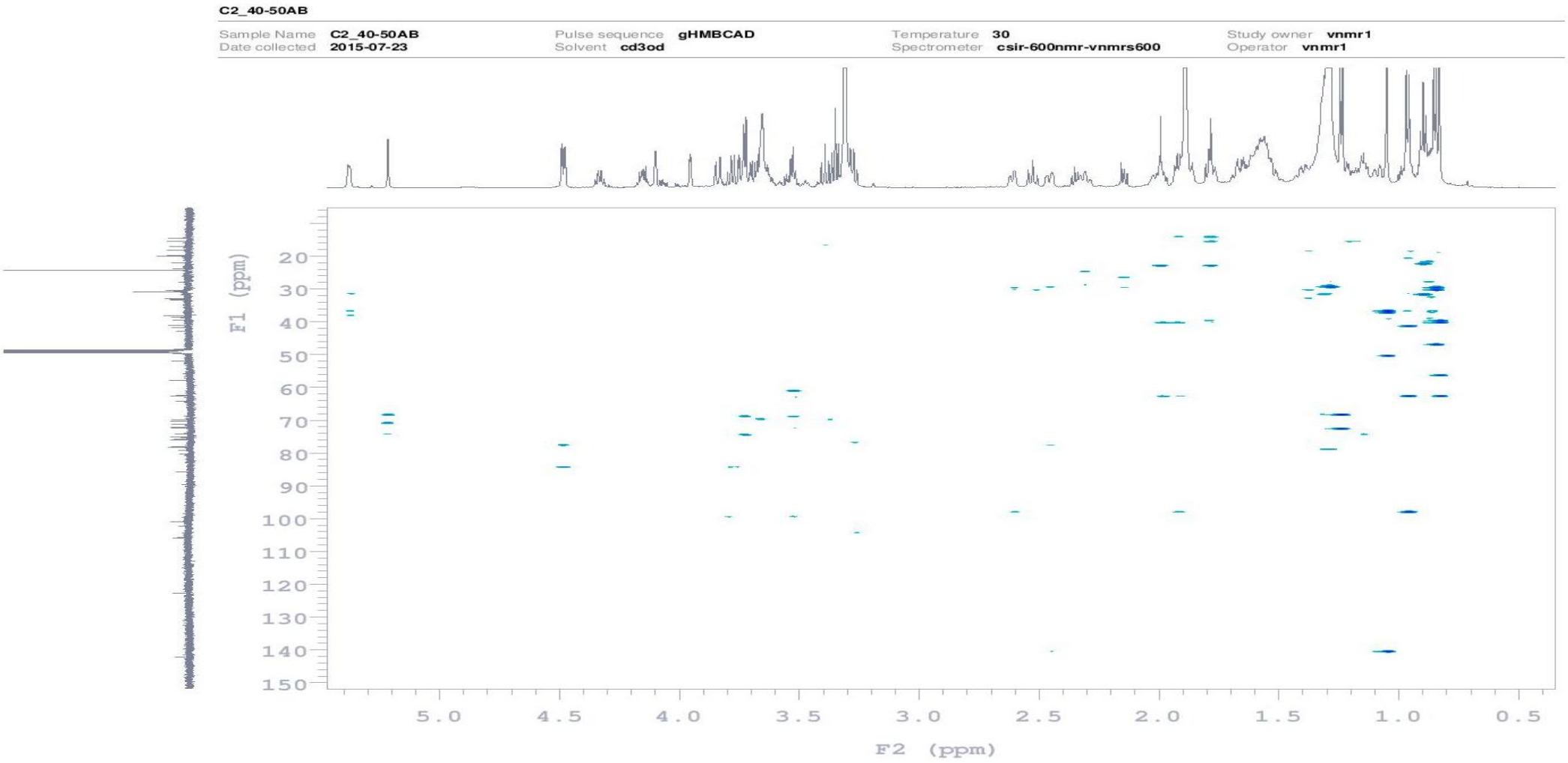

E: COSY for solasonine

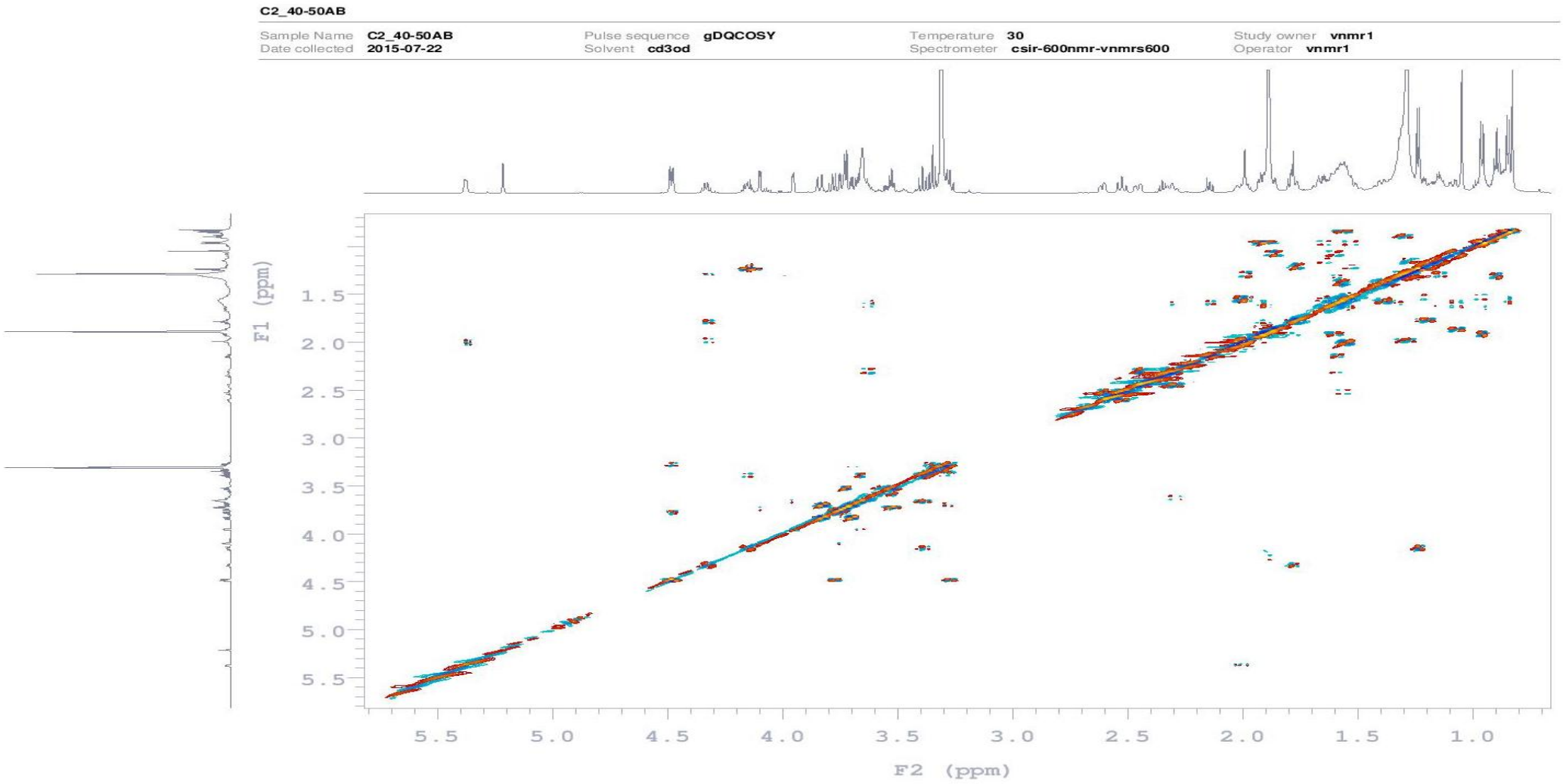

F: UPLC-TOF-MS chromatogram and fragmentation pattern for solasonine

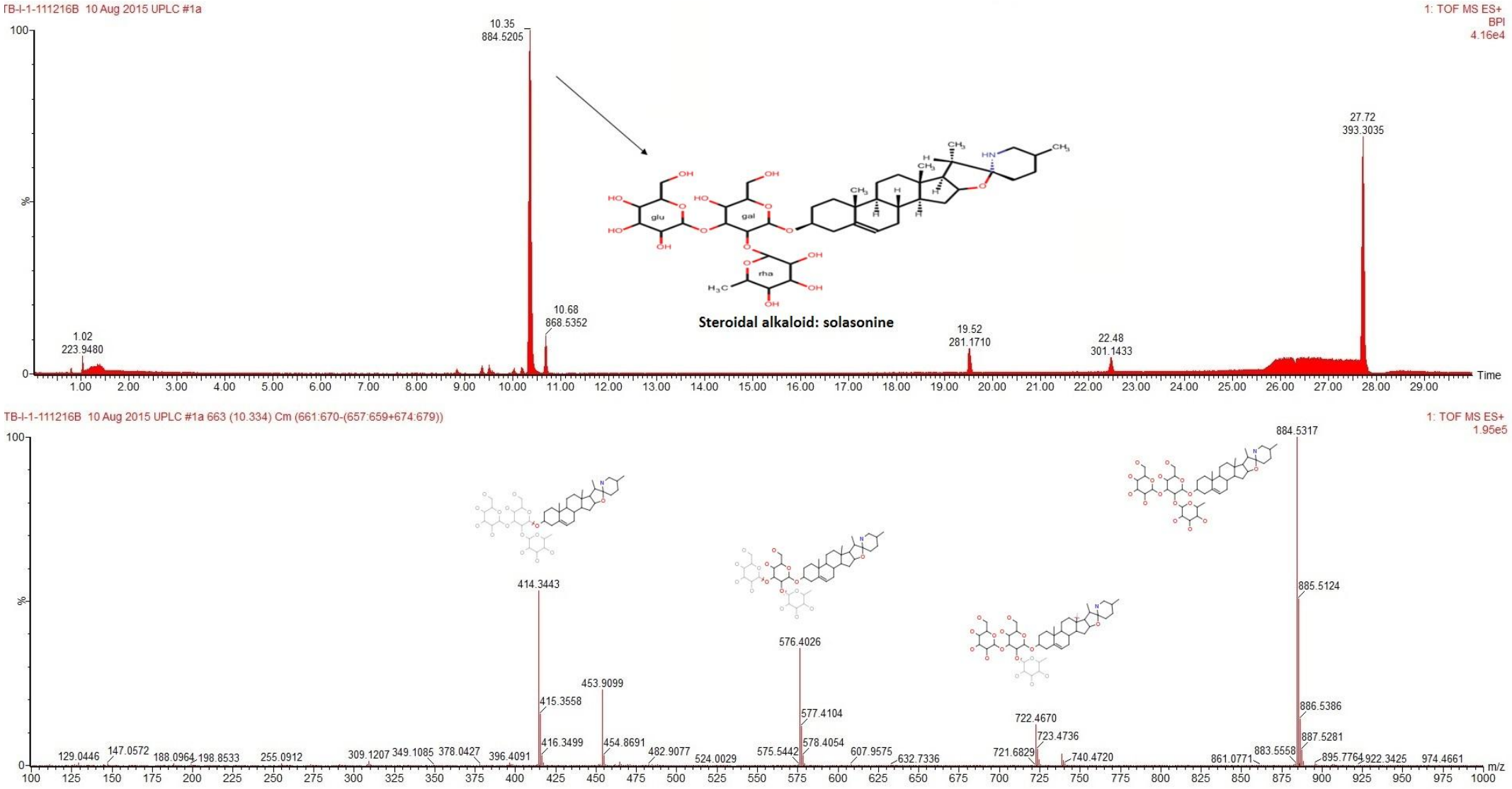

G: UPLC-TOF-MS empirical formula calculation for solasonine

Elemental Composition Report

Single Mass Analysis

Tolerance = 6.0 mDa / DBE: min = -1.0, max = 100.0
Element prediction: Off
Number of isotope peaks used for i-FIT = 4

Monoisotopic Mass, Even Electron Ions
6088 formula(e) evaluated with 3 results within limits (up to 50 best isotopic matches for each mass)
Elements Used:
C: 45-46 1H: 70-100 2H: 0-100 N: 1-1 O: 15-16

ESIPos VTOF 98%A2:02%B2 @ 0.4 60C SYNAPT HDMS G1
TB-I-1-111216B 10 Aug 2015 UPLC #1a 663 (10.334) Cm (661:670-(657:659+674:679)) 1: TOF MS ES+
1.95e+005

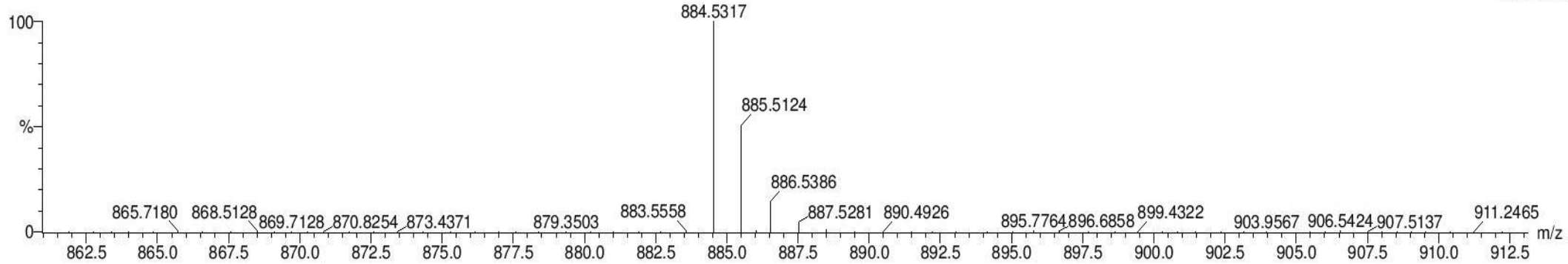

Minimum:				-1.0			
Maximum:		6.0	10.0	100.0			
Mass	Calc. Mass	mDa	PPM	DBE	i-FIT	i-FIT (Norm)	Formula
884.5317	884.5310	0.7	0.8	10.5	52.3	1.0	C46 1H70 2H4 N O15
	884.5341	-2.4	-2.7	9.5	52.3	1.1	C46 1H74 2H2 N O15
	884.5371	-5.4	-6.1	8.5	52.4	1.2	C46 1H78 N O15

Appendix V

A: UPLC-TOF-MS chromatograms of the crude extract (TB03)

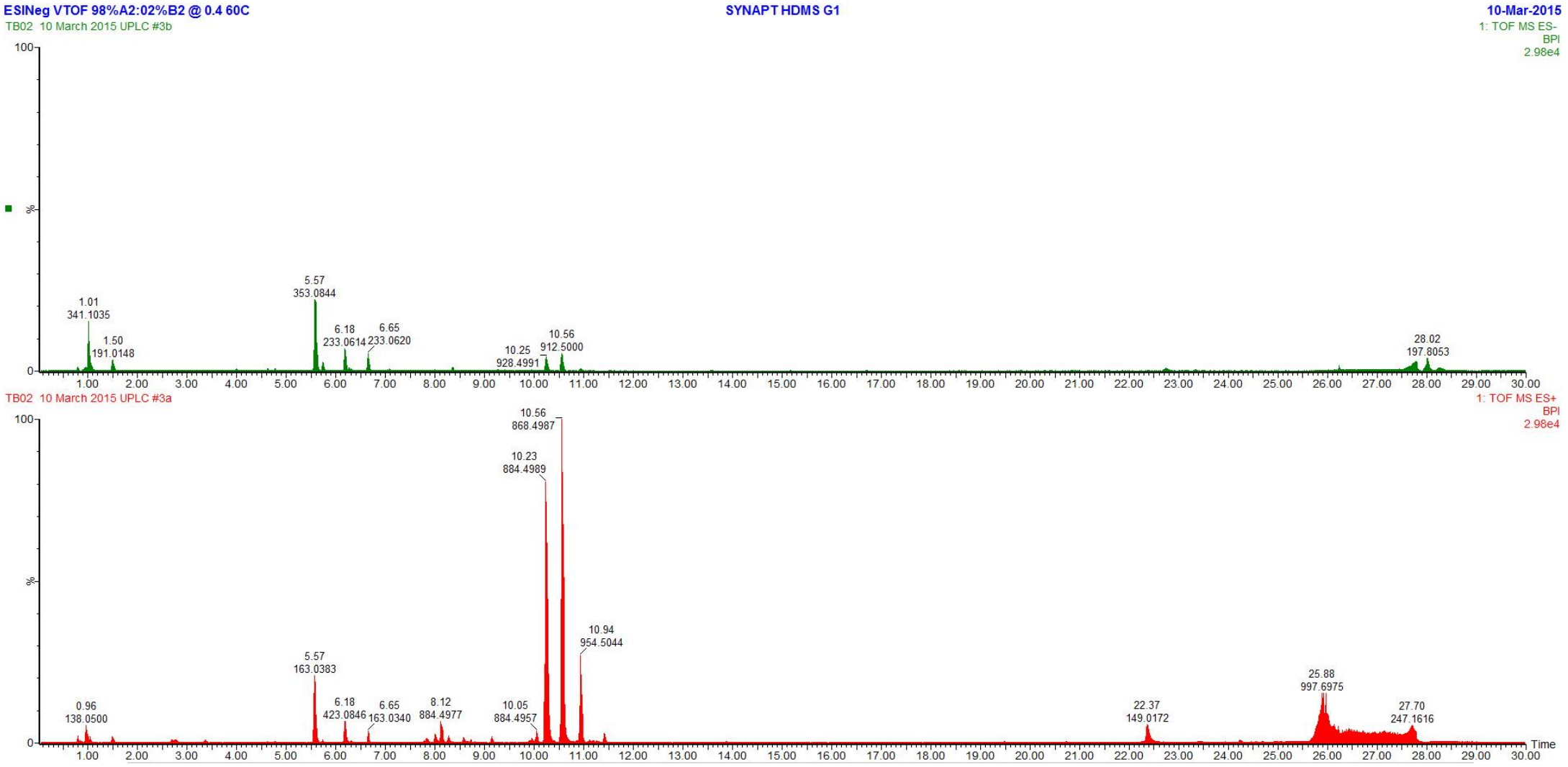

B: UPLC-TOF-MS chromatogram of the ether fraction (TB04)

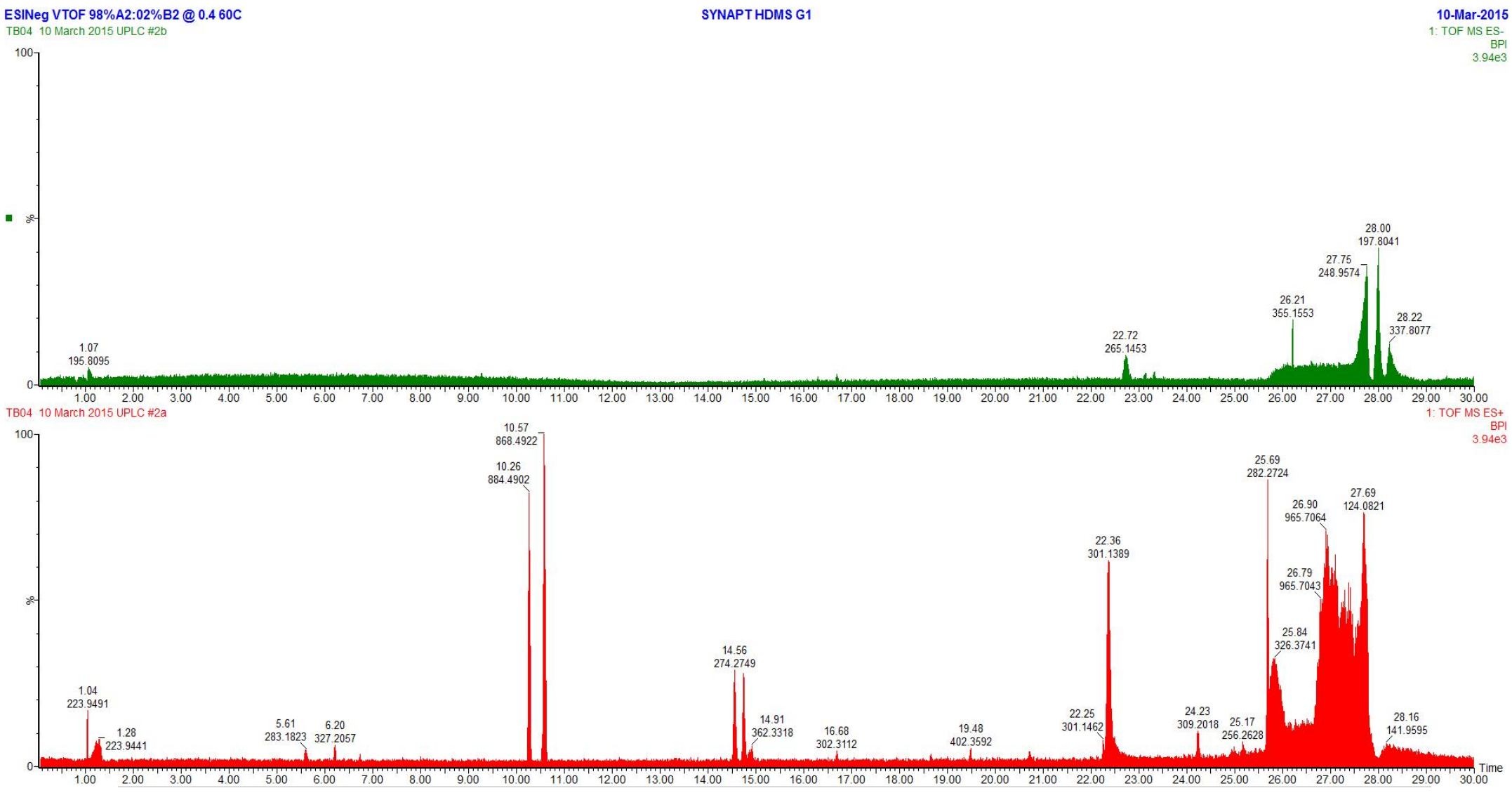

C: UPLC-TOF-MS chromatogram of the chloroform fraction (TB01)

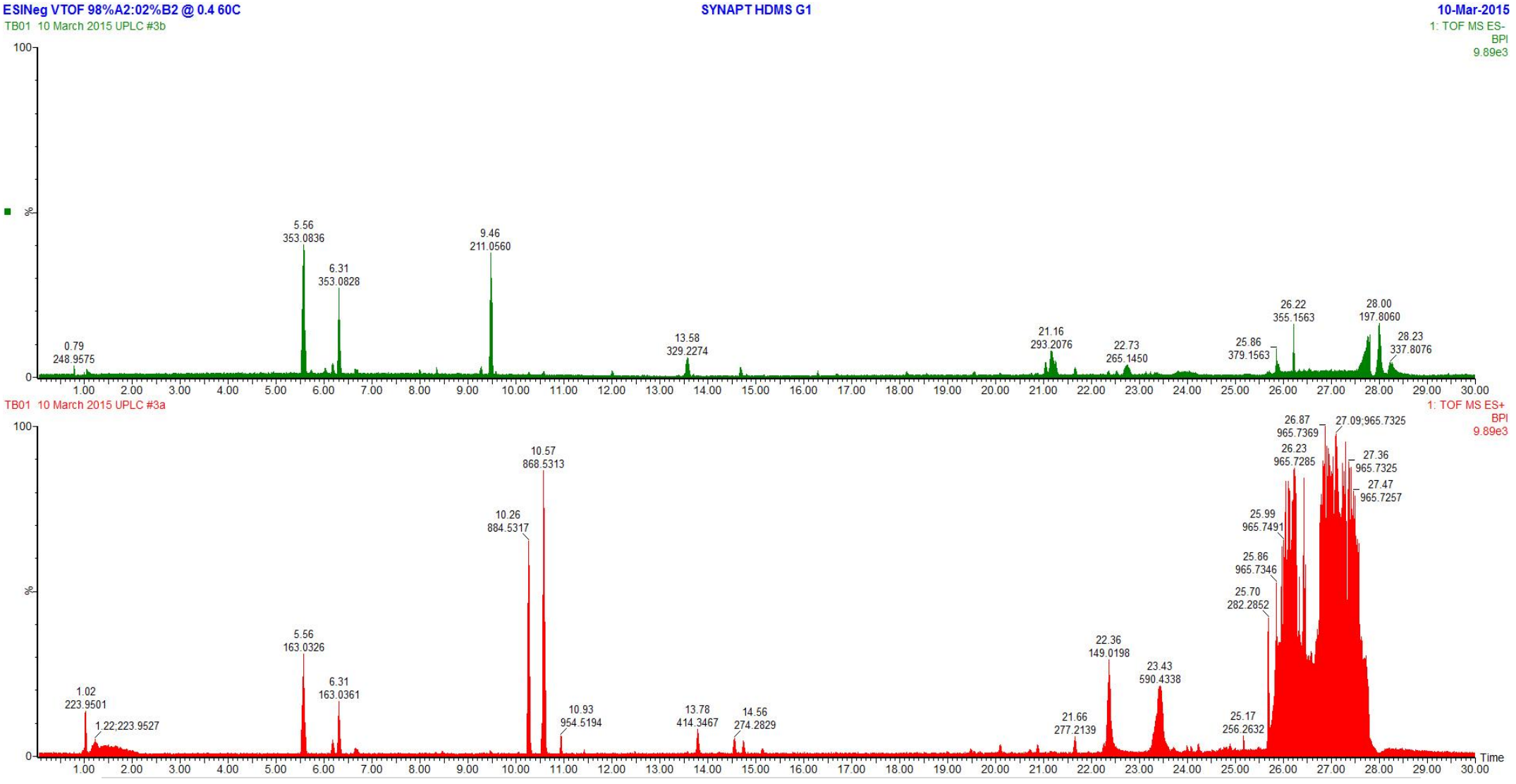

D: UPLC-TOF-MS chromatogram of the aqueous fraction (TB02)